LIMBURGS UNIVERSITAIR CENTRUM

ANALYSIS AND KINETICS OF MELAMINE-FORMALDEHYDE RESINS

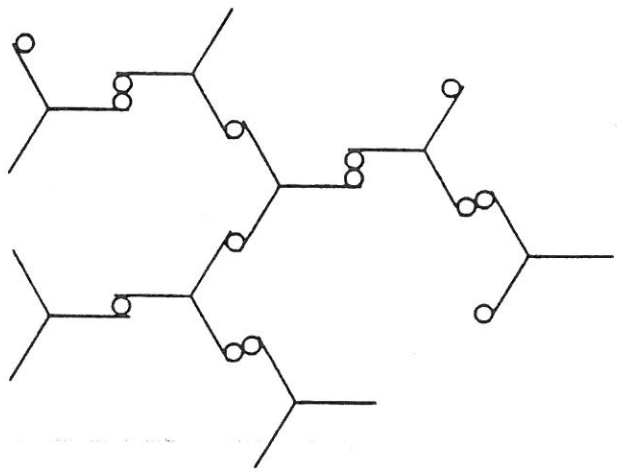

MARTINE SCHEEPERS

Promotoren Prof.Dr.J.Gelan
Prof.Dr.D.Vanderzande

INSTITUUT VOOR MATERIAALONDERZOEK

LIMBURGS UNIVERSITAIR CENTRUM
FACULTEIT WETENSCHAPPEN

ANALYSIS AND KINETICS OF MELAMINE-FORMALDEHYDE RESINS

Proefschrift voorgelegd tot het bekomen van de graad van
Doctor in de Wetenschappen
te verdedigen aan het Limburgs Universitair Centrum
door

MARTINE SCHEEPERS

Promotoren Prof.Dr.J.Gelan
Prof.Dr.D.Vanderzande

Diepenbeek 1994

Dankwoord

Tijdens de afgelopen vier jaar heb ik ervaren dat het zelfstandig werken aan de probleemstelling van dit proefschrift en het kritisch analyseren van resultaten centraal staan tijdens een promotie onderzoek. Ik wens dan ook iedereen te danken die hiertoe heeft bijgedragen.

Mijn ouders dank ik voor de studiemogelijkheden en de praktische hulp op alle mogelijke vlakken.

Ik heb dit promotie onderzoek kunnen voltooien in zeer benijdenswaardige omstandigheden. Prof.Dr.J.Gelan en Dr.P.Brandts ben ik zeer erkentelijk voor het creeëren van deze samenwerkingsmogelijkheden. Mijn promotors Prof.dr.J.Gelan en Prof.dr.D.Vanderzande ben ik dankbaar voor hun wetenschappelijke begeleiding en de vrijheid die mij geboden werd tijdens dit onderzoek. Een speciaal woord van dank wil ik richten tot Dr.P.Brandts voor de vele 'kostbare' uurtjes om te discussieren over de aanpak van problemen, het kritisch analyseren van resultaten en het onuitputtelijk aanbod aan voorstellen. Dr.R.Carleer was steeds bereid om mee te discussieren in de werkbesprekingen en hulp te verlenen daar waar nodig.

Tijdens dit onderzoek heb ik samengewerkt met tal van specialisten: Dr.P.Adriaensens op het gebied van NMR, Dr.B.Kip op het gebied van Raman spectroscopie, Prof.dr.J.Mullens op het gebied van thermische analyse en Dr.J.J.Nusselder op het gebied van kinetiek. Ik ben hen zeer dankbaar voor de vele waardevolle suggesties en voor hun hulp bij de interpretatie van de experimenten. Dr.V.Aarts wil ik bedanken voor het kritisch doorlezen van dit proefschrift.

Verder gaat mijn dank nog uit naar zowel mijn Belgische als Nederlandse collega's voor hun steun, meeleven en de zeer aangename werksfeer.

Tenslotte, maar zeker niet in het minst wil ik Jos nog bedanken voor zijn aanhoudende steun en het bijspringen in de huishoudelijke taken.

CONTENTS

PART I INTRODUCTION

PART II DEVELOPMENT OF TECHNIQUES

CHAPTER 1

CHEMISTRY OF MF RESINS

1 General introduction

Melamine-formaldehyde (MF) resins have been used for decades. Melamine was synthesized by Liebig in 1834 but production of MF resins did not start until 1936 [1]. Then MF resins moved rapidly into applications already established by urea and soon formulations for moulding, laminating, coatings, adhesives and paper and textile treating were manufactured throughout the industrialized world [2,3].

The rapid industrial development of MF resin technology has far out-distanced the capability to analyze the products. The hexa-functionality of melamine and the analytical inaccessibility of the cured resins are the main reasons for this. As a result, the industry optimizes the resin formulations on an empirical basis. The MF resin technology has undergone substantial evolutionary changes over the years to reduce formaldehyde emissions and to provide better overall performance of the applied coatings. In order to better optimize the properties and the performance characteristics of MF resins it is necessary to develop relationships between resin composition, resin structure and subsequent properties.

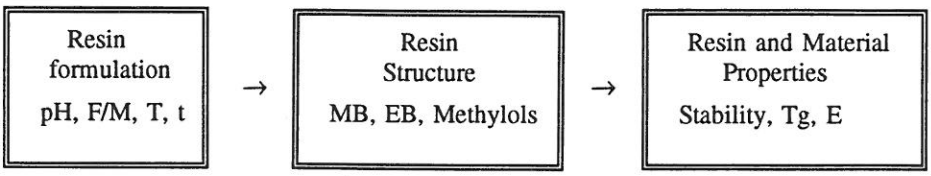

A more fundamental knowledge of chemistry and structure of MF resins will allow a more systematic development of improved resin formulations in place of empiricism. This systematic development of MF resins involves several phases: (i) synthesis of MF resins under a variety of reaction conditions including pH, F/M ratio, temperature and reaction time, (ii) characterization of MF resins in terms of methylene bridges

(MB), methylene-ether bridges (EB) and methylol groups as well in the early stage of the condensation as in the cured stage, this requires the development of techniques, (iii) correlation of chemical structure of low molecular weight resins with properties such as resin stability and correlation of chemical structure of finally cured resins with properties of three dimensional networks such a glass transition, E modulus , crosslink density and (iv) derivation of guidelines for optimum resin composition and properties.

An investigation was started at DSM Research in Geleen in cooperation with Limburg University at Diepenbeek to establish how the chemical structure of MF resins in the early stage of condensation and in the cured stage is influenced by variables in the resin formulation.

2 *Applications*

The remarkable versatility of MF resins results from the possible variations in the processing conditions. Resins on the basis of melamine-formaldehyde are similar to those based on urea-formaldehyde, but have some superior properties such as a better heat, water, stain and scratch resistance [3].

Laminates

The major use of MF resins is currently for the production of laminates [4]. Decorative paper is impregnated with MF resin and is then dried and partially cured. Laminates are pressed in a heated press where the final curing takes place. One can distinguish between low-pressure (LP), continuous pressed (CP) and high-pressure (HP) laminates depending on the composition of the laminate and the pressing conditions. LP laminates are mainly used for bodies of kitchen cabinets. CP laminates are used e.g. for fronts of kitchen cabinets and self-assembly furniture. HP laminates are mainly used for tabletops. HP laminates possess excellent heat and scratch resistance. Special hard-wearing HP laminates pressed onto a wood-based core are used as flooring.

Adhesives

Urea-formaldehyde resins represent the largest market of adhesives based on amino resins [5]. Melamine is often added to UF resins to upgrade the properties of the latter. Melamine adhesives exhibit a better water resistance compared to urea whereas urea adhesives are lower in cost. Blends of urea- and melamine formaldehyde resins are often used as adhesives to get the best balance between cost and performance.

Moulding compounds

Melamine resins may be blended with a filler to make a moulding compound. The moulding compound may be used as a powder or as granules to get the desired decorative appearance in the moulded article. Melamine moulding compounds filled with α-cellulose are e.g. used for plastic dinnerware [5]. The excellent electrical properties, hardness, heat resistance and strength of MF resins make them useful for a variety of industrial applications.

Coatings

Melamine-formaldehyde resins etherified with methanol or butanol are used in a wide range of coatings [6]. These alkylated resins are efficient crosslinkers for other resins like alkyds, polyesters, epoxy resins and certain types of acrylics. Melamine-based coatings exhibit excellent colour retention and resistance to wear and are mainly used in the automotive industry.

Other uses

MF resins are also used in the paper industry for a variety of applications. They are e.g. used to improve wet and dry strength, stiffness and the water resistance of paper, cartons and labels. They also find application as textile-finishing resins, providing wash- and wear properties to cellulosic fabrics. Melamine also makes paper and textile flame-retardant [7]. Water-soluble MF resins are used in tanning of leather or to improve adhesion to vulcanized rubber.

3 *Monomers*

Melamine

Melamine (2,4,6-triamino-s-triazine) is a white crystalline solid that decomposes and sublimes at approximately 354°C. It is only slightly soluble in water (30 g/l H_2O at 100°C) and is practically insoluble in most organic solvents.
Molecular structure calculations by ab initio quantum mechanical techniques and force field and semi-empirical methods, yield a not completely planar structure for melamine with torsional angles describing the position of the amine hydrogen atoms of about 8°. The amine rotational-energy barrier was found to be 20 kcal mol^{-1} implying that the $C\text{-}N_{amine}$ bond is a stiff bond hardly allowing rotation of the amine group at room temperature [8].

Formaldehyde

In the pure state, formaldehyde is a colorless, pungent-smelling reactive gas. The commercial chemical is handled either as a solution or as a solid polymer, paraformaldehyde [9]. Formaldehyde gas is very soluble in water and reacts with it to form methylene glycol

$$HCHO + H_2O \rightleftarrows HO\text{-}CH_2\text{-}OH \qquad (1)$$

and higher polyoxymethylene glycols

$$HO\text{-}CH_2\text{-}OH + n\ HCHO \rightleftarrows HO\text{-}CH_2\text{-}O(CH_2\text{-}O)_nH \qquad (2)$$

Formaldehyde is usually used as a 37% (by weight) aqueous solution. Aqueous formaldehyde is known as formalin. It is supplied in two types, unstabilized and methanol-stabilized.

4 *MF resin formation*

MF resin formation consists of two stages [3]. In the first stage, the slightly water soluble melamine dissolves in formalin and a series of addition and condensation reactions takes place to give a low molecular weight resin. The resin which may be concentrated can be used as an impregnant or as an adhesive. Spray-drying yields a solid. At this stage the resin is both fusible and soluble.

During the final curing process, the intermediates are transformed to the desired MF resins with the application of pressure, heat and/or an acid catalyst by reaction of amino- and methylol groups that are still available. During cure further chain extension and crosslinking take place to form an insoluble, infusible, three dimensional network.

4.1 *Addition of formaldehyde to melamine*

The first reaction is an addition of formaldehyde to melamine to introduce the methylol group and is shown in eq.3. This is known as the methylolation [10]. For convenience we always represent the melamine species minus one amino group by R.

$$R\text{-}NH_2 + CH_2O \rightleftarrows R\text{-}NHCH_2OH \qquad (3)$$

The addition reaction is catalysed by both acids and bases, hence it takes place over the entire pH range. Melamine has six amino hydrogens, so there are various possibilities for reaction with formaldehyde. The methylolation reactions can be represented as a series of competitive and consecutive equilibria. Nine distinct methylolmelamines are posssible because di-, tri- and tetra- methylolmelamine may each exist in two isomeric forms. The methylolation scheme, reported by Gordon et al. [10], is depicted in Scheme I.1.

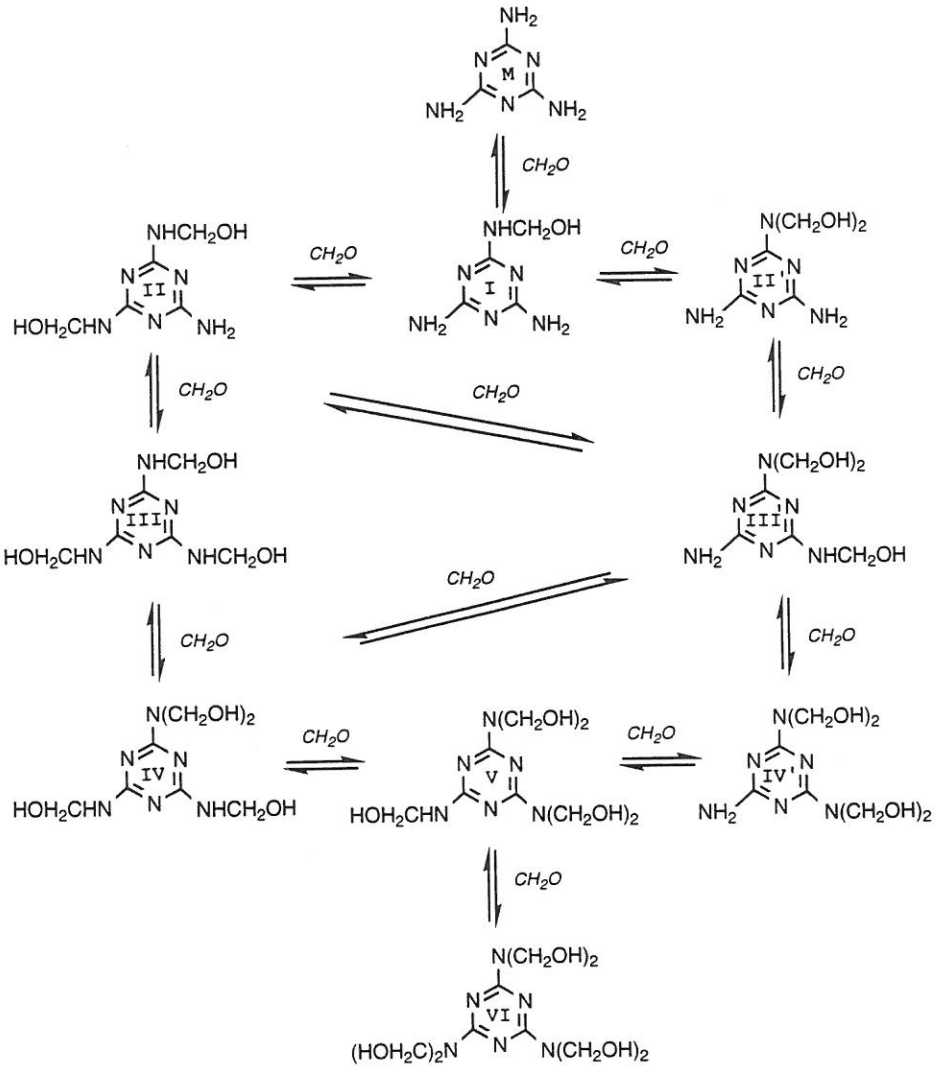

Scheme I.1 Methylolation scheme reported by Gordon et al.[10].

4.2 *Condensation reactions*

Methylolmelamines can undergo two types of condensation reactions. By condensation of a methylol group and an amino group a methylene bridge (eq.4) is formed and the mutual condensation of pairs of methylol groups results in a methylene-ether bridge (eq.5).

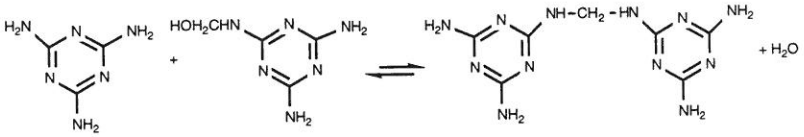

(4)

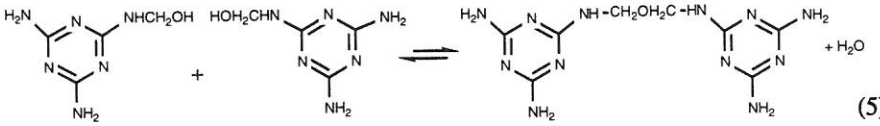

(5)

Beside these linear bridged structures, methylene and methylene-ether bridges can also be substituted by a methylol group or a second bridge. One has to imagine that the resin structure obtained by bonds created at random and consisting of methylol groups, methylene and methylene ether bridges has a rather irregular constitution. Furthermore, the methylene versus methylene-ether bridge formation depends on pH, F/M molar ratio, temperature and reaction time [3]. The analysis of the resin structure requires therefore selective analytical techniques for the determination of the various structural units in which formaldehyde can be incorporated.

4.3 *Control of MF reaction*

A somewhat troublesome side reaction encountered in the manufacture of MF resins is the conversion of formaldehyde to formic acid [9]. Often, the reaction mixture must be heated under alkaline conditions. This is favourable for the Cannizzaro reaction, in which two molecules of formaldehyde interact to yield one molecule of methanol and one of formic acid.

$$2\ HCHO + H_2O \rightarrow CH_3OH + HCOOH \qquad (6)$$

Unless this reaction is controlled, the resin solution may become sufficiently acidic to catalyze the condensation reaction and cause premature gelation of the resin solution. Hence, control of pH and water tolerance during reaction of melamine with formaldehyde is of paramount importance for the production of successful products.

5 *Analysis of MF resins*

Although the MF resin production started from 1936 and the MF resins moved rapidly into a variety of applications, it took a long time to elucidate the structure of them and some structural details are still lacking. Particularly, the methylene-ether bridge formation has been studied in less detail and the structure of cured MF resins has been studied only fragmentary because of the lack of a selective analytical technique. The reason for this slow progress is the intrinsic complexity of the MF products, caused by the dependence of the reaction path on pH, F/M molar ratio, concentration, temperature and reaction time. A major breakthrough in this field has occured due to modern analytical tools. Among these tools, chromatographic methods and ^{13}C NMR has probably offered the most significant progress.

Until thirthy years ago, analysis of MF resins relied on titrimetic methods [11-13] giving the free formaldehyde content by the sulfite method and the methylolformaldehyde content by the iodometric method. The methylolation reactions were investigated by following the consumption of free formaldehyde and the bridge formation was studied iodometrically from the decrease of methylol groups without further identification of the bridges.

Then, separation of the various methylolmelamines became possible by chromatographic methods. Paper chromatographic methods were initially used by Koeda [14] in 1954 for the separation of methylolmelamines. Braun and Legradic [15-18] first silylated the methylolmelamines by treatment with N-diethyltrimethylsilylamine before separation by gel permeation chromatography. They isolated six trimethylsilyl ethers of mono- to hexa-methylolmelamine by GPC on a preparative scale and characterized their isolated peaks by ^{1}H NMR and IR spectroscopy. In their analysis, trimethylolmelamine silyl ether was obtained in its symmetrical form only and dimethylolmelamine silyl ether only as the isomer with two monomethylolated amino groups. Tetramethylolmelamine silyl ether existed as a mixture of both possible isomers. Separation of the individual methylolmelamines by liquid chromatography has proved to be more successful than GPC [19,20]. In 1977 Tomita et al. [19] separated all nine methylolmelamines by LC with a reverse-phase

system and identified each of the isolated species by ^{1}H NMR.

A variety of techniques have been used to study the condensation reactions in MF resins. However, each study was performed under different combinations of pH, F/M ratio, concentration and temperature. Since the concentrations of the two types of bridges strongly depend on the reaction conditions and different authors used different techniques (different detection limits) discrepancies may be anticipated.

In initial studies [21-24] it was assumed that only methylene bridges are formed in the pH range 1-8.6 based on the determination of the reaction order in methylol groups.

Braun et al. [25] concluded that methylene-ether bridges are formed under alkaline conditions. They separated some linked species by GPC after treatment with N-diethyltrimethylsilylamine and then characterized them by IR (band at 1170 cm^{-1}) and ^{1}H NMR.

Anderson et al. [26] made use of two model compound systems, i.e., 2-amino-4, 6-diphenoxy-s-triazine and 2-amino-4, 6-diphenyl-s-triazine to investigate the possible course of methylolation and subsequent condensation steps in MF resins by using thin layer chromatography, ^{1}H NMR and IR spectroscopy. They found that condensation occurs at 120°C through methylene-ether bridge formation. Above 135°C methylene-ether bridges were converted to methylene bridges and formaldehyde was released.

In the 1970s solution ^{13}C NMR emerged as a very powerful technique for the analysis of MF resins [27-33]. ^{13}C NMR provides information on both the azine carbons and methylene carbons. The different azine carbon resonances were assigned to different methylolmelamines [27-31]. Tomita et al. [33] concentrated upon the types of bridges formed in the intermediate stages of the MF reaction. The formation of non-substituted as well as substituted methylene and methylene-ether bridges was shown for an MF resin prepared from F/M 3 and pH 9.

For the selective characterization of MF condensates a method has been developed by Gebregiorgis [34] which involves the removal of residual methylol groups, while leaving the bridges already formed practically unaffected. This method consists of a treatment of MF resin syrups with an aqueous ammonia solution to hydrolyse the methylol groups to free formaldehyde and subsequently convert the free formaldehyde quantitatively to hexamethylene tetramine (eq.7).

$$4\ NH_3 + 6\ CH_2O \rightarrow (CH_2)_6N_4 + 6\ H_2O \qquad (7)$$

However, the formation of some ring structures, i.e. two melamine units connected by a methylene-ether and a methylene bridge, was observed under these conditions. Spectroscopic evidence for the presence of both methylene and methylene-ether bridges in the methylol-free MF resins was obtained by ^{1}H NMR and FT-IR and ESCA measurements.

The usefulness of polarographic methods for the analysis of the MF reaction mixtures was investigated by Nastke et al. [35-37]. This study revealed that free formaldehyde, formaldehyde bound in methylol groups and in methylene bridges can be determined by polarography. They also described a chemical method for the determination of the oxidable formaldehyde. The formaldehyde bound in methylene-ethers could then be calculated as the difference between the oxidable formaldehyde and the methylol formaldehyde. Using a combination of polarography and mathematical modeling Nastke et al. showed that methylene and methylene-ether bridges are formed under acid and base reaction conditions, respectively [38].

During the final cure process the condensation reactions have been studied only fragmentary. O'Rourke [39] used ^{13}C CP/MAS NMR to examine the structure of cured MF resins. Ebdon et al. [3,32] investigated the structure of some fully-cured MF resins (prepared from F/M 1.5 and 3.0) by CP/MAS ^{13}C and ^{15}N NMR. ^{13}C CP/MAS NMR spectra show the conversion of methyol groups to methylene bridges. Methylene-ether bridges, however, overlap with residual methylol groups. Ebdon et al. checked the presence of residual methylol groups by studying the ^{15}N CP/MAS NMR spectra of the resins. They concluded that the resin prepared from F/M 1.5 contains predominantly methylene bridges and that prepared from F/M 3 contains an equal number of methylene and methylene-ether bridges.

6 Kinetics and mechanisms of MF reaction

6.1 Kinetics and mechanism of the addition reaction

Approaches made to the analysis of the kinetics of the addition reactions between melamine and formaldehyde began with following the consumption of formaldehyde by the sulphite method. A number of kinetic and thermodynamic constants were obtained in this way by Okano et al. [21], Sato et al. [40-44], Berge et al. [45,46] and Gordon et al. [10,47].

In 1952 Okano and Ogata [21] offered the first analytical kinetic data. The rate of reaction of melamine with formaldehyde to form methylol-substituted

products was determined at 35-40°C over a pH range of 3.0 to 10.6. It was concluded that methylolation is catalyzed by both acids and bases (Scheme I.2)
The methylolation was found to be reversible.

Scheme I.2

Base catalysis

$$R\text{-}NH_2 + OH^- \rightleftarrows R\text{-}NH^- + H_2O \quad (8)$$

$$R\text{-}NH^- + HOCH_2OH \rightleftarrows R\text{-}NHCH_2OH + OH^- \quad (9)$$

Acid catalysis

$$HOCH_2OH + H^+ \rightleftarrows HO(H)^+\text{-}CH_2OH \rightleftarrows {}^+CH_2OH + H_2O \quad (10)$$

$${}^+CH_2OH + R\text{-}NH_2 \rightleftarrows R\text{-}NHCH_2\text{-}O(H)^+H \rightleftarrows R\text{-}NHCH_2OH + H^+ \quad (11)$$

Sato et al. [40-44] studied the kinetics of the methylolation reactions in weakly acid media (pH 3-8) and in strongly acid media (pH 0.6-2.5). Second order kinetics has been observed for the methylolation reaction and the demethylolation follows a first order reaction. They proposed that methylolation follows general acid and base catalysis. By investigating the kinetics and mechanism of the methylolation in the presence of the hydrogen phosphate/phosphate buffer at pH 11.4-11.9, it was shown that the reaction takes place via a general base catalysis [44].

Berge et al. [45,46] reported a kinetic study on the acid and base catalysed decompositions of methylolmelamines (and methoxymethylmelamines). The decomposition of methylolmelamines was found to be subject to general acid and base catalysis.

Gordon et al. [10,47] further elucidated the kinetics of the addition reaction between melamine and formaldehyde. They utilized Koeda's method to conduct additional methylolation studies and illustrated that quantitative estimates of the nine possible methylolmelamines could be made using ^{14}C labeled formaldehyde. The experimentally obtained distribution of methylolmelamines was compared to that attainable in theory by assuming random methylolation behaviour. Some deviation from random behaviour was noted. The parameters which accounted for deviations from randomness were calculated. The first one accounts for a general substitution

effect due to successive methylolation of melamine and the second one was introduced to account for the reduced reactivity of secondary methylolmelamines compared to primary ones. Validity of these parameters was tested in computer simulations by Aldersley et al. [48]. The general substitution parameter was found to be close to 1 so that it could probably be ingored and the parameter accounting for localized substitution was found to be 0.61. Rate constants for methylolation and demethylolation were obtained as a function of pH (5.7-10.2), F/M ratio (0.5-15) and temperature (25-55°C). Good agreement was found with the values of the rate constants obtained by Okano and Ogata [21]. The pH dependence of the rate constant for methylolation is shown in Figure I.1. A value of 3.89 l mol^{-1} was found for the equilibrium constant of methylolation and this value was nearly independent of pH. The activation energy for the methylolation was calculated as 98.74 kJ/mole from rate constant data as a function of temperature. From K values as a function of temperature the heat of reaction was calculated as 12.30 kJ/mole for F/M 3 and as 11.72 kJ/mole for F/M 7.

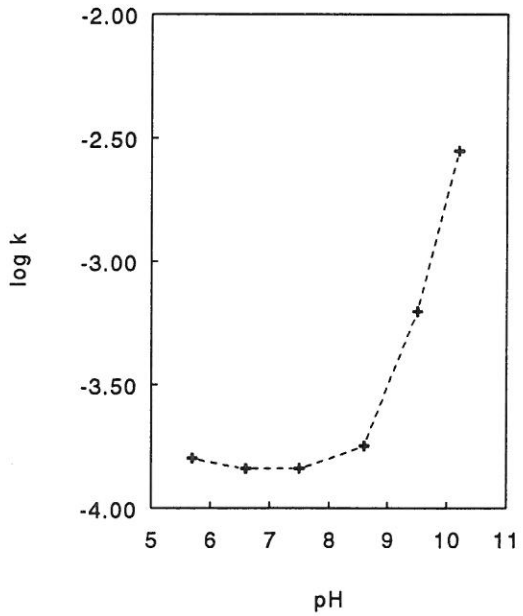

Figure I.1 Rate constants of methylolation at 45°C as a function of pH (data taken from ref. 47).

Tomita et al. [19] estimated equilibrium constants and rate constants for the individual reversible methylolation reactions from the quantitative analysis of the methylolmelamines and free formaldehyde by HPLC. The equilibrium constants (K in l mol^{-1}) for the various stages of MF addition at 48°C and pH 9 are shown in Scheme I.3 (symbols see Scheme I.1). It was concluded that methylolation of a primary nitrogen takes place more rapidly than that of a secondary nitrogen. The temperature dependence of each equilibrium constant was calculated, giving a ΔH value of -12.5 to -14.6 kJ $mole^{-1}$ for each methylolation. The equilibrium constants obtained by Tomita et al. [19] are associated with molecular species. By adding appropriate weightage functions to account for the various possibilities we calculated the equilibrium constants associated with functional groups. For example, the rate of the formation of mono-methylolmelamine will be $6k_1$ because F may attack any of the six hydrogens in melamine. Values of 3.0 ± 0.9 l mol^{-1} and 2.1 ± 0.7 l mol^{-1} were found for the equilibrium constant of the primary methylolation and the secondary methylolation, respectively.

Scheme I.3

Methylolation of a primary -NH

$K_{M,1}$	$K_{1,2}$	$K_{2,3}$
25	12	4.3

Methylolation of a primary -NH with a neighbouring tertiary N

$K_{2',3'}$	$K_{3',4}$	$K_{4',5}$
25	7.2	22

Methylolation of a secondary -NH

$K_{1,2'}$	$K_{2,3'}$	$K_{3,4}$	$K_{3',4'}$	$K_{4,5}$	$K_{5,6}$
0.9	1.8	2.9	0.5	1.3	0.7

6.2 *Kinetics and mechanisms of the condensation reactions*

On the contrary to the methylolation reactions, the kinetics of the condensation reactions has been studied in less detail. In works of Okano et al. [21], Sato et al. [22,23] and Berge et al. [24] the kinetics of the methylene bridge formation was studied from the decrease of methylol groups. Demethylolation and methylene-ether bridge formation were not taken into account.

Okano and Ogata [21] reported a value of 2.7 10^{-3} l mol-1s^{-1} for the rate constant of methylene bridge formation at 70°C and pH 4.9. They proposed the following mechanism for methylene bridge formation because of the considerable variations in reaction rates with varying pH values from 4 to 6.

$$R\text{-}NH\text{-}CH_2OH + H_3O^+ \rightleftarrows R\text{-}NH\text{-}CH_2^+ + 2\ H_2O \qquad (12)$$

$$R\text{-}NH\text{-}CH_2^+ + R\text{-}NHR' \rightleftarrows R\text{-}NH\text{-}CH_2\text{-}NR'\text{-}R + H^+ \qquad (13)$$

R' = H or CH_2-

Eq.(13) was suggested as the rate determining step.

Sato et al. [22,23,49] investigated the methylene bridge formation of mixtures of methylolmelamines (F/M=2, 3 and 6) in the pH range of 1-8 in a water-dimethylsulphoxide mixture as solvent in order to avoid demethylolation. It was found that the condensation rates of the mixtures of methylolmelamines exhibit maxima at approximately pH 4 as shown in Figure I.2. Several possibilities were discussed concerning the nature of the reactive species in methylene bridge formation. In acidic media, the methylolmelamine is in equilibrium with the conjugate acid (eq.14) and the carbonium ion (eq.15).

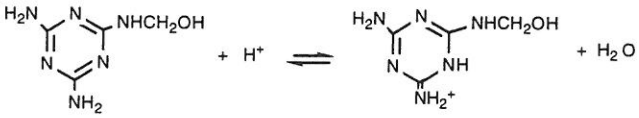

(14)

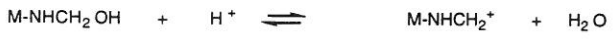

(15)

They claimed that the ring protonated methylol compound is the most likely dominating reactive specie. The structure of the conjugate acid has been demonstrated by Dixon et al. [50] on the basis of UV spectra. Based on the relationship between condensation rate and the acidity of the solution the following mechanism for methylene bridge formation was suggested: in the pH region 2-7 methylene bridges are mainly produced by reaction between a methylolmelamine molecule and its conjugate acid and in the strong acid range (pH<2) they result from reaction between the conjugate acids themselves (Scheme I.4)

Scheme I.4

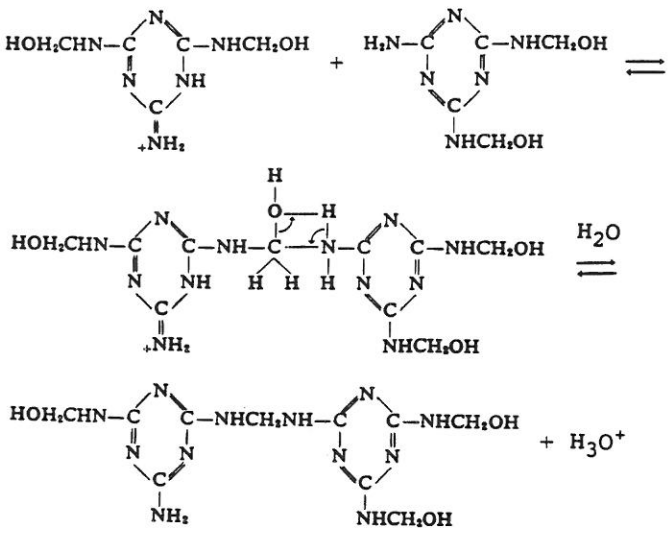

(16)

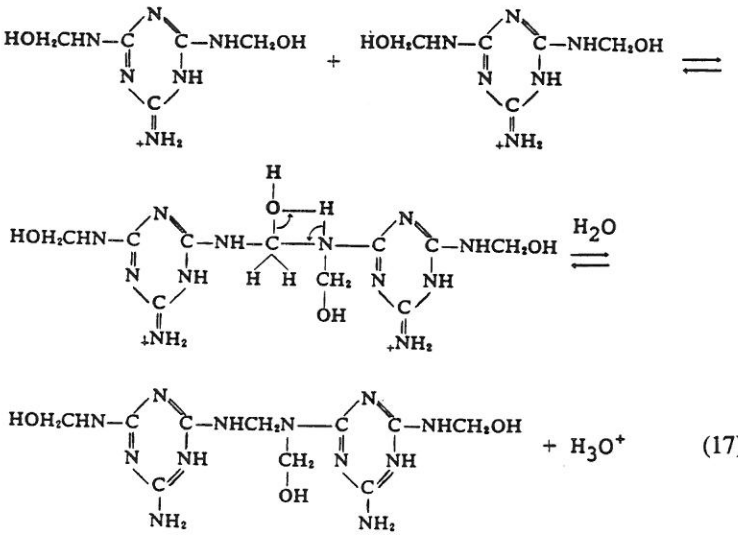

(17)

The methylene bridge formation was also studied in the pH region from 1 to 6 for the reaction between trimethylolmelamine and an excess of melamine by Berge et al. [24]. The same pH dependence of the rate constant of methylene bridge formation was found as that obtained by Sato et al. However, they supported the mechanisms first outlined by Okano et al [21].

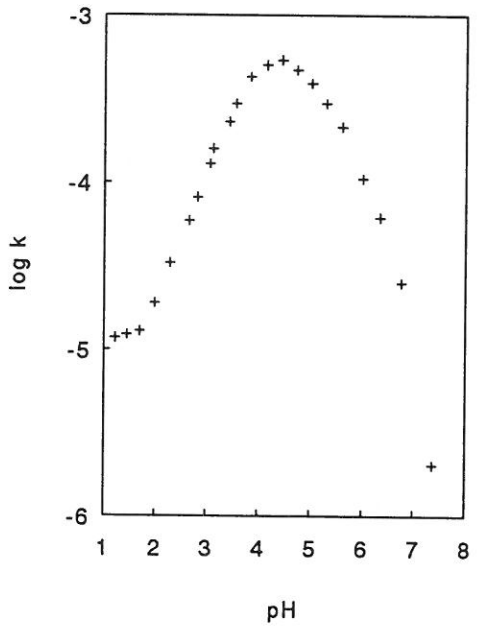

Figure I.2 Rate constants of methylene bridge formation at 35°C as a function of pH (data taken from ref. 23).

Nastke et al. [38] were the first to describe the methylolation, methylene, and methylene-ether bridge formation simultaneously. Rate constants for methylolation, demethylolation, methylene bridge formation, methylene-ether bridge formation and hydrolysis were estimated as a function of pH, F/M molar ratio, temperature and concentration. A kinetic model of the overall reaction was established and the rate constants were calculated by numerical methods. The rate constants for methylolation and demethylolation were found to be about 10 times higher than those obtained by Okano et al. [21] and Gordon et al. [47]. The values for the rate constants of methylene bridge formation obtained by the model were checked by comparing them with the values calculated from initial rate data (determined polarographically). Rate constants for methylene-ether bridge formation and hydrolysis could not be checked because methylene-ether bridges were not determined experimentally. The equilibrium constant for the reversible methylene-ether bridge formation at 80°C was shown to be 13-162 mol l^{-1} dependent on pH and F/M ratio. The activation energy determined for the methylene bridge formation was 76 kJ mol^{-1} at pH 8 and F/M 2. For the methylene-ether bridge formation and decomposition values of

27 and 28 kJ mol^{-1} were found, respectively. The pH dependence of the rate constants for methylene bridge formation for MF resins with various F/M ratios is shown in Figure I.3. Figure I.4 shows the pH dependence of the rate constants for methylene-ether bridge formation and hydrolysis for MF resins with various F/M ratios. They concluded that methylene and methylene-ether bridges are formed by acid- and base-catalyzed reactions, respectively. From Figure I.3 it can be observed that the rate constant of methylene bridge formation passes a minimum at pH 9 and increases as the pH increases at higher F/M ratio's. Based on this observation, they suggested that methylene bridges are formed not only in the acid media (Eqn. 18-21) but also from free Schiff's bases resulting from the base-catalyzed scission of methylene-ether linkages (Eqn. 22-24).

$$R\text{-}NHCH_2OH + H_3O^+ \rightleftarrows R\text{-}NHCH_2\overset{+}{\underset{H}{O}}\text{-}H + H_2O \quad (18)$$

$$R\text{-}NHCH_2\overset{+}{\underset{H}{O}}\text{-}H \rightleftarrows [\ R\text{-}NH\overset{+}{C}H_2 \leftrightarrow R\text{-}\overset{+}{N}H{=}CH_2\ ] + H_2O \quad (19)$$

$$R\text{-}NH\overset{+}{C}H_2 + H_2N\text{-}R \rightleftarrows R\text{-}NH\text{-}CH_2\overset{+}{\underset{H}{N}}\text{-}R \quad (20)$$

$$R\text{-}NH\text{-}CH_2\overset{+}{\underset{H}{N}}\text{-}R + H_2O \rightleftarrows R\text{-}NHCH_2NH\text{-}R + H_3O^+ \quad (21)$$

$$R\text{-}NH\text{-}CH_2OCH_2\text{-}NH\text{-}R + OH^- \rightleftarrows R\text{-}\bar{N}\text{-}CH_2OCH_2\text{-}NH\text{-}R + H_2O \quad (22)$$

$$R\text{-}\bar{N}\text{-}CH_2OCH_2\text{-}NH\text{-}R \rightleftarrows R\text{-}N{=}CH_2 + {}^-OCH_2\text{-}NH\text{-}R \quad (23)$$

$$R\text{-}N{=}CH_2 + R\text{-}NH_2 \rightleftarrows R\text{-}NH\text{-}CH_2\text{-}NH\text{-}R \quad (24)$$

A mechanism for methylene-ether bridge formation from Schiff's bases was also proposed by Nastke et al. (Eqn. 25-27).

$$R\text{-}NH\text{-}CH_2OH + OH^- \rightleftarrows R\text{-}NH\text{-}CH_2O^- + H_2O \quad (25)$$

$$R\text{-}NH\text{-}CH_2O^- + H_2C{=}N\text{-}R \rightleftarrows R\text{-}NH\text{-}CH_2OCH_2\text{-}\bar{N}\text{-}R \quad (26)$$

$$R\text{-}NH\text{-}CH_2OCH_2\text{-}\bar{N}\text{-}R + H_2O \rightleftarrows R\text{-}NH\text{-}CH_2OCH_2\text{-}NH\text{-}R + OH^- \quad (27)$$

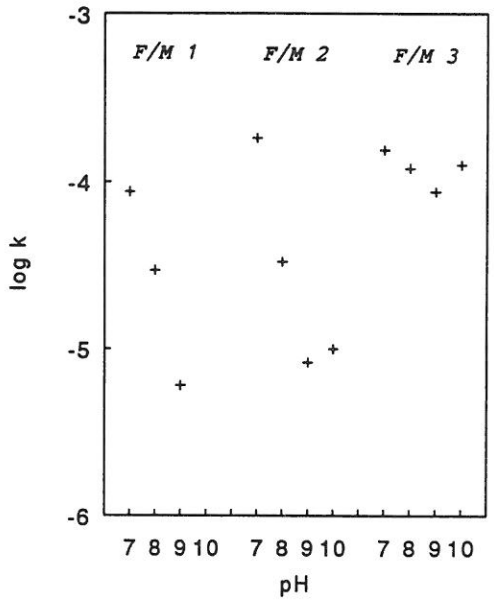

Figure I.3 Dependence of the rate constants of methylene bridge formation on pH at 80°C for different F/M ratios (data taken from ref. 38).

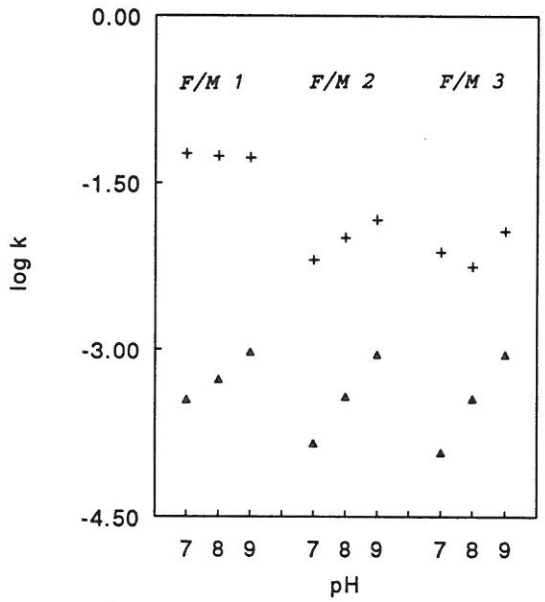

Figure I.4 Dependence of the rate constants of methylene-ether bridge formation (+) and cleavage (▲) on pH at 80°C for different F/M ratios (data taken from ref.38).

A number of authors have modeled the MF polymerization reaction. Among those Gupta et al. [51,52] and Kumar et al. [53,56] are the most important ones. The kinetic modeling of the MF polymerization reaction is a mathematical challenge because of the unequal sites of the reactive species. The model has to account for differences in reactivity between primary and secondary hydrogens and between internal and external hydrogens. Furthermore the reversibility of the reactions and the dissolution of melamine have to be taken into account.

7 *Aims of this study*

The main incentive of the work presented in this thesis is to obtain a better understanding of the relation between the resin structure and the factors governing them. This study is concentrated on " real life systems ", closely related to industrial practice. The first aim is therefore, to evaluate and to develop techniques for the characterization of the resin structure without disturbing the subtle equilibriain aqueous resin solutions as well as in cured MF resins. Determination of the kinetic constants of the condensation reactions in " real life systems " is the second aim. Finally, using these tools the chemical structure of MF resins and cured materials is studied as a function of some of the variables of the resin formulation with the purpose of relating resin structure to resin composition.

8 *Survey of the contents*

Chapter 1 contains a general introduction in the field of MF resins. The variety of applications is briefly reviewed. The progress in the analysis of the chemical structure of MF resins is presented. The kinetics and mechanisms of the addition reactions and condensation reactions are described. The development of techniques for the characterization of methylene bridges, methylene-ether bridges and methylol groups in MF resins is emphasized in order to advance the state of the art.

In Chapter 2 it is shown that ^{13}C NMR provides more detailed information on the structure of MF resins than is available from classical analytical methods. Particular attention is paid to the selective determination of methylene-ether bridges. A method to demonstrate the methylene-ether bridge formation is presented.

The usefulness of ^{13}C CP/MAS NMR for the characterization of cured MF resins is described in Chapter 3. Particular importance is ascribed to the attainable

resolution and the quantifiability of the spectra when it is desired to measure the curing conversion by means of ^{13}C CP/MAS NMR.

In Chapter 4, the possibility of using FT-Raman spectroscopy in the characterization of MF resins, is examined. The bands in the Raman spectra of MF resins are assigned based on a combination of literature band assignments on UF resins and a study of the Raman spectra of relevant model compounds and well-characterized MF resins. Furthermore, the quantification of the Raman bands is studied. The changes in the Raman spectra of MF resins during cure are illustrated. Finally, the utility of FT-Raman spectroscopy for the determination of the free melamine content in MF resins is described.

Chapter 5 deals with a DSC study on MF resin cure. However, particularly for MF resins which can cure by different mechanisms, support by spectroscopic techniques is required. Therefore two sets of partially cured MF resins are examined by a combination of DSC, ^{13}C CP/MAS NMR and FT-Raman spectroscopy. Enthalpies for methylene and methylene-ether bridge formation were estimated.

In Chapter 6 the kinetics of the methylene bridge formation, methylene-ether bridge formation and decomposition has been investigated for a standard F/M 1.7 resin with respect to pH and temperature. Both a molecular species approach and a functional group approach were used to estimate the rate constants of methylene bridge formation, methylene-ether bridge formation and hydrolysis.

The effect of variations in the resin formulation on the structure of MF resins during early stages of the resin formation is the subject of Chapter 7. The structure of the aqueous MF resins was analyzed by ^{13}C NMR. The effect of the following reaction parameters has been examined: (i) the pH, (ii) the F/M molar ratio and (iii) the solids content. The chemical aspects of the evolution of pH and water tolerance during the resin synthesis have been studied.

A systematic study on the structural dependence of cured MF resins on the initial reaction conditions is presented in Chapter 8. The structure of the cured MF resins was characterized by ^{13}C CP/MAS NMR and FT-Raman spectrosocpy. The effect of the following reaction parameters has been studied (i) initial formalin pH, (ii) F/M molar ratio, (iii) solids content, (iv) cure temperature and (v) p-toluene sulfonic acid as an acid catalyst.

Finally, abstracts are given in English and Dutch.

9 *References*

[1] Ger.Pat. 647,303 (1937) and Brit.Pat. 455,008 (1936), W.Hentrich and R.Köhler (to Henkel and Co.).

[2] I.H.Updegraff, Encyclopedia of Polymer Science and Engineering, Wiley, New York, 752 (1985).

[3] J.R.Ebdon, B.J.Hunt, M.Al-Kinany, *Spec.Publ.R.Soc.Chem.*, 87, 109 (1991).

[4] B.Arcement, *Plast.Laminates Semin.*, TAPPI, Atlanta, Notes, 25 (1980).

[5] P.O.Powers, 'Amino resins and Plastics', in Kirk-Othmer Encyclopedia of Chemical Technology, A.Standen, J.Scott, eds, 1st ed., 1, Interscience Publishers, Inc., New York, 741 (1947).

[6] D.R.Bauer, *Progr.Org.Coat.*, 14, 193 (1986).

[7] G.M.Crews, *Fire retard.Chem.Assoc.*, Lancaster, 119(6), 39 (1992).

[8] R.J.Meier, B.Coussens, *J.Mol.Struct.*, 209, 303 (1990).

[9] J.F.Walker, *Formaldehyde, American Chemical Society Monograph No.159, 3rd ed.*,Reinhold, New York (Chapman & Hall, London), 1964.

[10] M.Gordon, A.Halliwell and T.Wilson, *J.Appl.Polym.Sci.*, 10, 1153 (1966).

[11] F.Käsbauer, D.Merkel, O.Wittmann, *Z.Anal.Chem.*, 281, 17 (1976).

[12] G.Christensen, *Progress in Org.Coat.*, 5, 255 (1977).

[13] J.C.Morath, J.T.Woods, *Anal.Chem.*, 30(8), 1437 (1958).

[14] I.Koeda, *J.Chem.Soc. (Japan) Pure Chem.Section*, 75, 571 (1954).

[15] D.Braun and V.Legradic, *Angew.Makromol.Chem.*, 25, 193 (1972).

[16] D.Braun and V.Legradic, *Angew.Makromol.Chem.*, 34, 35 (1973).

[17] D.Braun and V.Legradic, *Angew.Makromol.Chem.*, 35, 101 (1974).

[18] D.Braun, W.Pandjojo, *Fres.Z.Anal.Chem.*, 294, 375 (1979).

[19] B.Tomita, *J.Polym.Sci.,Polym.Chem.Ed.* , 15, 2347 (1977).

[20] J.R.Ebdon, B.J.Hunt, W.T.S.O'Rourke, *Br.Polym.J.*, 19, 197 (1987).

[21] M.Okano and Y.Ogata, *J.Am.Chem.Soc.*, 74, 5728 (1952).

[22] K.Sato, *Bull.Chem.Soc.Jpn.*, 41, 7 (1968)

[23] K.Sato and T.Naito, *Polym.J.*, 5, 144 (1973).

[24] A.Berge, *Adv.Org.Coat.Sci.Technol.Ser*, 1, 23 (1979).

[25] D.Braun and V.Legradic, *Angew.Makromol.Chem.*, 36, 41 (1974).

[26] I.H.Anderson, M.Cawley and W.Steedman, *Br.Polym.J.*, 1, 24 (1966).

[27] G.A.Alvarez, R.G.Jones, M.Gordon, *Proceedings of the European Conference on Macromolecules*, Lerici, Rome, 149 (1978).

[28] A.J.J.de Breet, W.Dankelman, W.G.B.Huysmans, J.de Wit, *Angew.Makromol.Chem.*, 62, 7 (1977).
[29] H.Schindlbauer, J.Anderer, *Angew.Makromol.Chem.*, 79, 157 (1979).
[30] M.Dawbarn, J.R.Ebdon, S.J.Hewitt, J.E.B.Hunt, I.E.Williams and A.R.Westwood, *Polymer*, 19, 1309 (1978).
[31] J.R.Ebdon, B.J.Hunt, W.T.S.O'Rourke and J.Parkin, *Brit.Polym.J.*, 19, 197 (1987).
[32] J.R.Ebdon, B.J.Hunt, W.T.S.O'Rourke and J.Parkin, *Brit.Polym.J.*, 20, 327 (1988).
[33] B.Tomita, H.Ono, *J.Polym.Sci.Polym.Chem.Ed.*, 17, 3205 (1979).
[34] T.Gebregiorgis, Ph.D.Thesis, University of Essex, 1982.
[35] R.Nastke, K.Dietrich and W.Teige, *Acta Polym.*, 30, 522 (1979).
[36] R.Nastke, K.Dietrich and W.Teige, *Acta Polym.*, 31, 329 (1980).
[37] R.Nastke,K.Dietrich and F.Pragst, *Fres.Z.Anal.Chem.*, 319, 252 (1984).
[38] R.Nastke,K.Dietrich,G.Reinisch,G.Rafler, *J.Macromol.Sci.- Chem.*, A23(5), 579 (1986).
[39] S.O'Rourke, Ph.D.Thesis, University of Lancaster, 1984.
[40] K.Sato and S.Ouchi, *Polym.J.*, 10(1), 1 (1978).
[41] K.Sato and Y.Abe, *Kobunshi Ronbunshu*, 32, 687 (1975).
[42] K.Sato, *Bull.Chem.Soc.Jpn.*, 40, 2963 (1967).
[43] K.Sato, Y.Abe, K.Sugawara, *J.Polym.Sci.*, 13, 263 (1975).
[44] K.Sato, T.Konakahara, M.Kawashima, *Macromol.Chem.*, 183, 875 (1982).
[45] A.Berge, S.Gudmudson, J.Ugelstad, *Eur.Polym.J.*, 5, 171 (1969).
[46] A.Berge, B.Kvaeven, J.Ugelstad, *Eur.Polym.J.*, 6, 981 (1970).
[47] M.Gordon, A.Halliwell and T.Wilson, Chemistry of Polymerization Processes Monograph No.20, Society of Chemical Industry, London (1966).
[48] J.Aldersley, M.Gordon, A.Halliwell and T.Wilson, *Polymer*, 9(7), 345 (1968).
[49] K.Sato, *Bull.Chem.Soc.Jpn*, 40, 2963 (1967).
[50] J.K.Dixon, N.T.Woodberry, G.W.Costa, *J.Am.Chem.Soc.*, 69, 599 (1947).
[51] S.K.Gupta, A.K.Gupta, A.K.Ghosh, A.Kumar, *Frontiers in Chemical Reaction Engineering*, L.K.Doraiswamy, R.A.Mashelkar, Eds., Wiley Eastern, New Delhi, India, 1984.
[52] S.K.Gupta, *J.Appl.Polym.Sci.*, 31, 2805 (1986).
[53] A.Kumar, R.Chandra, *Polym.Eng.Sci.*, 27(13), 925 (1987).
[54] A.Kumar, V.Katiyar, *Am.Chem.Soc.*, 23, 3729 (1990).
[55] A.Kumar, *J.Appl.Polym.Sci.*, 34, 1367 (1987).
[56] A.Kumar, *J.Appl.Polym.Sci.*, 34, 1383 (1987).

CHAPTER 2

CHARACTERIZATION OF MF RESINS IN THE EARLY STAGES OF CONDENSATION BY ^{13}C NMR

1 Introduction

For the quantitative analysis of MF resins a selective analytical technique is required that can differentiate between the various formaldehyde species. Wet analytical methods have been used for a long time in MF resin analysis. They are based on the quantification of formaldehyde released after hydrolysis and the liberation of formaldehyde depends on the chemical structure in which formaldehyde was previously incorporated. Free formaldehyde, formaldehyde bound in methylol groups, formaldehyde bound in ethers and the total formaldehyde can be determined in this way. Christensen et al. [1] has summarized the pros and cons of the different chemical methods. Polarographic methods for the analysis of MF resins were developed by Nastke et al. [2,3]. They showed that free formaldehyde, formaldehyde bound in methylol groups and methylene bridges can be determined by polarography. A chemical method for the determination of the oxidable formaldehyde was also proposed. The ether-formaldehyde which corresponds to the total of formaldehyde bound in methylene-ether bridges, oligoacetals and oligooxymethylenes can then be calculated from the difference between the oxidisable and the methylol-formaldehyde. In the past 20 years ^{13}C NMR has emerged as a powerful technique for studying MF resins in the initial stage of condensation [4-9]. In particular, Tomita et al. [8] confirmed that methylene-ether bridges could be distinguished from methylol groups by solvent change of DMSO for water.

In this chapter, the use of ^{13}C NMR for the analysis of melamine-formaldehyde reaction mixtures will be evaluated. Particular attention is paid to methylene-ether bridge formation. The formation of methylene-ether bridges will be demonstrated by a combined ^{1}H and ^{13}C NMR study.

2 *Benefit of H_2O as solvent for the ^{13}C NMR analysis of MF resins*

Figure II.1 shows the ^{13}C NMR spectra of a freeze-dried MF resin dissolved in DMSO-d_6 (a) and an aqueous MF resin solution (b), both prepared from F/M 1.8, pH 7.7 and cured for 1 hour at 90°C. The ^{13}C NMR spectra of MF resins all exhibit resonances in two main regions. At around 165 ppm a series of resonances arise from the azine carbons of the melamine units whilst between 40 and 90 ppm several resonances are present that were attributed to methylene carbons derived from formaldehyde. From the spectra in Fig. II.1 it can be seen that the resolution in the methylene carbon region is considerably better using water as solvent. The resonances in the ^{13}C NMR spectra of the MF resins were assigned according to Tomita et al. [8] and are summarized in Table II.1.

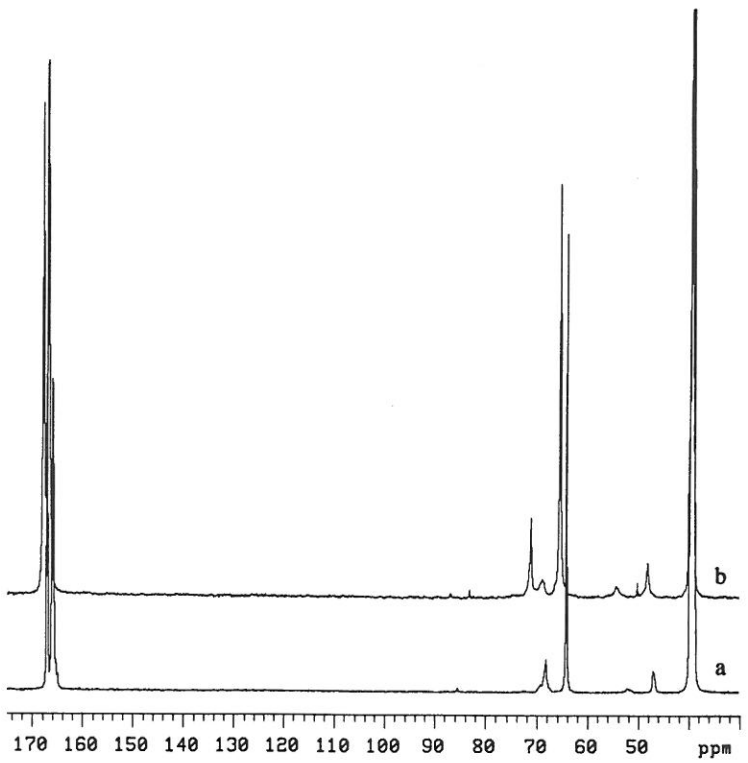

Figure II.1 ^{13}C NMR spectra of a freeze-dried MF resin in DMSO-d_6 (a) and an aqueous MF resin (b).

According to Tomita et al. the major advantage of the solvent change of DMSO for water is the separation of the carbon signals of methylene-ether bridges from those of methylol groups attached to tertiary nitrogens. The carbon signal at 69.7 ppm was assigned to methylene-ether bridges. However, the formation of methylene-ether bridges has not been demonstrated in a direct manner. In order to confirm the assignments of Tomita a method was developed to demonstrate the methylene-ether bridge formation. The features of this method will be given in the next section.

Table II.1 ^{13}C assignments of melamine formaldehyde resins according to Tomita et al. [8].

Name	Structure	δ(ppm)[1] DMSO-d_6	δ(ppm)[2] water
methylol group	-NH<u>C</u>H_2OH	64.8	65.5
	-NR'<u>C</u>H_2OH	69.8	71.6
methylene bridge	-NH<u>C</u>H_2NH-	47.3	47.9
	-NR'<u>C</u>H_2NH-	52.2	53.8
	-NR'<u>C</u>H_2NR'-		
methylene-ether bridge and hemiformal form of methylol group	-NH<u>C</u>H_2OCH_2NH-	69.8	69.7
	-NH<u>C</u>H_2OCH_2OH	69.8	69.7
	-NR'<u>C</u>H_2OCH_2NH-	73.0	75.0
	-NR'<u>C</u>H_2OCH_2OH	73.0	75.0
methylene glycol species	HO<u>C</u>H_2OH	82.1	83.0
	HO<u>C</u>H_2OCH_2OH	85.2	86.6
	H$(OCH_2)_n$O<u>C</u>H_2OCH_2OH	93.9	95.0
hemiformal form of methylol group	-NHCH_2O<u>C</u>H_2OH	86.2	87.1
	-NR'CH_2O<u>C</u>H_2OH	86.2	87.1

[1] Chemical shift was calculated by defining ^{13}C of DMSO-d_6 as 39.5 ppm.

[2] Chemical shift in water was calculated by defining ^{13}C external dioxane as 67.4 ppm.

R'= CH_2OH, CH_2- or CH_2O-

3 *Demonstration of methylene-ether bridge formation*

3.1 *Monitoring of the condensation reaction by ^{13}C NMR*

Figure II.2 (a and b) illustrates the methylene carbon region in the ^{13}C NMR spectra of the methylolmelamine mixture in DMSO-d_6 cured at 90°C for 0 and 11 hours, respectively. DMSO was used as solvent because it was revealed that the condensates formed in the latter stages remain soluble in DMSO and methylol-melamines only scarcely decompose in DMSO [10]. The resonances were assigned according to Tomita et al. [8]. The various structures in which formaldehyde is incorporated in MF-resins can be quantified by integrating the resonances in the region between 40 and 100 ppm. When assessing the intensity of the ^{13}C signals, care must be taken when integrating the $NH\underline{C}H_2NH$ signal because of the close proximity of the solvent DMSO resonance bands. The quantitative results of the functional group analysis are presented in Table II.2.

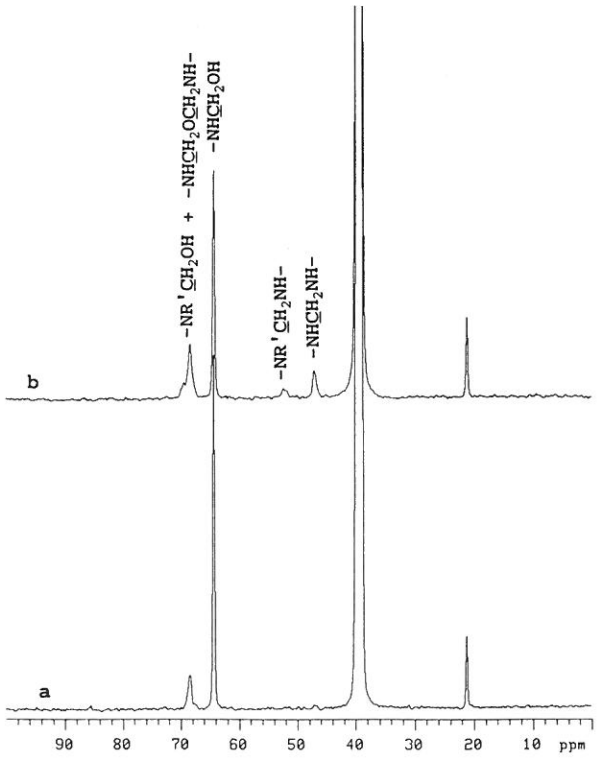

Figure II.2 ^{13}C NMR spectra from 0-100 ppm of the methylol-melamine mixture in DMSO-d_6 cured at 90°C for 0 (a) and 11 hrs. (b) respectively.

The total amount of methylene carbons was checked for all stages of the curing and it was found that it remained constant during cure for 11 hours at 90°C in DMSO and no liberation of formaldehyde could be detected. Curing for a longer time resulted in an apparent decrease of the total formaldehyde concentration. This is not unknown for ^{13}C liquid NMR on polymers and is generally due to extreme T_2 band broadening into the baseline due to restricted local molecular mobility. Within the methylene carbon region of the methylolmelamine mixture, a large signal from monomethylolated amino groups at 64 ppm and a smaller signal at 68.5 ppm were observed. It is possible that the methylolmelamine mixture already contains non-substituted methylene-ether linkages, as signals from this type of linkage overlap with signals from substituted methylol groups at 68.5 ppm. The spectrum shows no evidence for the presence of free formaldehyde as methylene glycol or polyoxymethylene oligomers (C-signals at 80-90 ppm). When the methylolmelamine mixture was heated at 90°C in DMSO-d_6 a decrease in the number of monomethylolated amino groups up to 40% was seen (Table II.2). Two new signals appeared in the spectra, i.e., the methylene bridge in which the two amino groups are monosubstituted at 47 ppm and the methylene bridge in which one of the two amino groups is disubstituted at 52 ppm, respectively (Figure II.2).

Table II.2 Quantitative data in mmole % derived from the ^1H and ^{13}C NMR spectra of the methylolmelamine mixture in DMSO-d6 as a function of cure time.

Cure time (hrs.)	0	2.5	3.5	7.5	11.0
H_2O	32.4	48.6	54.9	69.8	82.3
Azine $\underline{C}$	268.0	261.8	253.1	259.3	266.8
-NR'$\underline{C}H_2OH$ + -NH$\underline{C}H_2O$-	27.4	41.1	43.6	48.6	51.1
-NH$\underline{C}H_2OH$	137.1	114.7	106.0	91.0	82.3
-NH$\underline{C}H_2NH$-	-	7.5	8.7	12.5	21.2
-NR'$\underline{C}H_2NH$-	-	1.3	3.7	7.5	10.0
sum $\underline{C}H_2$'s	164.5	164.6	162.0	159.6	164.6

Note: R' = CH_2OH, CH_2N- or CH_2OCH_2-

The spectra also show an increase of the carbon signal at 68.5 ppm during cure. It is suggested that this increase is due to methylene-ether bridge formation derived from the condensation of pairs of methylol groups. Methylene-ether linkages, in which at least one of the two amino groups is disubstituted and which should appear at 73 ppm [8] were not observed.

Figure II.3 shows the changes in the azine carbon region of the methylol-melamine mixture with cure. The total concentration of azine carbons remains approximately constant during cure. Integration of the total azine carbon region gives a variation of about 5%. Several authors [3-5] reported that the distribution of methylolmelamines can be obtained from the precise analysis of the ring carbons. The ring carbons can essentially be classified into three sets of peaks, i.e., those bearing primary (167.7-166.7 ppm), secondary (166.7-165.4 ppm) and tertiary amino groups (165.4-164.4 ppm). Figure II.3 illustrates an increase in the number of azine carbons bearing secondary amino groups with cure relative to the number of azine carbons bearing primary amino groups.

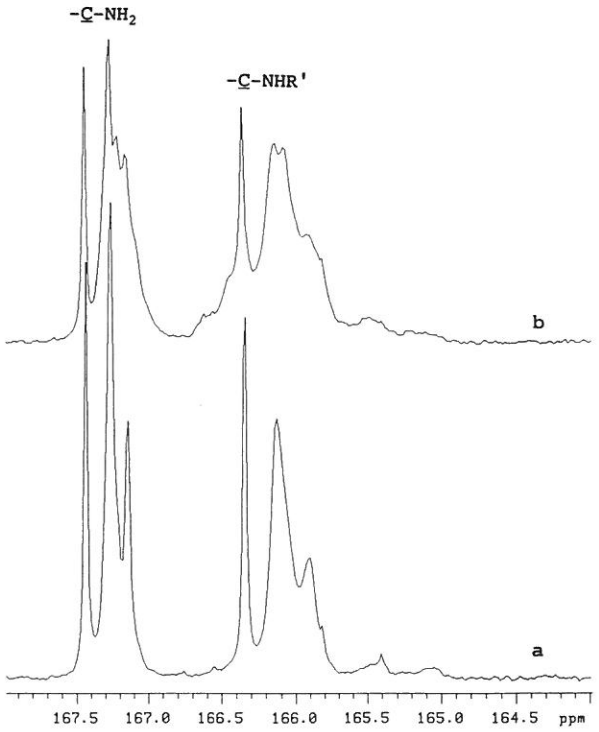

Figure II.3 Azine carbon region of the methylolmelamine mixture in DMSO-d_6 cured at 90°C for 0 (a) and 11 hrs. (b) respectively.

The condensation was further accompanied by the appearance of additional azine carbon peaks in the region of azine carbons bearing secondary amino groups. These new peaks were assigned to azine carbons bearing methylol substituted amino groups that have reacted to form non-substituted methylene and methylene-ether linkages.

3.2 Determination of water of condensation

Methylene and methylene-ether bridge formation are both accompanied by the elimination of water. The amount of water of condensation as a function of cure of the methylolmelamine mixture was determined by ^{1}H NMR on sealed NMR tubes, making use of toluene as internal standard. Figure II.4 (a and b) shows the ^{1}H NMR spectra of the methylolmelamine mixture cured at 90°C for 0 and 11 hours, respectively. The signal at 3.5 ppm arises from the protons of water. The water content was determined quantitatively by relating the area of this peak to that of the signal at 2.3 ppm due to the methyl protons of the toluene internal standard.

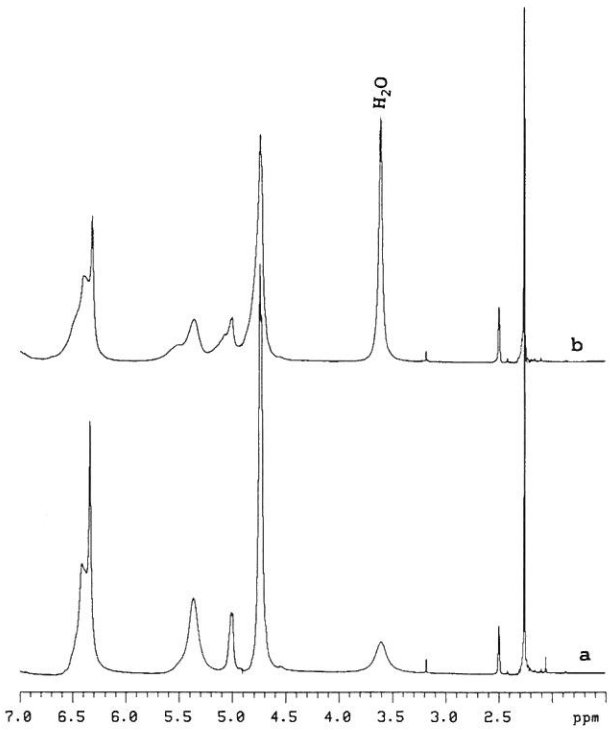

Figure II.4 ^{1}H NMR spectra of the methylolmelamine mixture in DMSO-d_6 cured at 90°C for 0 (a) and 11 hrs. (b) respectively.

The water contents presented in Table II.2, illustrate an increase in the amount of water with increasing time of cure. The amount of water from the condensation reactions was obtained after correcting for the water content of the original sample. The water contents obtained by ^1H NMR are in good agreement with those obtained by the low temperature Karl Fisher method. Figure II.5 shows the comparison of water contents obtained by both methods for some typical MF resins.

3.3 Discussion of methylene-ether bridge formation

In the following discussion the formation of methylene-ether bridges will be inferred in two ways. At first, they are calculated from the difference between the total amount of water of condensation and the amount of water liberated in the methylene bridge formation. Secondly, the number of monomethylolated amino groups coverted into methylene-ether bridges is calculated.

3.3.1 Relationship between the amount of water liberated and the number of bridges made

The condensation reaction can be followed quantitatively by the release of water during the formation of bridges, i.e., the formation of one mole of methylene bridges or methylene-ether bridges is accompanied by the elimination of one mole of water. The total amount of water liberated during several stages of the curing process is compared to the amount liberated by the methylene bridge formation in Table II.3. From the results in Table II.3 it can be concluded that the total amount of water generated cannot be exclusively attributed to the methylene bridge formation. The number of methylene-ether bridges can be calculated as the difference between the total amount of water of condensation and the amount of water liberated during methylene bridge formation (Table II.4).

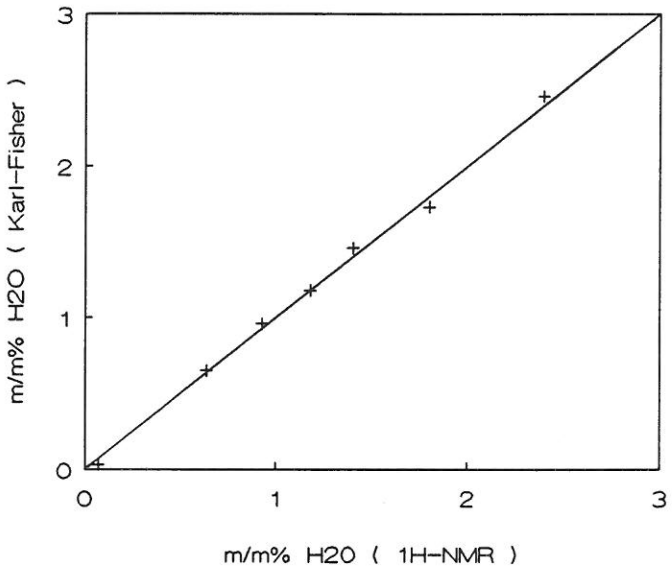

Figure II.5 Water contents obtained by the Karl Fisher titration method and by ^1H NMR of some typical MF resins.

Table II.3 Comparison of the total amount of water of condensation (mmole %) for several stages of the curing process with that liberated by the methylene bridge formation.

Cure time (hrs.)	Water of condensation	
	total	due to methylene bridge formation
2.5	16.2	8.8
3.5	22.5	12.4
7.5	37.4	20.0
11.0	49.9	31.2

3.3.2 *Relationship between the decrease in the number of monomethylolated amino groups and the increase in the number of bridges*

The quantitative results obtained from the ^{13}C NMR spectra are given in Table II.2. The monomethylolated amino groups can be consumed in several reactions. Eq.(1) describes the formation of a non-substituted methylene bridge. The total decrease in monomethylolated amino groups shown in Table II.2 cannot be exclusively explained by this reaction. The possible reactions, producing methylene bridges in which one of the two amino groups is disubstituted, are described in eq.(2) and eq.(3). It is assumed that the methylene bridges are substituted by a methylol group in the initial stages of reaction. This will be substantiated for aqueous MF resins in section 4.

$$\text{R-NHCH}_2\text{OH} + \text{R-NH2} \rightleftarrows \text{R-NH-CH}_2\text{-NH-R} + \text{H}_2\text{O} \qquad (1)$$

$$\text{R-NHCH}_2\text{OH} + \text{R-NHCH}_2\text{OH} \rightleftarrows \text{R-N(CH}_2\text{OH)-CH}_2\text{-NH-R} + \text{H}_2\text{O} \qquad (2)$$

$$\text{R-N(CH}_2\text{OH)}_2 + \text{R-NH}_2 \rightleftarrows \text{R-N(CH}_2\text{OH)-CH}_2\text{-NH-R} + \text{H}_2\text{O} \qquad (3)$$

Table II.2 shows that the total decrease of monomethylolated amino groups is still larger than those involved in the methylene bridge formation by considering either eq.(2) or eq.(3) for the substituted methylene bridge formation. This can be explained by the formation of non-substituted methylene-ether bridges of which the amount equals one half of the difference between the total decrease of monomethylolated amino groups and those involved in the methylene bridge formation. Good agreement with the results of the water of condensation determinations is achieved by assuming eq.(3) for the substituted methylene bridge formation (Table II.4). This is further supported by the changes in the azine carbon region with cure. Only eq.(3) beside eq.(1) can explain the observed increase of secondary amino groups bearing azine carbons as well as the decrease of azine carbons with primary amino groups.

Table II.4 Comparison of the amount (mmole %) of methylene-ethers determined from the number of monomethylolated amino groups involved in the condensation reaction (I) with that calculated from the water of condensation contents (II).

Cure time (hrs.)	I (mmole%)	II (mmole%)
2.5	7.5	7.4
3.5	11.2	10.1
7.5	16.8	17.4
11.0	16.6	18.7

3.4 Comparison with the aqueous MF resin

Based on the investigations dealt with in this section, we may conclude that both methylene and methylene-ether bridges are formed during condensation of this methylolmelamine mixture. One part of the aqueous methylolmelamine mixture that was freeze-dried to study the condensation reactions in DMSO-d_6, was cured for 1 hour at 90°C to verify the appearance of a distinct band at 69.7 ppm corresponding to methylene-ether bridges in water as solvent. The ^{13}C NMR spectrum of the aqueous MF resin solution (Fig.II.1b) clearly shows a distinct band at 69.7 ppm and this confirms the assignment of this band to methylene-ether bridges.

4 Review of the structural information of aqueous MF resins obtained by ^{13}C NMR

^{13}C NMR provides the most complete information about the structure of MF resins [8-11], more than is available from classical chemical analyses. In particular, methylene-ether bridges can be determined selectively. Furthermore it can differentiate between methylol groups attached to secondary and tertiary nitrogens and also between non-substituted and substituted methylene (ether) bridges. In this section the structural information obtainable by ^{13}C NMR will be reviewed.

Methylol groups

The number of monomethylolated aminogroups of an MF resin can be determined directly from the intensity of the carbon signal at 65.5 ppm.

The carbon signal at 71.6 ppm corresponds generally to the $NR'CH_2OH$ group. The substituent R' can either be a methylol group, a methylene- or a methylene-ether bridge. Figure II.6 illustrates the ^{13}C NMR spectra of an MF resin prepared from F/M 1.7 and pH 8 after methylolation (a) and after reaction for 90 min. at 95°C (b). With increasing time of condensation the appearance of a shoulder on the carbon signal at 71.6 ppm can be seen simultaneously with the substituted methylene bridges in the spectrum. This shoulder indicates the presence of methylol groups substituted on a methylene bridge that are shifted a little in chemical shift from the carbons of dimethylolated amino groups. It can be concluded that the substituted bridges for MF resins prepared from low F/M molar ratios are mainly substituted by a methylol group in the initial stage of the condensation as was observed from the appearance of that shoulder. In these cases, the number of dimethylolated amino groups can be calculated from the intensity of the carbon signal at 71.6 ppm after subtraction for the number of methylol groups substituted on the bridges.

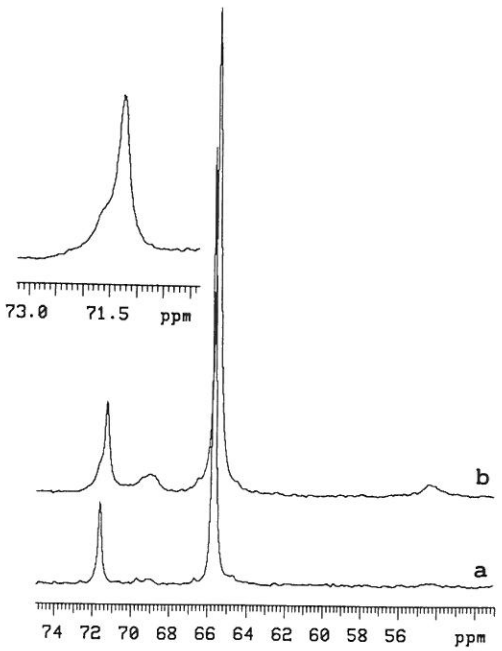

Figure II.6 ^{13}C NMR spectrum of an aqueous MF resin prepared from F/M 1.7 and pH 8 after methylolation (a) and after reaction for 90 min. at 95°C (b).

The number of methylol groups substituted on bridges can be obtained from the intensity of the substituted bridge carbons.

Methylene bridges

The amount of non-substituted methylene bridges and the methylene bridges in which one of the two aminogroups is disubstituted can be determined directly from the intensities of the carbon signals at 47.9 and 53.8 ppm, respectively.
The methylene bridges in which the two amino groups are disubstituted were considered to appear at 60 ppm based on the downfield shift of about 5 ppm when the nitrogen is substituted [9]. The substituent on the methylene bridge can either be a methylol group, a methylene or a methylene-ether bridge.

Methylene-ether bridges

It can be seen from the assignments in Table II.1 that the carbons of the hemiformal type of monosubstituted methylol ($NH\underline{C}H_2OCH_2OH$) may overlap with the carbons of the methylene-ether bridges, and those of disubstituted methylol ($NR'\underline{C}H_2OCH_2OH$) with the carbons of the substituted methylene-ether bridges. If these carbons correspond to the hemiformal type of methylol groups, the ^{13}C NMR spectrum should also show carbon resonances at 87 ppm corresponding to the dioxymethylene carbon of $NHCH_2O\underline{C}H_2OH$. The ^{13}C NMR spectrum of the MF resin (prepared from F/M 1.7 pH 10) in Figure II.7 shows a large signal at 69.7 ppm but no carbon resonances at 87 ppm, so the carbon signals at 69.7 ppm can be assigned exclusively to methylene-ether bridges.

The total number of methylene-ether bridges equals one half of the sum of the intensities of the carbon signals at 71.6 ppm and 75 ppm. The calculation of the amount of non-substituted and substituted methylene-ether bridges is more complex. In early stages of the condensation it can be assumed that for resins with low F/M ratios the substituted methylene-ether bridges are mainly substituted by a methylol group and that methylene-ether bridges in which both aminogroups are disubstituted are not present. In these cases the amount of non-substituted methylene-ether bridges equals one half of the difference between the intensities of the carbon signals at 71.6 and 75 ppm. The number of substituted methylene-ether bridges can be calculated directly from the intensity of the carbon signal at 75 ppm. In other cases, only the number of non-substituted and substituted methylene carbons involved in a methylene-ether bridge can be obtained from the ^{13}C NMR spectra.

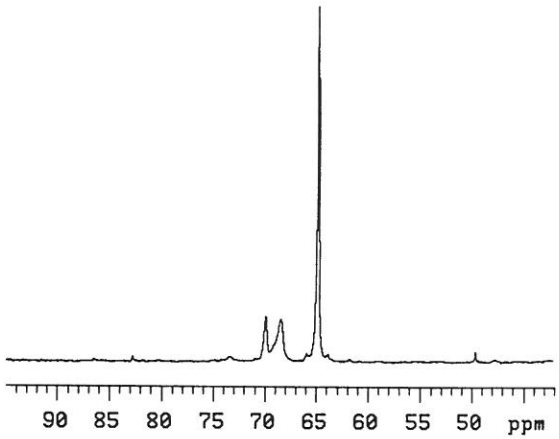

Figure II.7 ^{13}C NMR spectrum of an aqueous MF resin prepared from F/M 1.7 and pH 10 after methylolation.

Hemiformal types

Since the hemiformal form of a methylol group can exist in an aqueous MF resin [11], their analysis is of importance. The presence of hemiformal types can be observed from the carbon signals at 87.1 ppm.

Methylene glycol species

Formaldehyde is present as an equilibrium mixture of methylene glycol and low molecular weight polyoxymethylene glycols in aqueous solutions [11]. ^{13}C NMR provides differentiation between formaldehyde present as methylene glycol (at 83 ppm) and polyoxymethylene oligomers (at 86-95 ppm). From the sum of the intensities of the carbon signals of all methylene glycol species, the free formaldehyde content of an MF resin can be determined.

Triazine carbons

The azine carbon signals can essentially be classified into three sets of peaks, i.e., those bearing primary, secondary and tertiary amino groups. For MF resins prepared from low F/M molar ratios, the ^{13}C NMR spectra show some overlap of the azine carbons bearing a disubstituted aminogroup with those bearing a mono-

substituted aminogroup. Information about the mono- and disubstituted aminogroups can be better obtained from the methylene carbon region. The azine carbons bearing a primary aminogroup, on the contrary, are clearly resolved in the ^{13}C NMR spectra. As a result, the number of unsubstituted aminogroups in a MF resin can be determined from the relative number of azine carbons bearing an unsubstituted aminogroup.

F/M molar ratio

The formaldehyde content can be calculated from the sum of the intensities of the methylene carbons, all derived from formaldehyde, in the region between 40 and 95 ppm. The melamine content can be calculated from the intensity of all azine carbons which has to be divided by three because each melamine molecule contains three azine carbons. The formaldehyde to melamine molar ratios calculated in this way from the ^{13}C NMR spectra correspond within an error of ± 5% to those actually used in the preparation of MF resins.

5 *Conclusions*

The methylene-ether bridge formation during MF resin cure was demonstrated by a combination of ^{1}H and ^{13}C NMR spectroscopy. Good agreement was achieved between the number of methylene-ether bridges calculated from the amount of water of condensation liberated during condensation and that calculated from the number of monomethylolated amino groups consumed during condensation. This combined study has offered insight into the reaction pathways for the formation of methylol-substituted methylene bridges.

The structural details of MF resins obtainable by ^{13}C NMR can be summarized as follows. ^{13}C NMR can differentiate between methylol groups and methylene-ether bridge carbons attached to secondary and tertiary amino groups. The various methylene bridges, depending on their substitutent pattern, can be distinguished. The presence of hemiformal types of methylol groups can be observed. The free formaldehyde content and the number of unsubstituted amino groups can be determined. Finally, the F/M ratio of each MF resin can be calculated from the ^{13}C NMR spectrum.

6 *Experimental*

Sample Preparation

Methylolmelamine mixture

The methylolmelamine mixture was synthezised from melamine and 35.5% m/m aqueous formaldehyde in a F/M molar ratio of 1.8. The formalin was previously adjusted to pH 8.5 by the addition of 0.5 N aqueous sodium hydroxide solution. The methylolation was performed at 90°C for 35 minutes. After adjusting the pH to 7.7 by the addition of 0.5 N aqueous acetic acid, one part of the aqueous methylol-melamine mixture was cured for one hour at 90°C and the other part was cooled and then freeze-dried. The freeze-dried methylolmelamine mixture was the starting substance for the study of the condensation reaction in DMSO-d_6.

To a DMSO-d_6 solution containing 16.6% m/m of the freeze dried methylol-melamine mixture a known aliquot of toluene (2.4 % m/m) was added. Toluene was used as internal standard in the ^{1}H- and ^{13}C- NMR spectra. Definite amounts of this solution were weighed into NMR tubes. Each NMR tube was sealed-melted under vacuum to prevent any water from entering or disappearing from the NMR tube and then placed into an oven regulated at 90°C. After reaction times of 2.5, 3.5, 7.5, 11 and 16 hours, quantitative ^{1}H and ^{13}C NMR spectra were recorded.

Aqueous MF-resins

The aqueous melamine formaldehyde resins were synthesized from melamine, 32 % (m/m) aqueous formaldehyde and an appropriate amount of water resulting in a resin with a 50% solids content. The 32% formalin was previously adjusted to the desired pH by the addition of 1M aqueous sodium hydroxide solution. The resins were synthesized in a three necked vessel to allow insertion of pH and temperature probes and a stirrer. While stirring, the reaction mixture was heated at 95°C for a specific length of time.

Methods

NMR

^{1}H and ^{13}C NMR spectra were obtained on a Varian Unity-40 spectrometer. For the aqueous MF resins, DMSO-d6 was used as locking reagent. The NMR signal of DMSO was used as chemical shift reference in the ^{1}H (2.5 ppm) and ^{13}C (39.5 ppm) NMR spectra. The spin-lattice relaxation times (T_1) measured by the inversion recovery method are as follows: azine carbon $\underline{C}NH_2$ 1.86 ± 0.02 s, $\underline{C}NHR$ 2.47 ± 0.04 s, methylol carbon $NR\underline{C}H_2OH$ 0.20 ± 0.02 s, $NH\underline{C}H_2OH$ 0.18 ± 0.01 s, methylene bridge carbon $NH\underline{C}H_2NR$ 0.24 ± 0.13 s, $NH\underline{C}H_2NH$ 0.23 ± 0.04 s. The T_1's were 12.45 ± 0.10 s and 10.27 ± 0.15 s for the ortho and meta carbons of toluene, which were used as internal standard resonances for ^{13}C NMR. The quantitative carbon spectra of the methylolmelamine mixtures were obtained from 1000 scans and a preparation time of 70 seconds. For quantitative ^{13}C NMR measurements of the aqueous MF resins a preparation time of 12.5 seconds was used.

Karl Fisher titration

Small amounts of water were determined by the titration method introduced by Fisher [12] at -30°C. Bertz et al. [13] demonstrated that the water content in MF resins should be determined at -30°C to prevent interference (methylation) of the methylol groups during the analysis. To ensure a temperature of -30°C inside the titration flask, the titration vessel was connected with a cryostat (RCS lauda RC6). A model KF titrino 701 titrator (Metrohm) was used. The Karl Fisher reagent consists of iodine and sulfuric dioxide in pyridine-methanol solution. The endpoint was determined electrochemically by the dead stop technique using a microammeter which registrates a sudden increase of current when the platinum electrodes are depolarized. A polarisation voltage of 50 mV was used. The endpoint was taken at a residual current of 15μA.

7 *References*

[1] G.Christensen, *Progress in Org.Coat.*, 5, 255 (1977).

[2] R.Nastke, K.Dietrich, W.Teige, *Acta Polym.* 31, 329 (1980).

[3] R.Nastke, K.Dietrich, F.Pragst, *Fres.Z.Anal.Chem.*, 319, 252 (1984).

[4] G.A.Alvarez, R.G.Jones, M.Gordon, *Proceedings of the European Conference on Macromolecules*, Lerici, Rome, 149 (1978).

[5] M.Dawbarn, J.R.Ebdon, S.J.Hewitt, J.E.B.Hunt, I.E.Williams and A.R.Westwood, *Polymer*, 19, 1309 (1978).

[6] J.R.Ebdon, B.J.Hunt, W.T.S.O'Rourke and J.Parkin, *Brit.Polym.J.*, 20, 327 (1988).

[7] A.J.J. de Breet, W.Dankelman, W.G.B.Huysmans, J. de Wit, *Angew.Makromol.Chem.*, 62, 7 (1977).

[8] B.Tomita, H.Ono, *J.Polym.Sci.Polym.Chem.Ed.*, 17, 3205 (1979).

[9] H.Schindlbauer, J.Anderer, *Angew.Makromol.Chem.*, 79, 157 (1979).

[10] K.Sato, *Bull.Chem.Soc.Jpn.*, 40, 2963 (1967).

[11] J.F.Walker, *Formaldehyde, American Chemical Society Monograph No.159, 3rd ed.*,Reinhold, New York (Chapman & Hall, London), 1964.

[12] K.Fisher, *Angew.Chem.*, 48, 394 (1935).

[13] Bertz, Chr.Neundorf, G.Köhler, *Plaste und Kautschuk*, 10, 84 (1963).

A part of this Chapter is accepted for publication.

M.L.Scheepers, P.J.Adriaensens, J.M.Gelan, R.A.Carleer, D.J.Vanderzande, N.K.de Vries, P.M.Brandts, accepted for publication in *J.Polym.Sci. Polym.Chem.Ed.*

CHAPTER 3

STUDY OF THE CURE REACTIONS OF MF RESINS BY ^{13}C CP/MAS NMR SPECTROSCOPY

1 *Introduction*

As shown in the previous chapter, ^{13}C NMR is a very powerful technique for studying MF resins in the early stages of condensation. The final curing process has been studied only in part [1,2] despite the importance of structure in determining material properties and performance characteristics. Apart from the chemical complexity of MF resins, the insolubility of the cured resins preclude the use of liquid state analytical tools. A possible solution was found in high resolution solid state ^{13}C NMR consisting of a combination of cross polarization with high power ^{1}H decoupling and magic angle spinning [3,4]. A number of interesting CP/MAS NMR review articles concerning various areas of application, have been published by various authors [5-8].

With regard to ^{13}C CP/MAS NMR spectroscopy as an analytical tool, special attention is paid to the attainable resolution and quantifiability of the spectra. In this chapter the utility of ^{13}C CP/MAS NMR in the characterization of MF resins will be illustrated for two MF resins cured for various lengths of time. Besides the structural information, ^{13}C CP/MAS NMR can provide molecular mobility information from the analysis of $T_{1\rho}(^{1}H)$ values.

2 *Comparison to liquid state ^{13}C NMR*

Figure III.1 shows the ^{13}C CP/MAS NMR spectrum of an MF resin prepared from F/M of 1.7 at pH 7.6 and cured for 90 minutes at 100°C. Considerable broadening of the resonances arises as a result of the wider distribution of isotropic chemical shifts and of efficient spin-spin diffusion (short T_2-values) in the solid state. The assignment of chemical shifts is based on liquid state ^{13}C NMR results of soluble MF resins. The signals corresponding to azine carbons appear around 165 ppm without any fine structure. This is in contrast to the liquid state ^{13}C NMR [9-11] in

which the spectral region around 165 ppm does provide a good diagnostic tool for the determination of various azine carbon environments. The methylene carbon signals are however more revealing. Figure III.1 clearly shows four different methylene signals grouped into two sets of peaks. The former group (40-60 ppm) was attributed to the methylene carbons in non-substituted methylene bridges at 49 ppm and methylene bridges in which one of the two amino groups is disubstituted at 55 ppm. The 60-80 ppm region contains the monomethylolated aminogroups at 66 ppm and the carbons within the methylene-ether bridges giving rise to signals lying very close to those from methylol groups attached to tertiary nitrogens at 72 ppm.

In order to obtain the relative distribution of $N\text{-}CH_2\text{-}N$ and $N\text{-}CH_2\text{-}O$ structures it was necessary to resolve the overlapping methylene peaks in the ^{13}C CP/MAS spectrum. Based on the ^{13}C liquid NMR information the methylene region was deconvoluted into four resonances using the estimated band width, chemical shift, intensity and Lorentz fraction as starting parameters. It was found that 42% of the formaldehyde has been incorporated as methylene bridges and 58% as methylol groups and methylene-ether bridges.

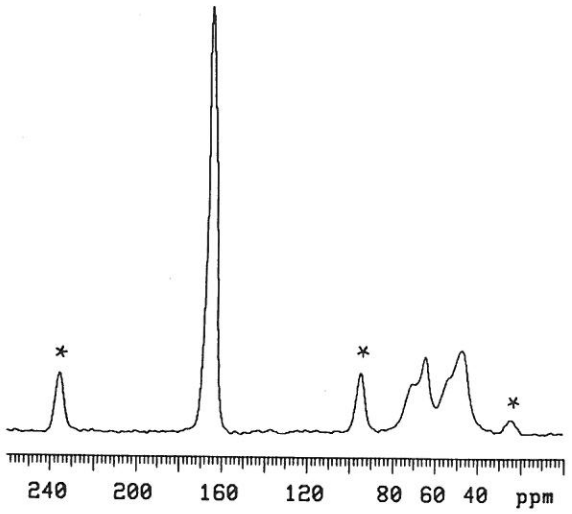

Figure III.1 *^{13}C CP/MAS NMR spectrum of an MF resin (F/M 1.7 pH 7.6 cured for 90 min. at 100°C) obtained with a contact time of 1 ms. Spinning sidebands are indicated by asterisks.*

3 *Quantifiability of the spectra*

In the conventional CP process under Hartman-Hahn conditions the ^1H and ^{13}C spin systems are spin locked in their rotating frames and are thermally in contact with each other, allowing exchange of energy. Since magnetization is transferred from protons to carbons, quantitative carbon measurements using a single contact time require that the polarization efficiency is the same for each kind of carbon. Since the magnetization transfer rate between protons and carbons is dependent on the separation distance, the molecular mobility and the carbon multiplicity quantitative conditions using a single contact time are almost never reached.
According to the theory of the CP process [12,13], the ^{13}C magnetization M(t), as a function of the contact time, can be described by eq.1.

$$M(t) = M_0/\lambda \, (1 - e^{-\lambda CT/T_c}) \, e^{-CT/T_{1\rho}(^1H)} \qquad (1)$$

$$\text{with } \lambda = 1 + T_c/T_{1\rho}(^{13}C) - T_c/T_{1\rho}(^1H)$$

where M_0 is the quantitative ^{13}C equilibrium magnetization. T_c is the time constant for the energy transfer between ^1H and ^{13}C spin systems and $T_{1\rho}(^1H)$ and $T_{1\rho}(^{13}C)$ are the spin-lattice relaxation times in their rotating frames. If T_c is much shorter than $T_{1\rho}(^{13}C)$ and $T_{1\rho}(^1H)$ and $\lambda \sim 1$ equation (1) reduces to

$$M(t) = M_0 \, (1 - e^{-CT/T_c}) \, e^{-CT/T_{1\rho}(^1H)} \qquad (2)$$

For long contact times ($CT >> T_c$) equation (2) further reduces to

$$M(t) = M_0 \, e^{-CT/T_{1\rho}(^1H)} \qquad (3)$$

Figure III.2 shows a semilogaritmic plot of the peak areas as a function of the contact time (CT) for three regions in a MF resin (F/M 1.7 pH 7.6 cured for 34 min. at 100°C) the azine carbon region, the region of the methylol groups and methylene-ether bridges and the region of methylene bridges. The corresponding spinning sidebands were included in the calculations of the peak areas of the azine carbon signals.

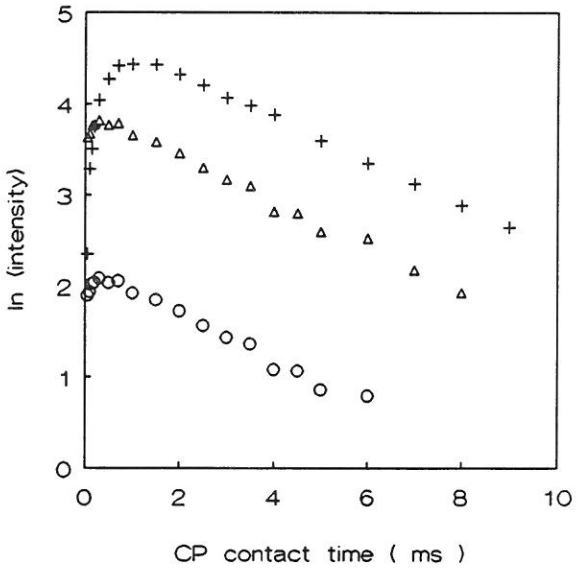

Figure III.2 CP process for three carbon regions of a MF resin (F/M 1.7 pH 7.6 cured for 34 min. at 100°C): azine carbons (+), methylene-ether and methylol carbons (▲) and methylene bridge carbons (o).

The proton $T_{1\rho}$ values were obtained by analyzing the decay of the carbon magnetization for long contact times in a cross polarization experiment. The magnetization transfer rate T_c can be determined by a non linear least square fit to eq.(2). $T_{1\rho}(^{13}C)$ was measured in a separate experiment. The $T_{1\rho}(^{13}C)$ pulse sequence can be found in Ref. [12]. The values for T_c, $T_{1\rho}(^{13}C)$ and $T_{1\rho}(^{1}H)$ are listed in Table III.1 and confirm the simplification of eq (1). It is noticed that quaternary C nuclei without ^{1}H nuclei within bonding distance cross-polarize more slowly than methylene C nuclei. Within experimental error the $T_{1\rho}(^{1}H)$ values of the various carbon regions are equal, suggesting efficient spin diffusion among the chemically different constituents, resulting in a single mean value for $T_{1\rho}(^{1}H)$ for all carbon types.

The quantitative M_0 value is determined by extrapolation of the straight line in the plot of the logarithmic intensities versus long contact times ($CT>>T_c$) to CT=0. From Table III.1 it can further be concluded that ratios of various methylene structures can be determined quantitatively in a single CT-experiment because both $T_{1\rho}(^{1}H)$ and T_c are identical for all methylene carbons.

Table III.1 Time constants T_c, $T_{1\rho}(^1H)$ and $T_{1\rho}(^{13}C)$ for an MF resin (F/M 1.7 pH 7.6 34 min. at 100°C).

carbon region	T_c (ms)	$T_{1\rho}(^{13}C)$ (ms)	$T_{1\rho}(^1H)$ (ms)
Azine carbons	0.373	2.439	3.843
Methylol groups methylene-ether bridges	0.024	1.310	3.624
Methylene bridges	0.020	1.630	3.620

Moreover, a fully relaxed liquid-like ^{13}C spectrum, where the intensity of each resonance line exactly reflects the concentration of the corresponding ^{13}C nucleus was obtained for the resin prepared from F/M 1.7 pH 7.6, cured for 34 min. at 100°C. A series of spectra acquired with different delay times under high power decoupling and magic angle spinning showed that the methylene carbons are fully relaxed when a delay of 360 s between successive acquisitions is used. In the methylene carbon region the fully relaxed spectrum is quite similar as the ^{13}C CP/MAS NMR spectrum shown in Fig.III.3. These results show that for cured MF resins the cross polarization technique can be applied with considerable saving in spectrometer time. Furthermore, the relative distribution of the methylene carbons in MF resins can be determined quantitatively from a single contact time for which the signal/noise ratio is maximal. Finally, formaldehyde eventually escaping from the mould during cure at higher temperatures can be measured from the ratio of $-CH_2-$ to azine carbons, which can be determined from a contact time study.

4 *Effect of curing on $T_{1\rho}(^1H)$*

From the variable contact time experiments changes in the $T_{1\rho}(^1H)$ values as a function of degree of cure were noticed. Therefore the $T_{1\rho}(^1H)$ values were measured more accurately with a more specific pulse sequence [12]. The time constants were derived from semilog plots of intensity versus time.

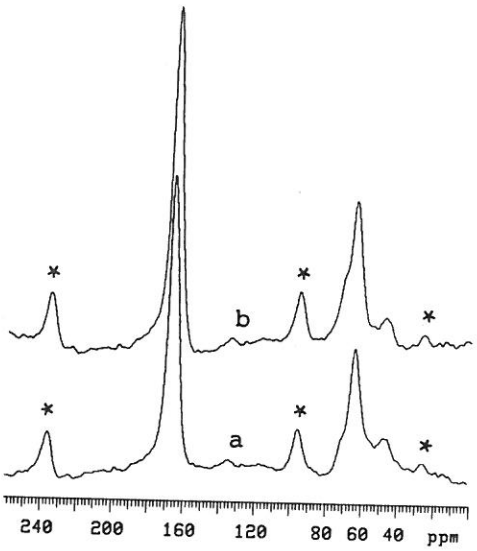

Figure III.3 Inverse gated high power decoupling spectrum (a) and ^{13}C CP/MAS NMR spectrum (b), obtained with a contact time of 1 ms of a MF resin (F/M 1.7 pH 7.6 cured for 34 min. at 100°C). Spinning sidebands are indicated by asterisks.

The $T_{1\rho}(^1H)$ values as a function of degree of cure for MF resins prepared from F/M 1.7 pH 7.6 are shown in Figure III.4. It should be noticed that these values represent an averaged value of the relaxation behavior of the ensemble of protons because the strong dipolar couplings give rise to efficient spin diffusion. So further interpretation in terms of various types of motions in the polymer is not possible. The changes in $T_{1\rho}(^1H)$ as a function of cure clearly demonstrate the sensitivity to changes in the averaged network mobility, so providing a criterion to determine the relative degree of cure. A decrease in $T_{1\rho}(^1H)$ with increasing extent of cure suggests that the MF networks are still relative mobile because the average correlation time of motion is situated in the so called extreme narrowing region, before the minimum point of the $T_{1\rho}(^1H)$ curve [11].

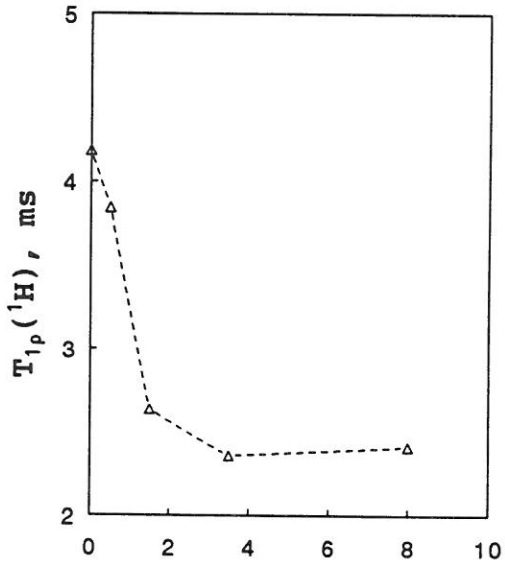

Figure III.4 ^1H spin-lattice relaxation times ($T_{1\rho}{}^1H$) in the rotating frame as a function of cure at 100°C for an MF resin (F/M 1.7 pH 7.6).

5 *Study of the cure reactions of two MF resins by ^{13}C CP/MAS NMR*

Two mixtures of methylolmelamines, prepared from F/M 1.7 pH 7.6 and F/M 6 pH 9 respectively, were cured at 100°C for various lengths of time. The ^{13}C CP/MAS NMR spectra of the MF resins with increasing time of cure are shown in Figure III.5 and 6 for the MF 1.7 and MF 6.0 resin, respectively. The spectra presented in Figure III.5 illustrate an increase in the concentration of N-CH_2-N structures relative to the concentration of N-CH_2-O structures during cure of the MF 1.7 resin. From the spectra in Figure III.6 it can be seen that only a few methylene bridges are formed during cure of the MF 6.O resin. Furthermore an increase in the number of substituted methylene and methylene-ether bridges is observed for the MF 6.0 resin, as indicated by the increased intensities at 55 pm and 77 ppm, respectively. The molar percentages of the various methylene carbons relative to the total formaldehyde content are listed in Tables III.2 and 3 for the MF 1.7 and MF 6.0 resin, respectively.

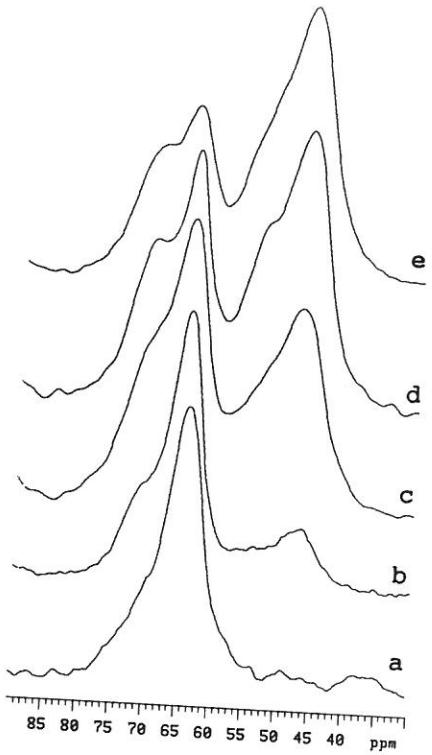

Figure III.5 ^{13}C *CP/MAS NMR spectra of a MF resin prepared from F/M 1.7, pH 7.6 cured for several lengths of time at 100°C: 0 hrs.(a), 0.5 hrs.(b), 1.5 hrs.(c), 3.5 hrs.(d) and 8 hrs.(e). All spectra were obtained with a contact time of 1 ms.*

Table III.2 Molar amounts of various methylene carbons relative to the total formaldehyde content from ^{13}C *CP/MAS NMR measurements for an MF resin (F/M 1.7, pH 7.6).*

Cure time (hrs.)	NR'CH_2OH	$NHCH_2OH$	NR'CH_2NH	$NHCH_2NH$	$NHCH_2OCH_2NH$
Liquid NMR					
0	16	80			
0.5	22	56	5	4	17
Solid NMR					
1.5		58		42	
3.5		43		57	
8		35		65	

R' = CH_2OH, CH_2N- or CH_2OCH_2-

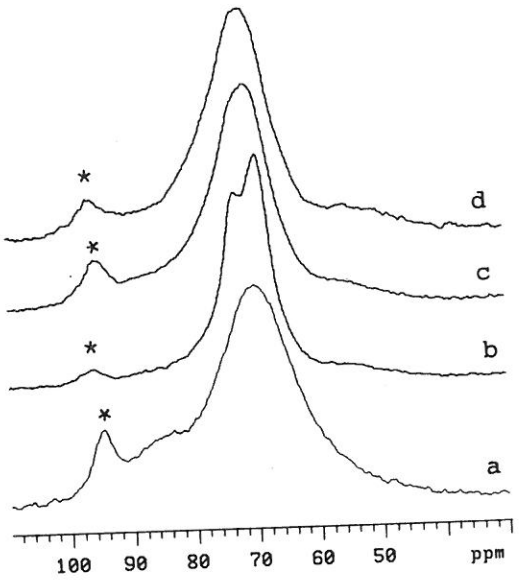

Figure III.6 Effect of cure time at 100°C on the ^{13}C CP/MAS NMR spectrum of MF resin prepared from F/M 6 and pH 9: 0 hrs.(a), 5 hrs.(b), 2 days (c) and 2 weeks (d). All spectra were obtained with a contact time of 1 ms. Spinning sidebands are indicated by asterisks.

Table III.3 Molar amounts of various methylene carbons relative to the total formaldehyde content from ^{13}C CP/MAS NMR measurements, for an MF resin (F/M 6.0, pH 9.0).

Cure time	$HOCH_2OH$ +oligomers	$NR'CH_2O$-	$NHCH_2O$- $NRCH_2OH$	$NHCH_2OH$	$NR'CH_2NH$
Liquid NMR					
0 hrs	26		62	12	
5.0 hrs	6		89	5	
Solid NMR					
7.5 hrs		96			4
2 days		96			4
2 Weeks		96			4

R' = CH_2OH, CH_2N- or CH_2OCH_2-

The integrated areas of the final MF resins, show that for the MF 1.7 resin approximately 65 mol % of the formaldehyde has been incorporated as methylene bridges and 35 mol % as methylol groups and methylene-ether bridges, whilst for the MF 6.0 resin the proportions are 4 mol % and 96 mol % respectively.
In summary it can be stated that the fraction of methylene bridges in cured MF resins can be determined by ^{13}C CP/MAS NMR. The major drawback is the overlap of the methylene-ether carbons with those of the residual methylol groups.

6 *Conclusions*

The results of this ^{13}C CP/MAS NMR study show that for cured MF resins the ^{13}C NMR cross polarization technique yields quantitative data. It was found that measurements carried out with a single CP contact time yield quantitative peak areas for the various methylene structures resulting in a considerable saving in spectrometer time.

The ^{13}C CP/MAS NMR technique provides a convenient, direct way for monitoring methylene bridge formation during cure of MF resins. By peak deconvolution one can further distinguish between non-substituted and substituted methylene bridges. Information about methylene-ether bridge formation however, cannot be obtained from ^{13}C CP/MAS NMR spectra because this resonance overlaps with the signals of the residual methylol groups.

Changes in the average mobility of the MF resin with cure were observed in the $T_{1\rho}(^1H)$ measurements offering a criterion to determine the relative degree of cure of a MF resin.

7 *Experimental*

MF resins

Two mixtures of methylolmelamines, prepared from F/M 1.7; pH 7.6 and F/M 6.0; pH 9.0 , respectively were cured for various times at 100°C. The MF resins were prepared according to the standard procedure, as described in chapter 2. The liquid samples (before the gelpoint) were freeze-dried to produce solid samples suitable for ^{13}C CP/MAS NMR studies. Since these MF resins were still soluble in DMSO-d6, they were analyzed as well by ^{13}C liquid as by ^{13}C CP/MAS NMR. Further curing leads to a viscous, hydrophobic resin which separates from the upper water layer. The cured resins were ground to powder and subsequently examined by ^{13}C solid state NMR.

NMR

^{13}C CP/MAS NMR spectra were recorded at room temperature on a Varian XL-200 spectrometer. Samples were run as powders in spinners of Si_4N_3 or zirconiumoxide with an internal volume of 300 µl. The aromatic signal of hexa-methylbenzene was used to adjust the Hartmann-Hahn settings and the magic angle. Typical spectral conditions were: resonance frequency 50 MHz, spectral width 20 000 Hz, 90° pulse width of 7 µs and a preparation delay of 2.0 s. Most of the spectra were recorded with a single contact time of 1 ms, except for some variable contact time experiments as will be described in the following sections. The spinning rate was set to 3.5 kHz resulting in methylene peaks free of aromatic carbon spinning sidebands. The spectra were externally referenced to hexamethylbenzene (aromatic carbon = 132.1 ppm). The inverse gated high power decoupling spectra (liquid-like spectra) were obtained by employing a 90° carbon pulse followed by acquisition under high-power decoupling and a 360 s delay between repetitive acquisitions. Spectral deconvolution has been performed on the overlapping bands in the methylene carbon region by standard Varian software. Best fits were obtained by describing the bandshape with a Lorentz function. The distribution of N-CH_2-N and N-CH_2-O structures can be determined with a standard deviation of 2%.

8 *References*

[1] S.O'Rourke, Ph.D.Thesis, University of Lancaster, 1984.

[2] J.R. Ebdon, B.J. Hunt, W.T.S. O'Rourke, J. Parkin, *Brit.Polym.J.*, 20, 327 (1988).

[3] A.Pines, M.G.Gibby, J.S.Waugh, *J.Chem.Phys.*, 59, 569 (1973).

[4] J.Schaefer, E.O.Stejskal, *J.Am.Chem.Soc.*, 98, 1031 (1976).

[5] R. Voelkel, *Angew.Chem.Int.Ed.Engl.*, 1988,27, 1468 (1988).

[6] J.R. Havens, J.L. Koenig, *Applied Spectr.*, 37(3), 226 (1983).

[7] D.R.G.Williams, P.E.M.Allen, G.P.Simon, *Materials Forum*, 13, 108 (1989).

[8] J.Schaefer, E.O.Stejskal, R.Buchdahl, *Macromolecules*, 10(2), 384 (1977).

[9] G.A.Alvarez, R.G.Jones, M.Gordon, *Proceedings of the European Conference on Macromolecules*, Lerici,Rome 149 (1978).

[10] M.Dawbarn, J.R.Ebdon,S.J.Hewitt, J.E.B.Hunt, I.E. Williams, A.R.Westwood, *Polymer*, 19, 1309 (1978).

[11] J.R.Ebdon, B.J.Hunt, W.T.S.O'Rourke, *Br.Polym.J.*, 19, 197 (1987).

[12] M.Mehring, 'Principles of High Resolution NMR in solids', Springer-Verlag, New York, USA (1983).

[13] R.A.Komoroski (Ed),'High Resolution NMR spectroscopy of Synthetic Polymers in Bulk', VCH, Deerfield Beach, 1986.

CHAPTER 4

INVESTIGATION OF MELAMINE-FORMALDEHYDE RESIN CURE BY FT-RAMAN SPECTROSCOPY

1 Introduction

From the ^{13}C CP/MAS NMR spectra, the desired level of structural detail was not achieved because of the overlap of the methylene-ether bridges with the residual methylol groups. There is scope for methods that provide a clear differentiation among the most important structural units of cured MF resins. Ebdon et al. [1] have explored the utility of ^{15}N CP/MAS NMR in the characterization of MF resins. This study has revealed that the relative proportions of methylol groups, methylene- and methylene-ether bridges can be obtained more rapidly from ^{13}C NMR spectra. FT-IR spectroscopy has been shown to have only limited capabilities in this regard [2-4]. Due to the high number of slightly different structures in the MF-resins the absorption bands are very broad and overlapping.

Hill et al. [5] have used FT-Raman spectroscopy to analyse the structures of urea-formaldehyde (UF) resins. The Raman spectra of several UF model compounds indicate that the methylene bending region (1400-1500 cm^{-1}) provides a clear separation between N-CH_2-O, indicative of methylol groups and methylene ether linkages, and N-CH_2-N, indicative of methylene linkages. They have also demonstrated that relative changes can be observed in the concentration of N-CH_2-N and N-CH_2-O moieties during the cure of UF-resins. The biggest advantage of Raman spectroscopy is the ease and versatility of sampling. Furthermore solid MF resins can be studied on a micron-scale or in situ during curing.

Therefore we decided to explore the use of Raman spectroscopy both qualitatively and quantitatively for the characterisation of MF resins. To our knowledge, there is no information in the literature concerning band assignments and interpretations of the changes in the Raman spectra of MF-resins during cure. In the first section of this chapter the bands in the Raman spectra of MF-adducts and resins are assigned based on a combination of literature band assignments on UF resins and a study of the Raman spectra of relevant model compounds and well-characterized MF-adducts and resins (HPLC,^{13}C NMR). The second section deals with the

quantification of the bands in the Raman spectra of MF-resins. In the third section, the changes in the Raman spectra during cure of the MF-resins are studied, making use of the results presented in previous sections. The determination of the free melamine content in MF resins by FT-Raman spectroscopy will be shown in the last section.

2 *Assignments of Raman bands in the spectra of MF-adducts and resins*

Figure IV.1 presents the FT-Raman spectra for 5 of the model compounds studied. Spectra of MF-adducts with varying F/M ratio are shown in Figure IV.2. Figure IV.3 shows the FT-Raman spectra of three MF resins with an increasing content of methylene-ether bridges. In Figure IV.4 FT-Raman spectra are shown of two MF-resins (F/M 1.7 and 6, pH 7.6 and 9.0, respectively) after methylolation (Figure 4b and d) and after curing at 100°C (Figure 4a and c). From Figure IV.4 it is obvious that several changes occur in the spectra during cure. However, in order to elucidate the structure of these resins, detailed assignment of the Raman bands is necessary. The spectral regions of interest, i.e., those changing with methylolation and curing will be dealt with separately.

3500-3100 cm^{-1} region

For melamine, a strong band is observed at 3127 cm^{-1} with a weaker additional feature near 3320 cm^{-1} and two weaker bands at 3417 cm^{-1} and 3467 cm^{-1} (Figure IV.1a). The former two bands correspond to the N-H stretching of interacting NH_2 groups while the latter two originate from free NH_2 groups [6]. The Raman spectra of mixtures of methylolmelamines prepared from low F/M ratio's show a broad band from 3050-3350 cm^{-1}, while the intensity of this band has strongly decreased for the methylolmelamine mixtures prepared from higher F/M ratios. Therefore, this band is assigned to secondary amines.

3100-2800 cm^{-1} region

In this region the bands are associated with C-H stretchings [6]. The Raman spectrum of formalin shows two intense bands at 2990 and 2930 cm^{-1} and two weaker bands at 2849 and 2804 cm^{-1} (Figure IV.1b). The mixtures of methylol-melamines possess three bands in this region at 3000 cm^{-1}, 2966-2977 cm^{-1} and at

2896-2909 cm^{-1} (Figure IV.2). The 2966-2977 cm^{-1} band is relatively strong in all cases. In infrared on UF-resins, this band is assigned to the symmetric CH stretching modes of ether, alcohol and N-CH_2-N groups [7]. The mixtures of methylol-melamines prepared with higher F/M ratio's show a distinct band at 3015 cm^{-1}.

It seems unlikely that this region will be useful for identification of the various types of methylenes in the MF-resins because of strong overlap of bands. However, because formaldehyde is the only source of C-H units in the MF-system, the C-H region might be useful for quantification of the formaldehyde content. It might be possible to determine the total amount of formaldehyde incorporated in several structural units from the C-H stretch region.

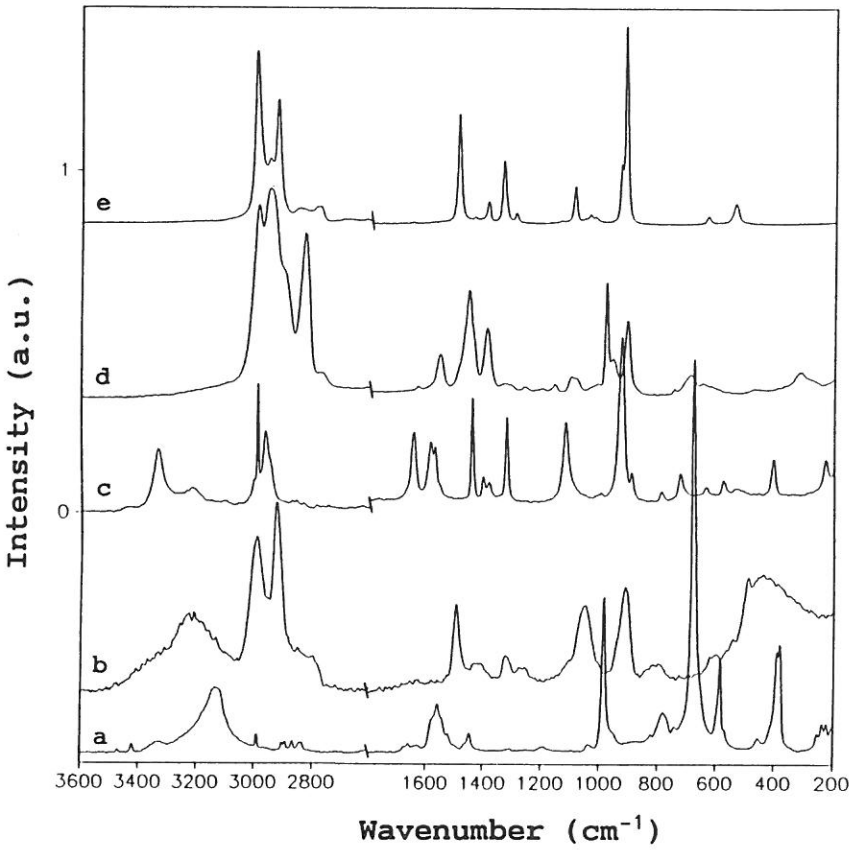

Figure IV.1 FT-Raman spectra of some model compounds: melamine (a), formalin (b), methylenediurea (c), hexamethoxymethylmelamine (d), paraformaldehyde (e).

1590-1500 cm^{-1} region

In the Raman spectrum of melamine a band extending from 1500-1590 cm^{-1} is observed (Fig.IV.1a). This range shows a series of frequencies and are attributed to NH_2 bending modes [6]. The Raman intensity of these modes decreases significant upon methylolation as can be observed from the Raman spectra of the methylol-melamine mixtures with various F/M ratio's (Fig.IV.2).

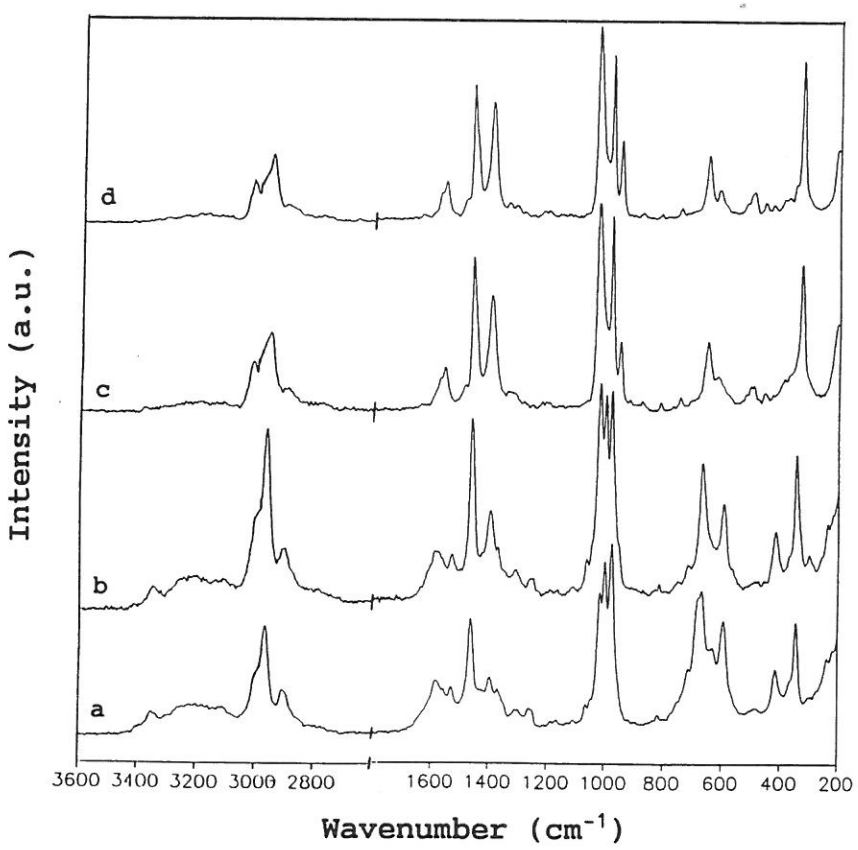

Figure IV.2 FT-Raman spectra from 500-3600 cm^{-1} of MF-adducts with different F/M ratio's: 2.1 (a), 3.2 (b), 5.5 (c) and 5.7 (d).

1500-1430 cm^{-1} region

This region has been assigned by Hill et al. to CH_2 bending in UF-resins [5]. The Raman spectra of several UF model compounds, studied by Hill et al., illustrated that this region provides a clear separation between N-CH_2-O groups at 1450 cm^{-1} and N-CH_2-N groups at 1435 cm^{-1}. In the present study, the Raman spectra of MF model compounds and well characterized MF-adducts and resins show that three bands can be distinguished in this region. The band at 1480-1490 cm^{-1} occurs in the spectra of paraformaldehyde and formalin (Figure IV.2e and 2b),i.e., in compounds containing the -O-CH_2-O- moiety. For compounds possessing the -NCH_2OH, -NCH_2OCH_3 and -NCH_2OCH_2N-units, i.e., mixtures of methylolmelamines (Figure IV.2) and hexamethoxymethylmelamine (Figure IV.1c), a strong band at 1450-1460 cm^{-1} is observed. The Raman spectra of methylene-diurea (Figure IV.1b) and cured MF resins (Figure IV.4a) show a distinct band at 1430-1440 cm^{-1}. The ^{13}C CP/MAS NMR spectrum of this MF-resin shows the presence of a relatively high amount of methylene linkages (Table III.2). Therefore, we assign this band to methylene linkages in MF-resins in line with the assignment for UF-resins.

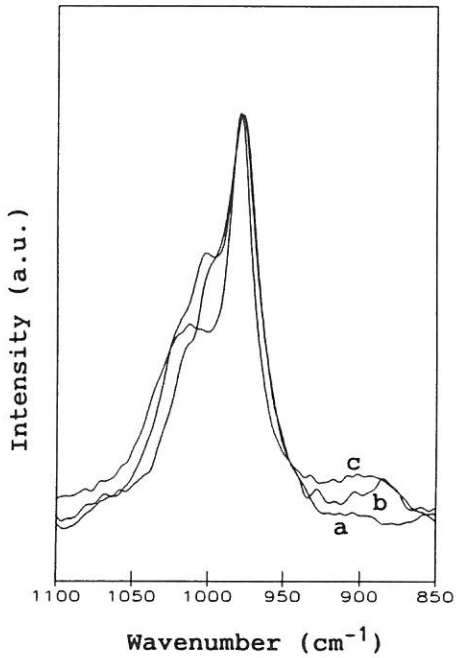

Figure IV.3 FT-Raman spectra from 850-1100 cm^{-1} of MF resins with various numbers of methylene-ether bridges: 0.02 (a), 0.21 (b) and 0.28 (c), calculated from the ^{13}C liquid NMR spectra.

The model compound spectra indicate that this spectral region provides differentiation among O-CH_2-O at 1490 cm^{-1}, N-CH_2-O at 1450-1460 cm^{-1} and N-CH_2-N at 1435 cm^{-1}. Melamine itself shows a band at 1443 cm^{-1}, that is attributed to a ring breathing mode [7].

1400-1360 cm^{-1} region

In the Raman spectra of methylolmelamine mixtures (Fig.IV.2) the band at 1390 cm^{-1} becomes more intens with a higher degree of methylolation. This band is assigned to a CH_2 motion in the methylol group.

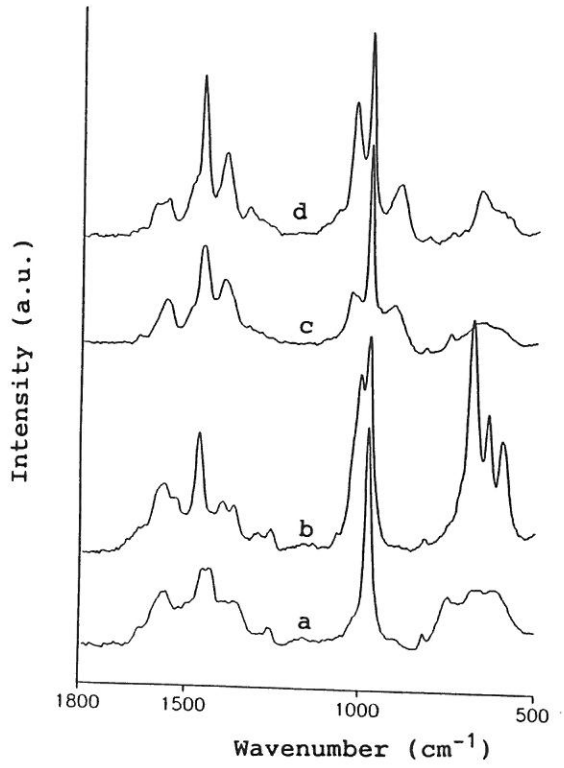

Figure IV.4 FT-Raman spectra from 500-1800 cm^{-1} of MF resins with different F/M ratios 1.7 and 6.0 respectively, after methylolation (b and d) and after curing at 100°C (a and c).

1030-950 cm^{-1} region

All spectra of melamine containing compounds show an intense band at 975 cm^{-1}. This characteristic band in the Raman spectra of trisubstituted triazines is attributed to the ring breathing vibration of the triazine ring [6].

The mixtures of methylolmelamines with low F/M ratio (Figure IV.2) show intense bands at 999 and 1015-1020 cm^{-1}. For higher F/M ratios, the latter band shifts to 1030 cm^{-1}. HPLC results in Table IV.2 demonstrate that the MF-adducts with low F/M ratio (sample 1-3) contain mainly mono-methylolated amino groups. In the MF-adducts with relatively high F/M ratio (sample 4,5) mainly di-methylolated amino groups are present. The spectra in Figure IV.4 show a significant decrease of these bands during cure. Although a definite assignment of these bands is still not possible, we assign these bands to vibrations of the methylol groups because these groups disappear with increasing degree of bridge formation, the 999 and 1015-1020 cm^{-1} for mono- and the 1030 cm^{-1} band for dimethylolated amino groups. Furthermore, the area of the 1000-1030 cm^{-1} bands relative to the area of the triazine band was correlated with the number of methylol groups (relative to the melamine content), determined by ^{13}C NMR. A reasonable correlation was found as shown in Fig.IV.5 and this fact further supports the assignment to vibrations of methylol groups.

920-900 cm^{-1} region

For n-alkyl ethers, the C-O-C symmetric stretch is located in the 930-830 cm^{-1} range [6]. Hill et al. [5] tentatively attributed the 906 cm^{-1} band of formalin to the C-O-C stretch. We confirmed this assignment: the Raman spectra of para-formaldehyde (Figure IV.1e) and hexamethoxymethylmelamine (Figure IV.1d) illustrate an intense band at 910 cm^{-1}. Compared to these model compounds, in the Raman spectra of MF resins (Figure IV.3) a broad band is observed in this region. The amount of methylene-ether bridges relative to the melamine content, calculated from the corresponding ^{13}C NMR spectra, are 0.02, 0.21 and 0.28 for the MF resins shown in Figure IV.3 from the bottom to the top respectively, with an increasing intensity of the 900 cm^{-1} band. The line width of the band at 900 cm^{-1} is broadened somewhat inhomogeneously probably because the great variety of environments surrounding the methylene-ether bridges in MF resins.

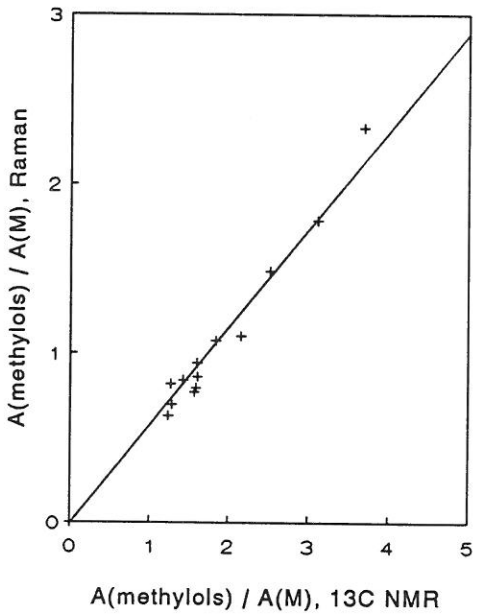

Figure IV.5 Correlation between the band area ratio methylol groups (1000 cm^{-1} bands) / melamine ring breathing (975 cm^{-1}) and the number of methylol groups determined by ^{13}C NMR.

680-670 cm^{-1} region

In the Raman spectrum of melamine an intense sharp band at 676 cm^{-1} is observed (Fig.IV.1a). This band is attributed to the 'in-plane' ring deformation of the triazine ring [6]. This band is practically absent in the Raman spectra of methylol-melamines. It is suggested that the intensity at 676 cm^{-1} vanishes upon methylolation.

3 *Quantitative analysis*

Historically, quantitative Raman spectroscopy has attracted little attention. This is largely due to experimental difficulties associated with conventional Raman spectroscopy. The development of FT-Raman spectrometers has offered a great step forward in solving these problems. Raman spectra can be measured very rapidly with an FT-spectrometer and as a consequence laser and spectrometer drift are less significant. Most FT-Raman instruments, using back scattering geometry, are

insensitive to the exact position of the sample in the sample area, this being one of the reasons why high reproducibility is possible. However, because we are interested in the quantification by means of Raman spectra of powders, it is still very risky to rely on absolute intensities since the scattering efficiency is particle size dependent. Therefore, we prefer to use relative intensities for quantitative work.

In the case of quantitative measurements using a NIR FT-Raman instrument the self absorption effect has to be considered. Everall and Lumsdon [8] studied the effect of sample alignment on the relative intensities of bands in an FT-Raman spectrum, excited by a Nd:YAG laser. They observed that by defocusing the sample relative to the collection optics, the intensities of strongly polarized bands near 1000 cm^{-1} were significantly decreased relative to other bands in the spectrum. Careful optimisation of sample position can yield reproducible relative intensities. Petty [9] demonstrated that self-absorption can affect NIR FT-Raman spectra. This perturbation of the spectrum will occur where the sample has an absorption band at the same frequency as the Raman scattering and results in a suppression of Raman bands relative to other bands in the spectrum. Therefore, the NIR absorption spectrum of a sample should always be recorded over the relevant spectral range and compared with the Raman data whenever quantitative measurements are being attempted.

MF-resins contain hydrocarbon-, hydronitrogen- and hydroxy fragments and therefore have C-H, N-H and O-H stretch overtones, which are likely to affect the NIR Raman spectra. Figure IV.6 shows the NIR absorption spectra of two MF-adducts with different F/M ratios. The spectra show that MF-adducts have significant absorptions in the Raman range, but the absorbances at a specific wavelength are the same for the various samples. Therefore, relative band areas are affected uniformly for the MF-resins studied.

Quantitative analysis of solids presents significant experimental difficulties. It is still possible to extract quantitative data from the spectra of solid samples making use of an internal standard or relative band ratios. First, a known amount of an inert reference with a characteristic Raman band can be added to the samples. This can have some undesirable consequences. The mixtures of methylolmelamines are very complex, with many competing equilibria. Adding a further component may perturb this system. Furthermore the inert reference should be homogeneously distributed through the samples. As a second possibility, one may choose one of the Raman bands of the MF-resins, e.g., the triazine ring breathing around 975 cm^{-1} or the C-H stretching around 3000 cm^{-1} as internal standard, provided that the Raman scattering cross section of these bands is independent on the degree of methylolation,

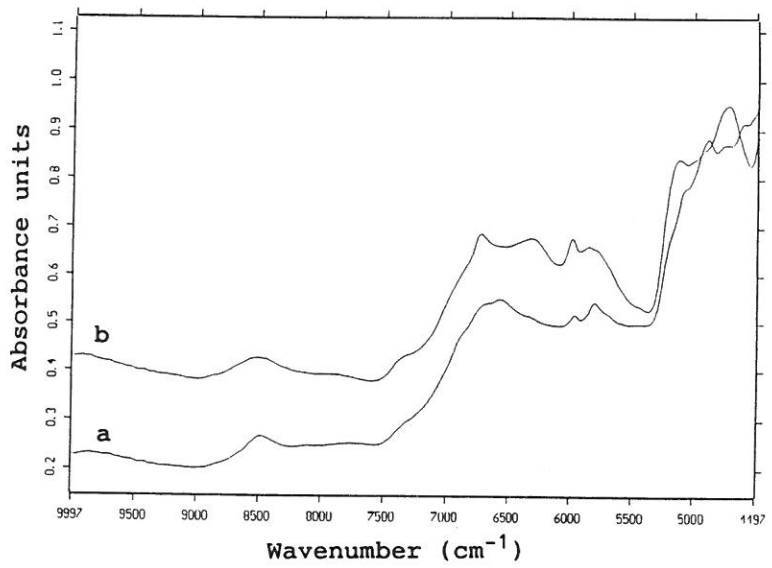

Figure IV.6 NIR absorption spectra of MF-adducts with different F/M ratio's 2 (a) and 6 (b), respectively.

the water content and the degree of curing. In order to study the possibility of quantification two sets of experiments were performed. In the first set of samples a known amount of DMSO-d_6 was added to solutions of methylolmelamines with a varying F/M ratio. The second set of samples was prepared by freeze-drying the solutions of the first set of samples.

3.1 Quantitative studies on solutions of methylolmelamines with various F/M ratios (DMSO-d_6 as internal standard)

Solutions of mixtures of methylolmelamines were prepared with different F/M ratios: 1.7; 2; 2.5; 3; 4; 5 and 6, respectively. Subsequently, a known amount of an inert reference, i.e., DMSO-d_6 with a characteristic Raman band was added to all the mixtures. In this way, the possibility of quantification was investigated by normalising the C-H stretch bands and the triazine band to the S=O stretching of DMSO-d_6 at 2134 cm^{-1}. The C-H stretch region and the region around 1000 cm^{-1} consist of several overlapping peaks. To resolve overlapping peaks, these two regions in the spectrum were deconvoluted.

The ratio of the area of the C-H stretching bands (normalised to the concentration of formaldehyde) and the area of the 2134 cm^{-1} band of DMSO-d_6 was found to be 0.219 with a standard deviation of 0.007. The ratio of the area of the triazine band at 975 cm^{-1} (normalised to the melamine concentration) and the area of the 2134 cm^{-1} of DMSO-d_6 was found to be 0.088 with a standard deviation of 0.002. This demonstrates that the sensitivity of the C-H stretching bands and the triazine band is not influenced by the F/M ratio. Figure IV.7 illustrates a good correlation between the ratio of the area of the C-H stretching bands to the area of the triazine band and the F/M ratio, determined by ^{13}C liquid NMR.

3.2 Quantitative studies on MF-powders

Experience with solids has been far less satisfactory than in the case of liquids. The quantitative analysis of freeze-dried MF-resins using DMSO-d_6 as internal standard presents significant experimental difficulties. The ratio of the area of the triazine band at 975 cm^{-1} (normalised to the melamine concentration) and the area of the 2134 cm^{-1} band of DMSO-d_6 is no longer constant. Compared to the results of the mixtures of methylolmelamines in the liquid phase, we found large deviations. This lack of correlation will be a result of the inhomogeneously distribution of DMSO-d_6 after freeze-drying. As a consequence DMSO-d_6 can no longer be used as internal standard. Secondly, free formaldehyde might be removed during freeze-drying.

Relative areas of bands of the MF resin itself might still be used to extract quantitative data from the spectra of solid samples. The ratio of the area of the C-H stretch region to the area of the triazine band was determined after resolving overlapping bands in the Raman spectra of MF-resins (prepared from F/M ratio 2, 3, 4, 5 and 6). The same correlation between the ratio of the area of the C-H stretching bands to the area of the triazine band and the F/M ratio was found as in the case of the liquid methylolmelamines (Fig. IV.7).

The results regarding the quantification indicate that both the 975 cm^{-1} triazine ring breathing and the 3000 cm^{-1} C-H stretching Raman scattering cross sections are not influenced by the degree of methylolation.

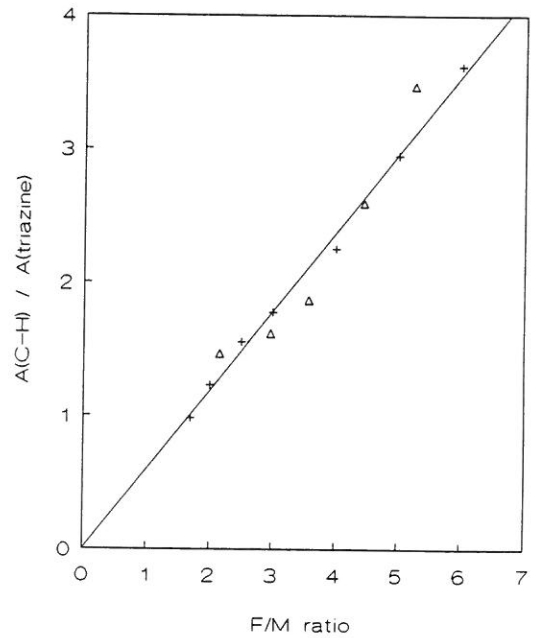

Figure IV.7 Band area ratio C-H stretch / melamine ring breathing versus F/M ratio for liquid mixtures of methylolmelamines (+) and freeze dried MF-powders (Δ).

4 Resin spectra

Both the triazine ring breathing at 975 cm^{-1} and the C-H stretching bands at 3000 cm^{-1} seem to be suitable for quantification. It is not expected that melamine, in contrast to formaldehyde, disappears during cure and therefore all Raman spectra were quantified on the same relative basis by normalizing the measured band areas to that of the triazine band in each spectrum.

The model compound spectra indicate that several spectral regions provide differentiation among the most important structures, i.e., methylol groups, methylene- and methylene-ether bridges in cured MF-resins. Those regions include the methylene bending region (1430-1460 cm^{-1}), the region around 1000 cm^{-1} linked to methylol groups and the C-O-C stretch region around 900 cm^{-1}.

In the methylene bending region we can differentiate between O-CH_2-O, N-CH_2-O and N-CH_2-N. The methylene bending region of the Raman spectra of a MF-resin (prepared with F/M 1.7 at pH 7.6) is shown in Figure IV.8 for different cure times.

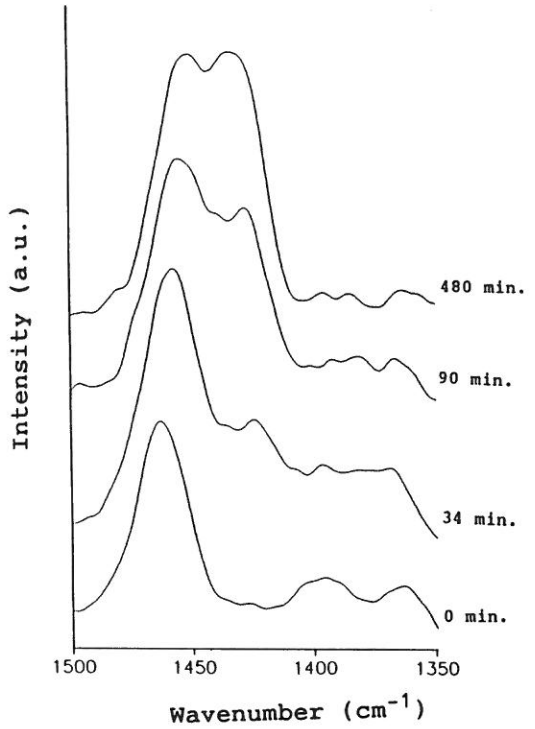

Figure IV.8 FT-Raman spectra from 1350-1500 cm^{-1} of an MF-resin (F/M 1.7; pH 7.6) cured for several lengths of time at 100°C.

The initial band at 1460 cm^{-1} shifts to 1450 cm^{-1} during cure. At present, no explanation for this frequency shift is known. The effect of cure time is observed in a change in the relative intensities of the 1450 and 1435 cm^{-1} bands. The concentration of N-CH_2-N groups at 1435 cm^{-1} increases with cure relative to the concentration of N-CH_2-O groups. Figure IV.9 shows the distinct differences in this spectral region between MF-resins prepared with different F/M ratios of 1.7, 3.5 and 6, respectively. The observed relative concentrations of N-CH_2-O and N-CH_2-N moieties are consistent with the ^{13}C CP/MAS results from these resins. Methylene linkages dominate in the case of resins with a low F/M ratio. For resins prepared from a higher F/M ratio no distinct methylene bending of the methylene bridge at 1430 cm^{-1} is observed.

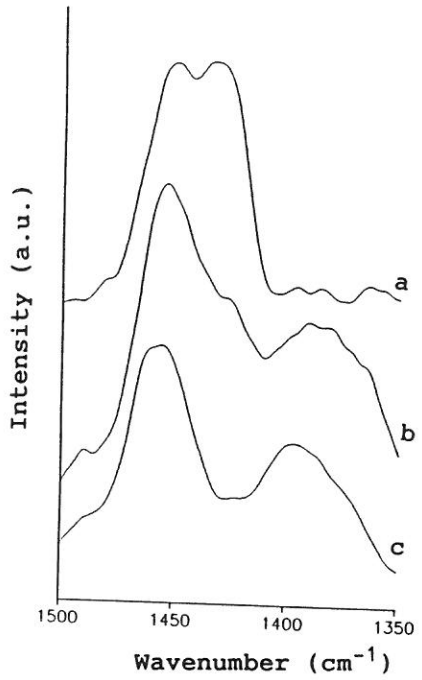

Figure IV.9 Comparison of the 1350-1500 cm^{-1} region of three cured MF resins prepared from F/M=1.7(a); 3.5(b) and 6(c) at 100°C.

The concentration of methylol groups decreases with cure. This is manifested by a decrease of bands in the region around 1000 cm^{-1}. The decrease of the area of the 999 and 1017 cm^{-1} bands during cure at 100°C of the MF resin (F/M 1.7; pH 7.6) is shown in Figure IV.10. Figure IV.11 shows the area of the 1030 cm^{-1} band of the MF resin (F/M 6; pH 9) against cure time at 100°C. Initially, a distinct band appears at 950 cm^{-1} and the 1030 cm^{-1} band increases in intensity. Basic conditions after the methylolation promote further addition reactions with formaldehyde. This observation was also confirmed by means of HPLC- and FT-IR measurements. After curing for 6 hrs., the intensities of the 950 cm^{-1} and 1030 cm^{-1} bands begin to decrease progressively with cure.

The C-O-C stretch region can be used to identify the presence of methylene ether linkages in cured MF resins. In the Raman spectra of the cured MF resins a broad band is seen in this region in comparison with the Raman spectra of model compounds. Figure IV.12 presents the 850-1100 cm^{-1} spectral region for the cured MF resins with different F/M ratios of 1.7, 3.5 and 6, respectively.

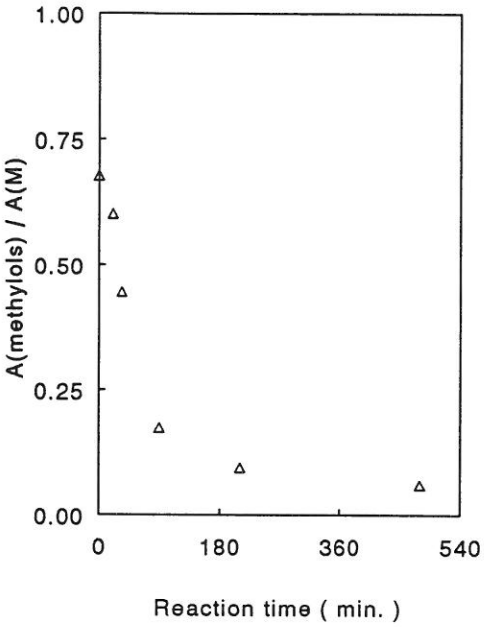

Fig.IV.10 Band area ratio of methylols (999 + 1017 cm^{-1}) and melamine (975 cm^{-1}) during cure of an MF resin (F/M 1.7, pH 7.6).

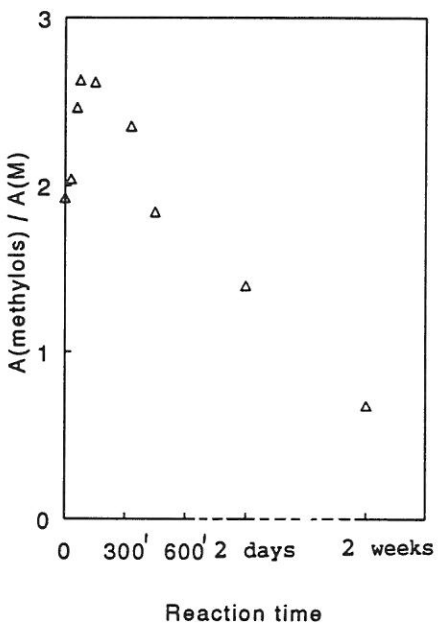

Fig.IV.11 Band area ratio of methylols (1030 cm^{-1}) and melamine (975 cm^{-1}) during cure of an MF resin (F/M 6, pH 9).

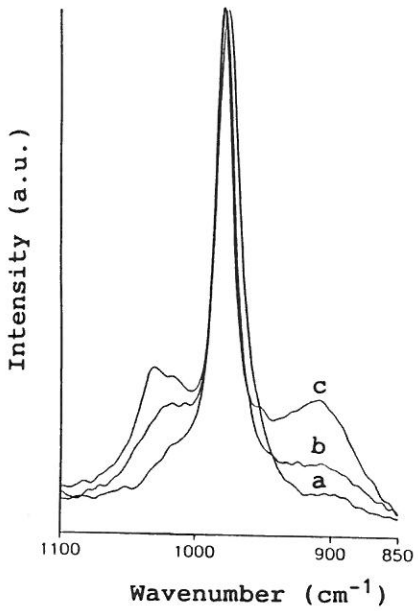

Figure IV.12 Comparison of the 850-1100 cm^{-1} region of three cured MF resins prepared from F/M 1.7(a), 3.5(b) and 6(c) at 100°C.

The broad (910-930 cm^{-1}) band is more intense for resins with higher formaldehyde contents indicating a higher number of methylene-ether bridges at high F/M ratios.

Finally, we have observed an additional change in the Raman spectra during cure. Close inspection of the Raman spectra of the cured MF resins reveals that the intensity of the 750 cm^{-1} band increases simultaneously with the 1435 cm^{-1} band (Fig.IV.4).

5 *Free melamine content*

In the Raman spectrum of melamine intense sharp bands at 676 and 975 cm^{-1} are observed (Fig.IV.13a). These bands are attributed to deformations of the triazine ring [6]. Surprisingly, the 675 cm^{-1} band is almost absent in the spectra of MF resins, whereas the band at 975 cm^{-1} is unchanged both in intensity and in frequency (Fig.IV.13b).

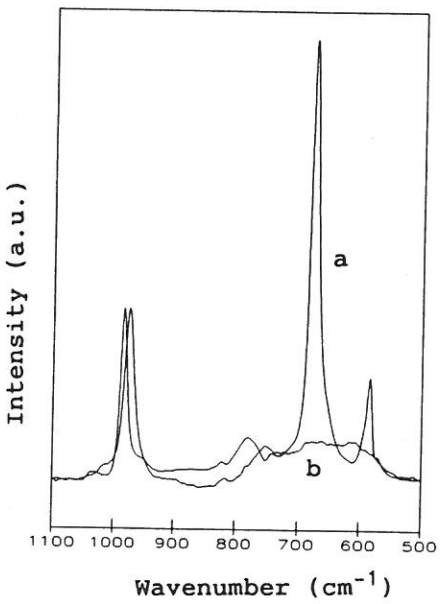

Figure IV.13 FT-Raman spectra from 1100-500 cm^{-1} of melamine (a) and a methylolmelamine mixture prepared from F/M 1.7 (b).

The Raman spectra of well-characterised MF-adducts and resins (HPLC, NMR) with varying F/M ratio, indicate that the 676 cm^{-1} band changes dramatically in intensity as the melamine ring is substituted. For MF resins that contain free melamine, as was determined by HPLC, the 676 cm^{-1} band is still present. These data suggest that it might be possible to use the intensity of the 676 cm^{-1} for the determination of the free melamine content in MF resins. In the third part it was shown that the band at 975 cm^{-1}, assigned to the triazine ring breathing vibration, can be used for quantification of the total melamine content of an MF resin. This suggests that the ratio R,

$$R = \frac{A_{676} / A_{975}}{R_M} \times 100\ \% \qquad (1)$$

can be used to quantify the % of melamine that is present in the unsubstituted form (A_{676} and A_{975} are the areas of the band at 676 cm^{-1} and 975 cm^{-1} , respectively, $R^M = A^M_{676} / A^M_{975}$ which was calculated from the Raman spectrum of pure melamine). Spectrum deconvolution has been carried out on the cluster of peaks around 1000 cm^{-1}. As a reference method, the determination of free melamine contents of soluble MF resins was carried out by HPLC after water extraction [10]. Table IV.1 shows the comparison of the % free melamine obtained by HPLC and those by Raman spectroscopy of some typical soluble MF resins. The percentage of free melamine obtained from eq.(1) by Raman spectroscopy is in good agreement with those obtained by HPLC. This Raman spectroscopic method can be applied for the determination of the free melamine content of cured MF resins. In this case it is impossible to use HPLC because of the insolubility of the resins.

Table IV.1 Percentage free melamine obtained by HPLC and Raman spectroscopy.

Resin No.	HPLC	Raman spectr.
1	19.5	19.4
2	13.0	11.6
3	13.5	12.8
4	16.3	15.9
5	10.8	8.9
6	40.6	39.2

It remains a surprising fact that the 676 cm^{-1} ring mode vanishes upon methylolation, whereas the 975 cm^{-1} band has a constant intensity upon methylolation. In order to understand this and further to support the current interpretation of the experimental data, a theoretical analysis of these Raman frequencies was performed by Dr. R.J.Meier. The 975 cm^{-1} and 676 cm^{-1} frequencies were calculated for several methylolmelamines, i.e., monomethylolmelamine, the two different trimethylolmelamines, and hexamethylolmelamine. The frequency at 676 cm^{-1} was not found for any of the methylolmelamines. An entire change of the character of vibration in conjunction with the loss of the symmetry properties explains the loss of intensity of the 676 cm^{-1} Raman band upon methylolation. The frequency for the ring mode corresponding to the 975 cm^{-1} band is practically constant, and since the character of the mode is also unchanged the Raman intensity is expected to be constant as well.

In conclusion, it is shown that FT-Raman spectroscopy can be used to determine the free melamine content in MF resins. In contrast to the conventional HPLC method, the Raman spectroscopic method can be directly applied to cured resins.

6 *Conclusions*

In this Chapter ^{13}C NMR, HPLC and FT-Raman measurements were combined to characterize uncured and cured MF-resins. From this combination of data we have achieved a significant clarification of the interpretation of MF Raman spectra. Nevertheless, it is also clear that there are still regions in the Raman spectra of MF resins where the interpretation remains tentative. Several distinct changes occur in the Raman spectra during methylolation and MF resin cure and these now appear to be consistent with the crosslinking process of these MF-resins. The major changes and their interpretations are the following. The decrease of methylol groups due to condensation can be observed from the decrease in intensity of the bands around 1000 cm^{-1}. Examination of the 1400-1500 cm^{-1} region during resin cure demonstrates that relative changes can be observed in the concentrations of $-NCH_2N-$ (1435 cm^{-1}) and $-NCH_2O-$ groups (1450-1460 cm^{-1}). The presence of methylene-ether bridges can be seen from the broad band at 910-930 cm^{-1}. The free melamine content in MF resins can be determined from the ratio of the 676 cm^{-1} and the 975 cm^{-1} bands. This was further supported by a theoretical analysis of Raman frequencies.

It is shown that FT-Raman spectroscopy is a useful complement to other techniques, such as solid state NMR for the characterization of cured MF-resins. It seems also possible to extract semi-quantitative data from FT-Raman spectra.

7 *Experimental*

Materials

Various mixtures of MF-adducts were prepared by dissolving the requisite amount of melamine in 30-35% formalin, previously adjusted to pH 8.5 by the addition of 0.1 N aqueous sodium hydroxide. The MF mixtures used in this study, were prepared from F/M molar ratios of 1.7, 2, 2.5, 3, 4, 5 and 6. After reaction at 90°C for times varying between 10 and 45 min until the melamine was completely dissolved, ^{13}C liquid NMR and Raman spectra were recorded. One part of these mixtures of methylolmelamines was freeze-dried. The other MF resins examined in this study were prepared as earlier described in Chapters 2 and 3. The cured MF resins were ground to powder. The powders could be directly examined by Raman spectroscopy without further treatment.

Methods

Raman spectroscopy

Raman spectra were recorded on a Bruker, Model FRA 106 FT-Raman spectrometer, attached to a Bruker IFS 66 spectrometer. At 1064 nm laser excitiation was provided by a Nd:YAG laser, with laser power in the 100 mW range. All spectra were recorded at 4 cm^{-1} resolution. Positioning of the sample cell along the instrument's optical axis was controlled by a micrometer screw. The liquid samples were held in a cuvette, which was silvered on the rearface to provide back-reflection. Powders were held in an aluminium sample cell (Bruker). Typical scan times varied between 2 and 5 minutes.

In order to study the possibility of quantification, it was necessary to resolve some overlapping peaks in the Raman spectra of MF-resins. All collected spectra were transferred to a PC for further analysis. The fitting procedure was performed with Spectra Calc software (Galactic Industries Corp.). With the used apodisation (Blackman-Harris) and resolution (4 cm^{-1}) it turned out that bands could be well described with a Lorentzian band shape.

NMR

^{13}C liquid NMR spectra from soluble MF-resins have been obtained on a Varian unity-400 spectrometer. ^{13}C liquid NMR was used to determine quantitatively the number of methylene bridges, methylene-ether bridges and methylol groups of MF resins that were used as references in this study. It was also used for the determination of the F/M ratio of several adduct mixtures.

Solid state CP/MAS ^{13}C NMR spectra were recorded on a Varian XL-200 spectrometer. The two sets of MF resins prepared from F/M 1.7 at pH 7.6 and F/M 6 at pH 9 respectively, characterized by ^{13}C CP/MAS NMR (Chapter 3) were used as references in this Raman study. Similar conditions as described in chapters 2 and 3, were used for recording the ^{13}C NMR spectra.

HPLC

A model 1050 High Performance Liquid Chromatograph (Hewlett Packard), equipped with a UV spectrophotometric detector set at 235 nm, was operated at room temperature for the determination of the free melamine content and the quantitative analyses of methylolmelamines (MM). A stainless steel reversed-phase HPLC column (125 mm x4 mm ID) was used with nucleosil 120-5 C18 (Machery & Nagel) as stationary phase. The eluents used were acetonitrile and water (50 mg triethylamine/ l water adjusted to pH 7 with phosphoric acid) at a combined flow rate of 1 ml/min. The solvent programme was set initially to 100% water and 0% acetonitrile and then progressively changed to 90% water and 10% acetonitrile over the analysis period of 25 minutes.

We derived the following molar relative response factors: melamine 1.00 (defined); monomethylolmelamine 1.18; N,N'-dimethylolmelamine 1.79; N,N',N''-trimethylolmelamine 2.36; N,N,N',N''-tetramethylolmelamine 2.96; pentamethylolmelamine 3.94 and hexamethylolmelamine 4.81. Quantitatively, these values compare well with those derived by Ebdon et al. [10]. However, small systematic differences, which probably find their origin in the different composition and pH of the eluent, do not influence our conclusions. Our relative response factors were applied in the HPLC analysis of adduct mixtures made by reacting 2.1, 2.7, 3.2, 5.5 and 5.7 mol of formaldehyde, respectively, per mol of melamine. The analysed composition of these mixtures is given in Table IV.2. The HPLC-data in Table IV.2 show that the mixtures of methylolmelamines prepared from F/M ratios less than 3 contain mainly mono, di- and trimethylolmelamine. Starting from F/M ratios greater than 3 results in the

formation of tetra-, penta- and hexamethylolmelamine. In those cases where the total amount of methylolmelamines does not add up to approximately 100%, the presence of oligomers was seen.

Table IV.2 Relative amounts of melamine and methylolmelamines (MM) in the adduct mixtures prepared from F/M ratios 2.1, 2.7, 3.2, 5.5 and 5.7 respectively; calculated from the areas of the chromatogram peaks and the relative molar response factors given in the text.

sample	1	2	3	4	5
F/M [a]	2.1	2.7	3.2	5.5	5.7
melamine	1.0	<0.5	<0.5	<0.5	<0.5
mono-MM	9.8	3.8	0.7	<0.5	<0.5
di-MM	15.0	19.7	10.1	<0.5	<0.5
tri-MM	35.5	61.5	46.7	<0.5	<0.5
tetra-MM	2.4	11.7	19.4	6.9	<0.5
penta-MM	<0.5	1.0	5.8	21.0	6.7
hexa-MM	–	–	–	69.4	72.6

[a] The F/M ratio of the freeze-dried MF powders was determined by ^{13}C liquid NMR. The deviations from 100% are due to analysis errors or the presence of oligomers in the adduct mixtures.

8 *References*

[1] J.R.Ebdon, B.J.Hunt, W.T.S.O'Rourke, J.Parkin, *Br.Polym.J.*, 20, 327 (1988).

[2] T.Gebregiorgis, Ph.D.Thesis, University of Essex, 1982.

[3] D.Braun, V.Legradic, Angew.Makromol.Chem., 36, 41 (1974).

[4] G.E.Myers, *J.Appl.Polym.Sci.*, 26, 747 (1981).

[5] C.G.Hill Jr, A.M.Hedren, G.E.Myers, J.A.Koutsky, *J.Appl.Polym.Sci.*, 29, 2749 (1984).

[6] F.R.Dollish, W.G.Fateley, F.F. Bentley, Characteristic Raman Frequencies of Organic Compounds, J.Wiley, New York, 1973.

[7] S.S.Jada, *J.Appl.Polym.Sci.*, 35, 1573 (1988).

[8] N.Everall, J.Lumsdon, *Vibr.Spectr.*, 2, 257 (1991).

[9] C.J.Petty, *Vibr.Spectr.*, 2, 263 (1991).

[10] J.R.Ebdon, B.J.Hunt and W.T.S.O'Rourke, Br.Polym.J., 19, 197 (1987).

One part of this Chapter has been published and another part is submitted for publication.

M.L.Scheepers, J.M.Gelan, R.A.Carleer, P.J.Adriaensens, D.J.Vanderzande, B.J.Kip, P.M.Brandts, *Vibr.Spectr.*, 6, 55 (1993).

M.L.Scheepers, R.J.Meier, L.Markwort, J.M.Gelan, D.J.Vanderzande and B.J.Kip, submitted for publication in *Vibr.Spectr.*

CHAPTER 5

STUDY OF THE CURE REACTIONS BY DIFFERENTIAL SCANNING CALORIMETRY

1 Introduction

One of the most widely used methods for studying the cure behaviour of thermosets is Differential Scanning Calorimetry (DSC) [1-3]. It has been the most common technique used to elucidate cure kinetics. Kay and Westwood [4] have investigated the kinetic parameters associated with the curing of MF resins impregnated into cellulose paper from the analysis of a single temperature scan. The extent of cure of partially cured resins can be determined by relating the residual exothermic energy to the total heat of reaction. DSC has the additional benefit that the increase in the glass transition temperature with cure can also be monitored. DSC can also be used to determine reaction enthalpies.

In order to derive ΔH values for methylene and methylene-ether bridge formation by DSC a number of problems must be overcome. The cure of MF resins is undoubtedly complex and is a summation of several competing reactions. MF resins can cure by formation of either methylene bridges or methylene-ether bridges and water of condensation is liberated. Since DSC can only provide information about the overall cure process, spectroscopic tools are required to provide information on the chemical structures formed during crosslinking. Therefore a careful study has been carried out in which two sets of partially-cured resins have been examined by a combination of DSC, ^{13}C CP/MAS NMR and Raman spectroscopy. The two MF resins used differ in F/M molar ratio and initial pH, and consequently differences in cure behaviour, related to their chemical composition, are expected.

In this chapter, the experimental procedure for the determination of ΔH for curing of MF resins is presented. Secondly, the ΔH's of the MF resins with different degrees of pre-cure have been measured by DSC and the pre-cured and finally cured MF resins were characterized by ^{13}C CP/MAS NMR and FT-Raman spectroscopy. Finally, ΔH's for methylene and methylene-ether bridge formation have been derived from the measured ΔH values and the concentrations of methylene and methylene-ether bridges formed during the cure cycles.

2 *DSC measurement of MF resin cure*

Two sets of MF resins prepared from F/M 1.7 pH 7.6 and F/M 6 pH 9, respectively, were pre-cured for several lengths of time at 100°C. Measurement of the residual heat of reaction of these partially-cured MF resins was not straightforward. The experimental difficulties resulting from the vaporization of water of condensation will now be discussed.

1. MF resins cure by a condensation type mechanism, this leads to extra complications. The exothermic cure reaction is altered by a competitive endothermic vaporization of water of condensation. At atmospheric pressure the exothermic cure reaction and endothermic vaporization of water of condensation are competitive and the net energy change detected by DSC does not give usuable information. Condensation reactions therefore require encapsulation or pressurization if the curing exotherm is to be observed [4,5]. We made use of sealed capsules in which pressure (to 24 atmospheres) can build up during the course of the reaction.

2. It is recommended that the residual heat of reaction of partially cured resins is determined from scanning experiments [1]. However, during a dynamic scan a continuous alternation of undersaturation and saturation of water vapor occurs dependent on the amount of water liberated during condensation and that evaporated at a certain temperature. When investigating the cure by an isothermal method on the contrary, the saturated vapor pressure of water is reached within one or two minutes. This is the time a sample cell needed to heat up to the desired temperature. Afterwards further vaporization of water can be neglected. But this approach also has problems in both the initial and final stages of reaction. The MF resin (F/M 1.65 pH 7.3) was cured by the isothermal method at temperatures varying from 90°C to 150°C until no further cure was detectable in terms of heat flow. The total heat of reaction varied with cure temperature in the manner shown in Table V.1. It is recognised that undercure may contribute to the low values at lower temperatures. When samples of this resin, which have been isothermally cured, were scanned at temperatures above the prior cure temperature further reaction was observed, as shown in Fig. V.1.

Table V.1 Apparent heats of reaction obtained from isothermal measurements.

Cure temperature (°C)	ΔH (kJ/mole melamine)
100	-22.9
110	-24.7
120	-25.4
130	-25.3
135	-23.6
140	-22.1
150	-19.0

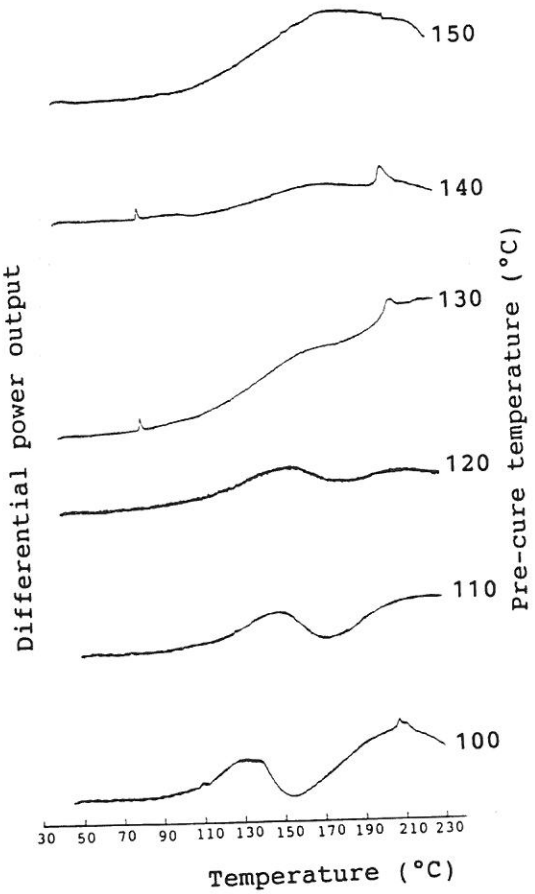

Figure V.1 Dynamic scans at 10° C / min. on MF resins (F/M 1.65 pH 7.3) previously cured to apparent completion at temperatures from 100°C to 150°C.

The subsequent scan reveals a residual exotherm of -3.3 kJ/mole M for the resin cured at 100°C and the residual exotherm diminishes as the pre-cure temperature increases (-2.1 and -0.6 kJ/mole M for the resins cured at 110°C and 120°C, respectively) to vanish at 130°C. Fig.VI.1 further shows that the glass transition occurs at the cure temperature, indicating that as soon as the resin vitrifies further reaction is very slight and no longer detectable with the isothermal method. The decrease of ΔH above 120°C results from the unrecorded portion of the reaction occuring during heating of the sample. This is derived from the large increase of the percentage conversion at a certain time with increasing cure temperature.

In this study the residual heat of reaction of each partially-cured sample was determined under isothermal conditions at 120°C.

3. Water is an unavoidable constituent and can become involved as well in the chemistry of curing as in plasticizing the cured thermoset. Variations in the amount of water can affect both the rate of cure and ultimate extent of cure. To determine the effect of water on curing, the heat of reaction was measured for a freeze-dried MF resin with variable amounts of water added. Figure V.2 shows the reaction enthalpy for a MF resin (F/M 1.7 pH 7.6) as a function of the water content.

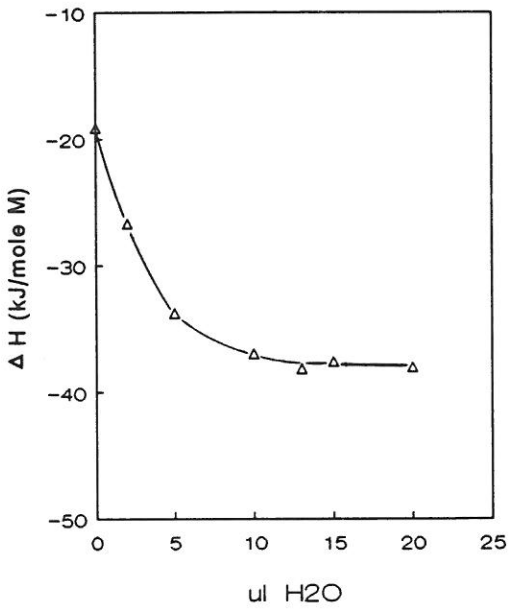

Figure V.2 Reaction enthalphy as a function of the amount of water added to the MF resin (F/M 1.7 pH 7.6).

Initially an increase in the ΔH value with an increasing amount of added water can be seen. Then the ΔH value levels off and reaches a maximum value. Therefore to each partially-cured MF resin examined in this study an identical amount of water (10µl) was added resulting in a resin with a solids content of 0.5 (comparable to aqueous MF resin solutions) and then the capsule was quickly sealed.

4. It is absolutely necessary to prevent any loss of sample because this will affect the measured heat flow. After the isothermal cure was completed the capsules were reweighed and compared to the initial weight. Weight loses were negligible during isothermal runs at 120°C.

5. Sample sizes of 10-11 mg were used to minimize thermal gradients in these heavy sample pans. No significant changes in ΔH were observed as the sample size is varied between 5 and 20 mg. The reproducibility of the reaction enthalpy was examined and was found to be 3 J/g sample weight.

In conclusion, to each partially-cured MF resin water was added resulting in a resin with a solid content of 0.5 and the residual heat of reaction was measured under isothermal conditions at 120°C. Then, the heat of reaction ($\Delta H_{react.}$) was calculated from the difference between ΔH for the uncured MF resin and the residual ΔH's for the partially-cured resins.

$$\Delta H_{react.} = \Delta H_{uncured} - \Delta H_{res.} \qquad (1)$$

3 *Chemical structure of pre-cured and finally cured MF resins*

Before an evaluation of the measured ΔH's is made it is necessary to ascertain which reactions occur during cure in order to determine the reaction enthalpies for methylene and methylene-ether bridge formation. ^{13}C CP/MAS NMR and Raman spectroscopy were used for the characterization of the two sets of MF resins that were pre-cured for various lengths of time. The ^{13}C CP/MAS NMR results of the two series of MF resins are summarized in Tables III.2 and III.3. These data show that the MF(1.7) resin cures mainly by formation of methylene bridges whilst in the MF(6.0) resin only 4% of the total formaldehyde was incorporated as methylene bridges. The ^{13}C CP/MAS spectra provide no quantitative information about methylene-ether bridge formation because of the overlap with the residual

methylol groups. Methylene-ether bridge formation and the presence of residual methylol groups can be observed from the corresponding FT-Raman spectra [6]. The broad band at 900 cm^{-1}, representing methylene-ether bridges is more intense for the MF(6.0) resin indicating a higher number of methylene-ether bridges for the MF(6.0) resin compared to the MF(1.7) resin (Fig.IV.4). For each partially-cured MF resin the number of residual methylol groups per melamine unit was determined from the ratio of the area of the 1000 cm^{-1} bands to the area of the triazine band at 975 cm^{-1}. For the MF(1.7) resin the number of methylol groups decreases with increasing time of cure as shown in Fig.IV.9. The number of methylol groups for the MF(6.0) resin increases initially and decreases progressively with cure after curing for 6 hours at 100°C, as shown in Fig.IV.10. The number of methylene bridges of the MF resins with different degrees of pre-cure relative to that of the uncured resin is determined by ^{13}C CP/MAS NMR. The number of methylene-ether bridges of the various partially-cured MF resins relative to that of the uncured resin is calculated as one half of the difference between the total number of methylol groups consumed in the condensation (obtained from the Raman spectra) and the methylene bridges (obtained by ^{13}C CP/MAS NMR). No further differentiation between non-substituted and substitued bridges was made.

In the next section these spectroscopic data are related to the measured ΔH's by DSC. Then, it is required that curing by DSC results in the same final MF structure for each partially-cured MF resin within a given set. The MF resin samples obtained after isothermal cure at 120°C in DSC were characterized by FT-Raman spectroscopy, indicating no significant structural differences for the MF resins within a given set.

4 *Comparison of the spectroscopic data with the heat flow data at 120°C*

Table V.2 shows the mole of methylene bridges and methylene-ether bridges per mole melamine for the two sets of MF resins together with the heat of reaction obtained from DSC measurements. The heat of reaction was not referred to the over-all weight of the sample but expressed per mole melamine.

In the simplified hypothesis that (i) the cure reactions contribute principally to the DSC heat flow and (ii) it is not differentiated between non-substituted and substituted bridges, enthalpies for the methylene and methylene-ether bridge formation can be obtained from a linear least squares fit to eq.(2) using the data in Table V.2.

$$\Delta MB.\Delta H_{MB} + \Delta EB.\Delta H_{EB} = \Delta H_{reac.} \quad (2)$$

This results in ΔH values of -30 ± 6 kJ/mole for methylene bridge formation and -19 ± 8 kJ/mole for methylene-ether bridge formation. It is interesting to compare the values determined in this work with the reaction enthalpy for the methylolation determined by Gordon et al. [7]. They obtained a value of -12.3 kJ/mole for the methylolation of melamine from the variation of the equilibrium constant with temperature. Thus despite the simplifying assumptions which have to be made, reasonable estimates of the enthalpies for methylene and methylene-ether bridge formation were obtained using a combination of DSC, ^{13}C CP/MAS NMR and FT-Raman spectroscopy.

Table V.2 Number of methylene (MB) and methylene-ether bridges (EB) formed during pre-cure with the corresponding heats of reactions obtained by DSC for two sets of MF resins.

F/M 1.7 pH 7.6

MB mole/mole M	EB mole/mole M	$\Delta H_{react.}$ kJ/mole M
0.15	0.02	- 4.35
0.31	0.14	-10.41
0.61	0.33	-24.74
0.90	0.28	-33.19
1.04	0.26	-35.55

F/M 6.0 pH 9.0

MB mole/mole M	EB mole/mole M	$\Delta H_{react.}$ kJ/mole M
0.24	0.18	-11.46
0.24	0.77	-21.05
0.24	1.28	-34.52
0.24	2.10	-43.78

5 *Conclusions*

The residual heat of reaction of the partially cured MF resins was determined isothermally at 120°C. $\Delta H_{react.}$ was calculated from the difference between the reaction enthalpy for the uncured MF resin and the residual reaction enthalpies of the partially-cured resins.

The determination of the enthalpies for methylene and methylene-ether bridge formation from DSC requires support by spectroscopic techniques providing detailed structural information, such as ^{13}C CP/MAS NMR and Raman spectroscopy. The enthalpy of methylene bridge formation (-30 ± 6 kJ/mole) is more exotherm than that of the methylene-ether bridge formation (-19 ± 8 kJ/mole). Despite the simplifying assumptions involved in the DSC measurement of MF resin cure, the enthalpies obtained for the methylene and methylene-ether bridge formation are plausible. Thus it can be concluded that the measurement conditions used for the kind of system examined in this study, give reliable data on the curing process of condensation resins.

6 *Experimental*

MF resins

The preparation of the two sets of partially-cured MF resins has been described before in chapter 3. ^{13}C CP/MAS NMR and FT-Raman measurements were performed on the powders. For the DSC measurements, water was added to each partially-cured MF resin resulting in a resin with a solids content of 0.5.

Methods

DSC

A differential scanning calorimeter, Perkin Elmer DSC-2, was used to measure the residual heats of reaction of the partially-cured MF resins. Large Volume Capsules (O-ring sealed, stainless steel sample containers) were used in all runs. LVC's eliminate the interfering effects of the heat of vaporization by suppressing the vaporization of solvents. If properly sealed, the capsules could withstand internal pressures up to 24 atmospheres which corresponds with an equilibrium water vapor pressure at 225°C. They have a capacity of 60 µl. The weight of the sample cell is 330 mg and this obviously provides a greater thermal inertia than does the standard sample pan. It was therefore necessary to recalibrate both temperature and energy scales using indium and lead metals. The sample size used was 10-11 mg and the samples were all solids. Runs were always made using an empty cell as reference.

13C CP/MAS NMR

Typical conditions for recording the ^{13}C CP/MAS NMR spectra have been given in Chapter 3.

FT-Raman

The experimental details of the FT-Raman measurements have been described in Chapter 4.

7 *References*

[1] A.Turi, Thermal Characterisation of Polymeric Materials, Academic Press, New York, 1981.

[2] G.Allen and J.C.Bevington, Comprehensive Polymer Science, 1, Pergamon Press, 1989.

[3] M.J.Richardson, *Pure and Appl.Chem.*,64(11), 1789 (1992).

[4] R.Kay and A.R.Westwood, *Eur.Polym.J.*,11, 25 (1975).

[5] M.Ezrin, G.C.Claver, *Appl.Polym.Symp.*,8, 159 (1969).

[6] M.L.Scheepers, J.M.Gelan, R.A.Carleer, P.J.Adriaensens, D.J.Vanderzande, B.J.Kip, P.M.Brandts, *Vibr.Spectr.*, 6, 55 (1993).

[7] M.Gordon, A.Halliwell and T.Wilson, *J.Appl.Polym.Sci.*, 10, 1153 (1966).

CHAPTER 6

KINETICS OF THE CONDENSATION REACTIONS

1 Introduction

The chemical structure of an MF resin is probably one of the most important factors which determines the properties of the low molecular weight resins such as storage stability, water tolerance etc. and is strongly influenced by the reaction conditions. When the cure of MF resins is studied in more detail two steps can be identified: the methylolation and the condensation. The former has been described in detail as a function of pH, F/M ratio and temperature [1-5]. On the contrary, the latter has been studied in much lesser detail. Initially the pH dependence of the rate constant of methylene bridge formation was determined by titrimetric methods while the methylene-ether bridge formation was not taken into account [5-8].
Nastke et al. [9] used a combination of polarography and mathematical modeling to describe methylolation, methylene and methylene-ether bridge formation. Modeling was used because the methylene-ether bridges could not be detected selectively. Rate constants for methylolation, demethylolation, methylene bridge formation, methylene-ether bridge formation and decompostion were estimated as a function of pH, F/M ratio, temperature and concentration.

In this chapter the evolution of various chemical structures such as methylene and methylene-ether bridges , methylol groups, free amino groups has been determined for an MF resin with a F/M ratio of 1.7 as a function of pH and temperature by means of ^{13}C NMR and HPLC. Using ^{13}C NMR the following functional groups in an MF resin can be determined quantitatively $-NH_2$, $NHCH_2OH$, $-N(CH_2OH)_2$, $-NHCH_2NH-$, $-NR'CH_2NH-$, $-NHCH_2OCH_2NH-$, $-NR'CH_2OCH_2NH-$ and CH_2O. HPLC provides information on the changes in the concentrations of melamine, methylolated species and various dimers in an MF resin. Kinetic constants were calculated from these data assuming a second order reaction model.

2 *Approaches to rate constant determination*

Two different approaches were used to determine the rate constants of the methylene and methylene-ether bridge formation and hydrolysis (i) the molecular species approach and (ii) the functional group approach. In the first approach the rate constants for the formation and hydrolysis of distinct molecular species were estimated. The concentrations of the molecular species were determined by HPLC. In the second approach, rate constants were estimated from concentrations of the functional groups ($-NH_2$, $-NHCH_2OH$, $-N(CH_2OH)_2$ ....) as a function of time. These concentrations were determined by ^{13}C NMR. The results of the ^{13}C NMR measurements are tabulated in Tables 12-25 (see appendix).

2.1 *Molecular species approach*

In a first approach the rate constants for the methylene dimelamine formation, methylene-ether dimelamine formation and decomposition are estimated from the quantitative analysis of melamine species by HPLC. The various possible reaction path-ways for the formation and decomposition of methylene dimelamine and methylene-ether dimelamine are given in Scheme VI.1. For convenience, melamine and a reacted formaldehyde species are represented by  and o, respectively.
The kinetic rate equations for the two dimers are given in eqn. (1) and (2).

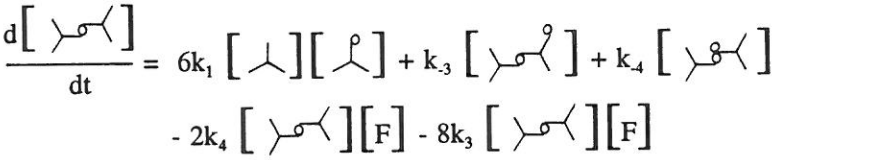

$$\frac{d[\quad]}{dt} = 6k_1[\quad][\quad] + k_{-3}[\quad] + k_{-4}[\quad] - 2k_4[\quad][F] - 8k_3[\quad][F]$$

$$+ \textit{trimer formation and decomposition} \qquad (1)$$

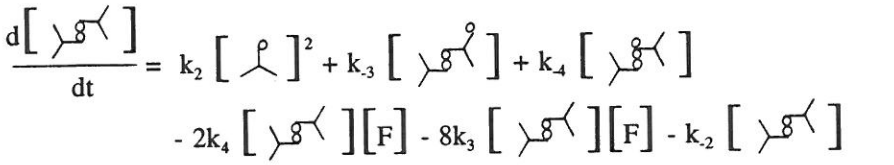

$$\frac{d[\quad]}{dt} = k_2[\quad]^2 + k_{-3}[\quad] + k_{-4}[\quad] - 2k_4[\quad][F] - 8k_3[\quad][F] - k_{-2}[\quad]$$

$$+ \textit{trimer formation and decomposition} \qquad (2)$$

Scheme VI.1

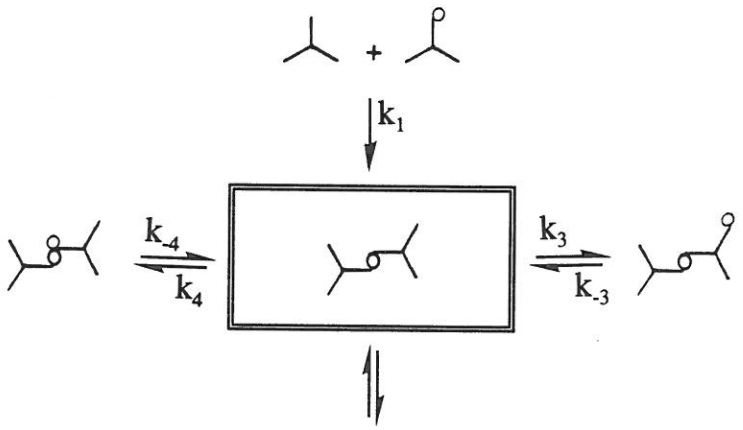

Trimer formation and decompostion

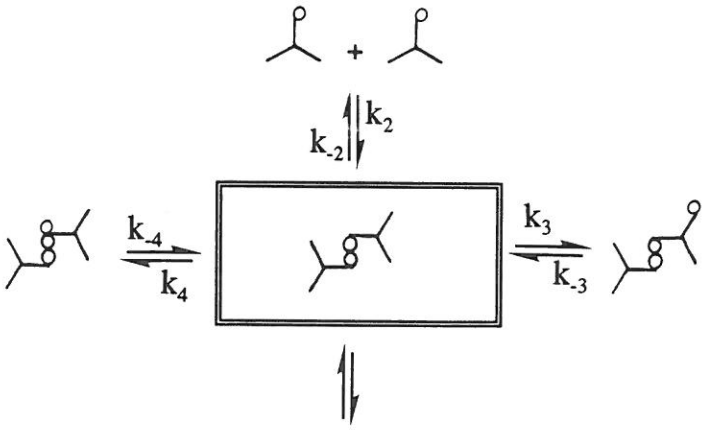

Trimer formation and decompostion

The following rate constants for the reaction between the various melamine species are used.

k_1 Rate constant for methylene bridge formation by reaction of a primary amino group and a methylol group substituted on a secondary nitrogen.

k_2,k_{-2} Rate constants for methylene-ether bridge formation and decomposition by reaction between two methylol groups substituted on secondary nitrogens.

k_3,k_{-3} Rate constants for methylolation and demethylolation of primary amino groups.

k_4,k_{-4} Rate constants for bridge methylolation and demethylolation. It is assumed that the reactivity of the secondary amino nitrogen of both types of bridges is similar.

The concentration of water is included in the rate constants for the reverse reactions. To get a good estimate of the rate constants of dimer formation and hydrolysis various melamine species must be taken into account. Unfortunately, the limited set of data does not permit a complete solution of the set of differential equations (eqn.1 and 2). However, a number of plausible simplifications can be made based on the following assumptions. (i) trimer formation was not taken into account. This seems reasonable because the reactions were studied in the initial stage and the number of dimers compared to the number of melamine remained low (maximal 0.06) (ii) equilibrium is established all the time for the reversible methylolation of a methylene (ether) bridge, as will be shown in the functional group approach. As a result the following terms can be expressed as

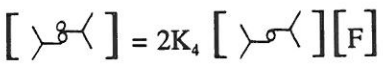

(3)

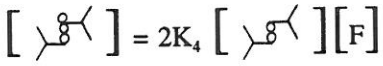

(4)

In this case, the differential equations can be reduced to eqn. (5) and (6).

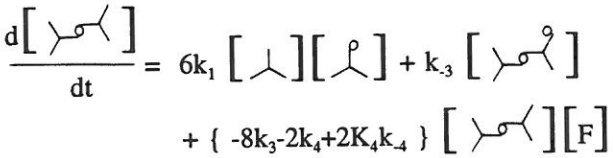

(5)

$$\frac{d[\ ]}{dt} = k_2 [\ ]^2 + k_{-2} [\ ] + k_{-3} [\ ] + \{ -8k_3 - 2k_4 + 2K_4k_{-4} \} [\ ][F] \qquad (6)$$

The rate d[ ] / dt was obtained by measuring the tangents on the curve of the concentration as a function of time. The rate constants k_1, k_2 and k_{-2} were determined by a non linear least square fit to eqn. (5) and (6).

2.2 *Functional group approach*

During condensation methylene bridges are formed by the reaction between -NH and $-NCH_2OH$ groups (eq.7) and methylene-ether bridges are formed by reaction between two $-NCH_2OH$ groups (eq.8).

$$R\text{-}NR'CH_2OH + HNR'\text{-}R \rightarrow R\text{-}NR'CH_2R'N\text{-}R + H_2O \qquad (7)$$

$$2\ R\text{-}NR'CH_2OH \rightleftarrows R\text{-}NR'CH_2OCH_2R'N\text{-}R + H_2O \qquad (8)$$

It is assumed that the reactivity of a -NH or $-NCH_2OH$ group is independent of the substitutent pattern (either non substituted or methylol substituted or bridged) of the melamine ring R on which these groups are located. This assumption has been made by a number of authors [10-12] in the kinetic modeling of MF polymerization.
By ^{13}C NMR the following functional groups can be determined $-NH_2$, $-NHCH_2OH$, $-N(CH_2OH)_2$, $-NHCH_2NH-$, $-NR'CH_2NH-$, $-NHCH_2OCH_2NH-$, $-NR'CH_2OCH_2NH-$ and CH_2O. The substituent R' can either be a methylol group or a methylene (ether) bridge. However, it is assumed that the methylene and methylene-ether bridges are substituted by a methylol group. This is substantiated by the appearance of a distinct shoulder on the carbon resonance at 71.6 ppm as was argued earlier in Chapter 2. So, the formation of methylene (ether) bridges substituted by a second bridge is not taken into account.

Scheme VI.2 summarises the reactions generating linear and methylol-substituted methylene and methylene-ether bridges. Both linear methylene and methylene-ether bridges can only be formed from one reaction path given in eq.(9) and eq.(10), respectively. The methylene bridge substituted by a methylol group can

result from three routes: reaction of (i) a di-methylolated and an unsubstituted amino group (eq.11), (ii) two mono-methylolated amino groups (eq.12) and (iii) methylolation of a linear bridge (eq.13). There are two modes of formation of a methylol substituted methylene-ether bridge: (i) reaction of a mono- and di-methylolated amino group (eq.14) and (ii) methylolation of a linear bridge (eq.15).

Scheme VI.2

$$R\text{-}NH_2 + R\text{-}NHCH_2OH \xrightarrow{k_1} R\text{-}NHCH_2NH\text{-}R + H_2O \qquad (9)$$

$$2R\text{-}NHCH_2OH \underset{k_{-2}}{\overset{k_2}{\rightleftarrows}} R\text{-}NHCH_2OCH_2NH\text{-}R + H_2O \qquad (10)$$

$$R\text{-}NH_2 + R\text{-}N(CH_2OH)_2 \xrightarrow{k_5} R\text{-}NR'CH_2NH\text{-}R + H_2O \qquad (11)$$

$$2\ R\text{-}NHCH_2OH \xrightarrow{k_6} R\text{-}NR'CH_2NH\text{-}R + H_2O \qquad (12)$$

$$R\text{-}NHCH_2NH\text{-}R + CH_2O \underset{k_{-4}}{\overset{k_4}{\rightleftarrows}} R\text{-}NR'CH_2NH\text{-}R + H_2O \qquad (13)$$

$$R\text{-}N(CH_2OH)_2 + R\text{-}NHCH_2OH \underset{k_{-7}}{\overset{k_7}{\rightleftarrows}} R\text{-}NR'CH_2OCH_2NH\text{-}R + H_2O \qquad (14)$$

$$R\text{-}NHCH_2OCH_2NH\text{-}R + CH_2O \underset{k_{-4}}{\overset{k_4}{\rightleftarrows}} R\text{-}NR'CH_2OCH_2NH\text{-}R + H_2O \qquad (15)$$

R = melamine residue, R' = CH_2OH

The following rate constants characterizing the reactions between the various functional groups are used.

k_1 Rate constant for methylene bridge formation by reaction of a primary amino group and a methylol group substituted on a secondary nitrogen. A similar value of the rate constant was defined to that of the dimer formation because it is assumed that the degree of substitution of the melamine ring does not change the reactivity of a given nitrogen or methylol group.

k_2,k_{-2} Rate constants for methylene-ether bridge formation and decomposition by reaction of two methylol groups substituted on a secondary nitrogen. Similar values were defined to these of the dimer formation, as was argued above.

k_4,k_{-4} Rate constants for methylolation and demethylolation of a methylene (ether) bridge.

k_5 Rate constant for methylol-substituted methylene bridge formation by reaction of a primary amino group and a methylol group substituted on a tertiary nitrogen.

k_6 Rate constant for methylol-substituted methylene bridge formation by reaction of a secondary amino group and a methylol group substitued on a secondary nitrogen. It is assumed that the reactivity of a given amino nitrogen or methylol group is different for a primary and a secondary amino group or methylol group.

k_7,k_{-7} Rate constant for methylol-substituted methylene-ether bridge formation and decomposition by reaction between a methylol group substituted on a secondary nitrogen and a methylol group substituted on a tertiary nitrogen.

The following set of rate equations for the various bridges can be derived.

$$d[\text{-NHCH}_2\text{NH-}]/dt = 2k_1\,[\text{-NH}_2][\text{-NHCH}_2\text{OH}] + k_{-4}\,[\text{-NR'CH}_2\text{NH-}] - 2k_4\,[\text{-NHCH}_2\text{NH-}][F] \quad (16)$$

$$d[\text{-NHCH}_2\text{OCH}_2\text{NH-}]/dt = k_2\,[\text{-NHCH}_2\text{OH}]^2 + k_{-4}\,[\text{-NR'CH}_2\text{OCH}_2\text{NH-}] - k_{-2}\,[\text{-NHCH}_2\text{OCH}_2\text{NH-}] - 2k_4\,[\text{-NHCH}_2\text{OCH}_2\text{NH-}][F] \quad (17)$$

$$d[\text{-NR'CH}_2\text{NH-}]/dt = 4k_5\,[\text{-N(CH}_2\text{OH)}_2][\text{-NH}_2] + 2k_6\,[\text{-NHCH}_2\text{OH}]^2 + 2k_4\,[\text{-NHCH}_2\text{NH-}][F] - k_{-4}\,[\text{-NR'CH}_2\text{NH-}] \quad (18)$$

$$d[\text{-NR'CH}_2\text{OCH}_2\text{NH-}]/dt = 2k_7\,[\text{-N(CH}_2\text{OH)}_2][\text{-NHCH}_2\text{OH}] + 2k_4\,[\text{-NHCH}_2\text{OCH}_2\text{NH-}][F] - k_{-4}\,[\text{-NR'CH}_2\text{OCH}_2\text{NH-}] - k_{-7}\,[\text{-NR'CH}_2\text{OCH}_2\text{NH-}] \quad (19)$$

It may be mentioned that the concentration of water is included in the rate constants for the hydrolysis reactions.

Determination of the rate constants by a non linear least square fit to eqn. (16) to (19) resulted in large errors in some of the rate constants. Since the set of data is limited it is necessary to find a way which permits the reduction of the number of fit parameters in the analysis of k_1, k_2, k_{-2}, k_5, k_6, k_7 and k_{-7}. First, the combined ^{13}C and ^1H NMR study, described in Chapter 2 has offered insight into the reaction pathways for the formation of methylol-substituted methylene bridges. It was

shown that these bridges are formed by the reaction pathway given in eq.(11) rather than that given in eq.(12). So the formation of methylol-substituted methylene bridges by reaction pathway given in eq.(12) is not taken into account. Secondly, when a pseudo equilibrium for the methylolation of methylene and methylene-ether bridges is observed the formation rate must be directly balanced with the decomposition rate according to eq.(20)

$$2\,k_4\,[\text{-NHCH}_2\text{NH-}][F] = k_{-4}\,[\text{-NR'CH}_2\text{NH-}] \qquad (20)$$

The equilibrium constant is the following:

$$K_4 = k_4 / k_{-4} = [\text{-NR'CH}_2\text{NH-}] \,/\, (2[\text{-NHCH}_2\text{NH-}][F]) \qquad (21)$$

The rates of methylolation and demethylolation ($\sim 10^{-1}$-10^{-2}) are fast with respect to the rate of bridge formation ($\sim 10^{-6}$) so it can be assumed that methylolation is in equilibrium all the time. Furthermore, the [-NR'CH_2NH-]/([-NHCH$_2$NH-]) ratio was found to be constant (~0.44) during the time the reaction was studied as can be seen from the data in Tables 12-26 (see appendix). The concentration of free formaldehyde measured by HPLC, remained nearly constant all the time.
At equilibrium the [-NHCH$_2$NH-][F]-term can be expressed as a function of [-NR'CH_2NH-]:

$$2k_4\,[\text{-NHCH}_2\text{NH-}][F] = k_4 \,/\, (K_4\,[\text{-NR'CH}_2\text{NH-}]) \qquad (22)$$

Thirdly, the methylol-substituted methylene-ether bridge formation and hydrolysis are not taken into account because these bridges are formed only slightly at this F/M ratio.

As a consequence the set of differential equations can be simplified to:

$$d[\text{-NHCH}_2\text{NH-}]/dt = 2k_1\,[\text{-NH}_2][\text{-NHCH}_2\text{OH}] + \{k_{-4}\text{-}(k_4/K)\}\,[\text{-NR'CH}_2\text{NH-}] \qquad (23)$$

$$d[\text{-NHCH}_2\text{OCH}_2\text{NH-}]/dt = k_2\,[\text{-NHCH}_2\text{OH}]^2 - k_{-2}\,[\text{-NHCH}_2\text{OCH}_2\text{NH-}] + \{k_{-4}\text{-}(k_4/K)\}\,[\text{-NR'CH}_2\text{OCH}_2\text{NH-}] \qquad (24)$$

$$d[\text{-NR'CH}_2\text{NH-}]/dt = 4k_5\,[\text{-N(CH}_2\text{OH)}_2][\text{-NH}_2] + \{(k_4/K)\text{-}k_{-4}\}\,[\text{-NR'CH}_2\text{NH-}] \qquad (25)$$

The rate d[ ] / dt was obtained by measuring the tangents on the curve of the concentration as a function of time. The rate constants k_1, k_2, k_{-2}, and k_5 were determined by a non linear least square fit to Eqn.(23) to (25).

3 *Rate constants*

The rate constants k_1, k_5, k_2, and k_{-2} estimated by both a molecular species approach and a functional group approach are presented in Tables VI.1 and VI.2. The rate constants are expressed in kg resin solution mol^{-1} s^{-1}.

Table VI.1 Rate constants of unsubstituted, k_1 and methylol-substituted, k_5 methylene bridge formation.

T (°C)	pH	$k_1.10^6$ [a]	$k_1.10^6$ [b] (kg $mol^{-1}s^{-1}$)	$k_5.10^6$ [a]
85	7.5	5.4 ± 0.6	3.8 ± 0.2	4.4 ± 0.7
	8.0	2.0 ± 0.3	1.4 ± 0.2	1.0 ± 0.5
	9.0	0.13 ± 0.05	0.32 ± 0.01	
	9.25	0.2 ± 0.1	0.20 ± 0.01	
	9.5	0.20 ± 0.08	0.13 ± 0.05	
90	7.5	7.7 ± 0.8	4.9 ± 0.2	8.0 ± 1.5
	8.0	2.2 ± 0.5	1.8 ± 0.1	2.4 ± 0.6
	9.0	0.3 ± 0.1	0.36 ± 0.02	
	9.5	0.24 ± 0.06	0.4 ± 0.1	
95	7.5	11.3 ± 0.9	6.9 ± 0.6	9.1 ± 1.6
	8.0	2.9 ± 0.5	2.7 ± 0.2	3.2 ± 0.3
	9.0	0.8 ± 0.3	2.0 ± 1.1	
	9.25	0.4 ± 0.2	0.5 ± 0.2	
	9.5	0.4 ± 0.1	0.6 ± 0.1	

[a] Group approach, [b] molecular species approach.

Table VI.2 Rate constants for methylene-ether bridge formation, k_2 and decomposition, k_{-2}.

T (°C)	pH	$k_2.10^6$ [a]	$k_2.10^6$ [b]	$k_{-2}.10^4$ [a]	$k_{-2}.10^4$ [b]
		(kg mol^{-1}s^{-1})		(s^{-1})	
85	7.5	3.3 ± 0.9	2.3 ± 0.2	2.3 ± 1.0	1.3 ± 0.3
	8.0	1.5 ± 0.5	1.2 ± 0.1	0.3 ± 0.2	0.7 ± 0.1
	9.0	2.3 ± 0.3	2.2 ± 0.1	0.5 ± 0.2	0.7 ± 0.1
	9.25	5.4 ± 0.5	4.4 ± 0.1	1.1 ± 0.1	1.3 ± 0.2
	9.5	9.4 ± 0.6	8.3 ± 0.6	1.3 ± 0.4	1.5 ± 0.4
90	7.5	2.4 ± 1.0		1.6 ± 0.4	
	8.0	2.0 ± 0.6	1.5 ± 0.1	1.9 ± 1.0	0.9 ± 0.3
	9.0	2.8 ± 1.0	4.1 ± 0.2		1.0 ± 0.2
	9.5	15.9 ± 0.9	17.8 ± 1.6	3.6 ± 0.7	3.0 ± 0.5
95	7.5	3.8 ± 0.1	3.7 ± 0.3	1.6 ± 0.3	2.4 ± 0.6
	8.0	5.8 ± 2.0	3.1 ± 0.4		2.1 ± 0.3
	9.0	8.1 ± 0.7		2.0 ± 0.4	2.7 ± 1.1
	9.25	20.2 ± 1.0	13.5 ± 0.8	5.4 ± 0.4	5.7 ± 0.4
	9.5	37.6 ± 3.0	36.2 ± 4.0	7.9 ± 1.0	

[a] Group approach, [b] molecular species approach.

From the data presented in Tables VI.1 and 2 the following conclusions can be drawn. First, it can be concluded that the rate constants of -$NHCH_2NH$- and -$NHCH_2OCH_2NH$- bridge formation of the group and molecular species approach are rather similar. The small differences may be attributed to the fact that the trimer formation has not been taken into account in the molecular species approach.
Secondly, the rate constants of the methylol substituted methylene bridge formation are rather similar to those of unsubstituted bridge formation, as shown in Table VI.4. Thirdly, it was found that the equilibrium constant for methylene-ether bridge formation ($K= k_2/k_{-2}$) decreases with a decreasing pH value. Theoretically, K should be independent of pH. It should be stressed, however, that the error in K is considerably larger at lower pH values. In the pH range 9-9.5 an averaged value for K at 90°C of 0.05 ± 0.01 kg mol^{-1} was obtained. However, in the pH 7-8 region a value of 0.017 ± 0.006 kg mol^{-1} for K at 90°C was found.

Finally, the deviation of concentrations calculated via kinetic rate constants from experimental concentrations was estimated by a Fortran computer program developed by Dr.J.J.H.Nusselder (DSM Research) in order to check our rate constants of the bridge formation. By means of a series of numerical integrations of supplied kinetic rate constants the program can estimate the molar concentration of the various functional groups at any given time of reaction. Rate constants of methylolation and demethylolation were taken from literature. For methylolation and demethylolation of primary amino groups rate constant data were estimated from values at 45°C determined by Gordon et al. [1] and using an activation energy of 98.74 kJ mol^{-1}. The rate constants for the addition of a second methylol group were calculated by taking into account a substitution effect of 0.6 [1,13]. The rate constant for the hydrolysis of dimethylolated amino groups was calculated from the equilibrium constant (2.1 [2]) and the rate constant for the forward reaction. The initial concentrations of the various functional groups were also fed into the computer. The resulting concentrations of the various methylene and methylene-ether bridges were compared with the experimentally observed ones. The input data for the calculation of the concentrations for the resins prepared from F/M 1.7 and pH 7.5, 8 and 9.5 at 85°C are listed in Table VI.3. The calculated and experimental plots are shown for these three MF resin formulations in Figures VI.1, 2 and 3, respectively.

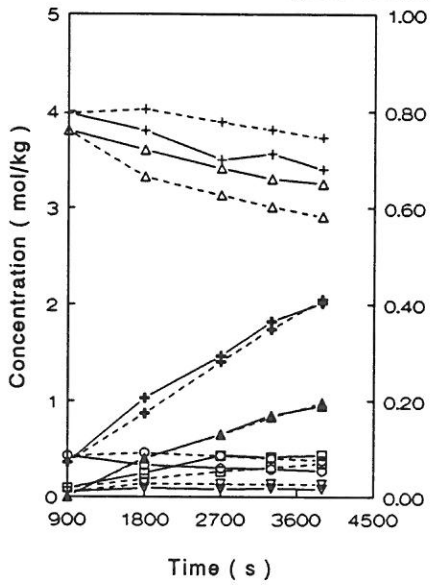

Fig.VI.1 Experimental (–) and calculated (--) concentration-time relationships for the MF resin with F/M 1.7 pH 7.5 at 85°C. Left + -NH_2, ▵ -$NHCH_2OH$, ○ -$N(CH_2OH)_2$, ▿ CH_2O, Right + -$NHCH_2NH$-, ▴ -$NR'CH_2NH$-, □ -$NHCH_2OCH_2NH$-

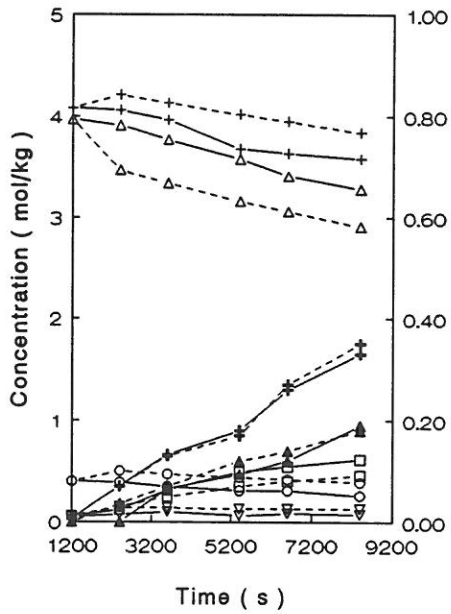

Figure VI.2 Experimental and calculated concentration-time relationships for the MF resin with F/M 1.7 pH 8 at 85°C. Symbols see Fig. VI.11

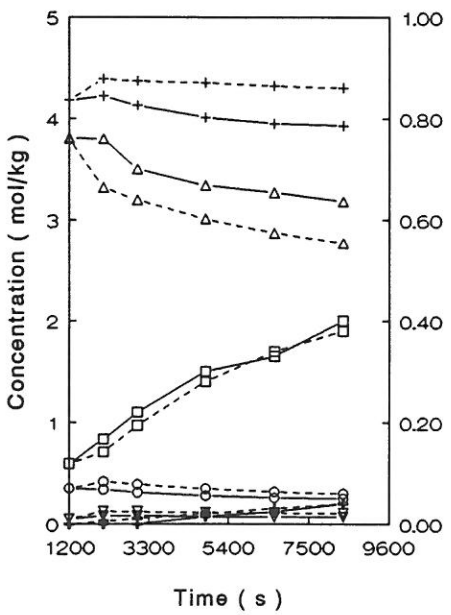

Figure VI.3 Experimental and calculated concentration-time relationships for the MF resin with F/M 1.7 pH 9.5 at 85°C. Symbols see Fig. VI.11

Table VI.3 Input data for the calculation of the concentrations of the various functional groups from kinetic rate constants.

	F/M 1.7, 85°C pH 7.5	8	9.5	F/M 2, 80°C pH 8 [9]
Rate constants, $lmol^{-1}s^{-1}$				
$k_{m1} .10^3$	9.3	9.3	40.1	3.6
$k_{-m1} .10^3$	3.1	3.1	13.5	1.1
$k_{m2} .10^3$	5.6	5.6	24.3	1.5
$k_{-m2} .10^3$	2.7	2.7	12.2	0.7
$k_1 .10^6$	5.4	2.0	0.2	3.3
$k_2 .10^6$	3.3	1.5	9.4	10000.0
$k_{-2} .10^4$	1.3	0.3	1.3	3.8
$k_5 .10^6$	4.4	1.0	-	-
Concentrations, $molkg^{-1}$				
$-NH_2$	4.00	4.08	4.18	1.5
$-NHCH_2OH$	3.80	3.97	3.80	
$-N(CH_2OH)_2$	0.43	0.40	0.35	
$-NHCH_2NH-$	0.07	0.07	-	
$-NR'CH_2NH-$	-	-	-	
$-NHCH_2OCH_2NH-$	0.02	0.01	0.12	
$-NR'CH_2OCH_2NH-$	-	-	-	
CH_2O	0.05	0.05	0.05	1.0

List of symbols k_{m1}, k_{-m1} Rate constants for methylolation and demethylolation of *primary* aminogroups, k_{m2}, k_{-m2} Rate constants for methylolation and demethylolation of *mono-methylolated* amino groups, k_1, k_2, k_{-2} and k_5 are expressed in kg $mol^{-1}s^{-1}$, see text.

It can be concluded that the concentration-time plots calculated with the experimentally determined rate constants are almost identical with the experimental plots for the bridges. The deviations for the free amino groups and methylol groups may be attributed to the use of the rate constants for methylolation and demethylolation determined in dilute solutions [1,2]. Similar agreements were found for the MF resins prepared under the other reaction conditions. These satisfying conformities indicate that (i) the rate constants of methylene bridge formation, methylene-ether bridge formation and decomposition are good and (ii) the assumptions made in the analysis of the rate constants are plausible.

4 *Comparison of the rate constants with literature data*

The kinetics of the methylene bridge formation has been studied by a number of research groups [5-9] while that of the methylene-ether bridge formation has only be studied by Nastke et al. [9] However, all studies were carried out in dilute solutions and each study was performed under different combinations of temperature, pH, concentration and reaction media as shown in the introduction. In order to compare our data with those reported in literature our rate constants were extrapolated to other temperatures by using the activation energies tabulated in Table VI.7. It is assumed that k is not influenced by F/M ratio.

It is clear from the data in Table VI.4 that the k_1 rate constants differ significantly from those of Nastke et al. [9] Better agreement is found with the value reported by Sato et al. [7] although the data are strongly extrapolated.

For the rate constants of methylene-ether bridge formation, k_2 even larger differences (~ 10^4) are found between the data obtained in our investigations and those reported by Nastke et al. [9] (Table VI.5). Therefore we repeated an experiment of Nastke et al. For the MF reaction with $[F]_0$ = 1 mol l^{-1} and F/M 2 at pH 8 and 80°C we found the following values: k_1 2.87 10^{-6}, k_2 1.11 10^{-6} and k_{-2} 4.92 10^{-5}. These data fit rather well with our previous data and do strongly deviate from the data of Nastke et al. [9].

Table VI.4 Rate constants of methylene bridge formation, comparison with literature data

T °C	pH	$k_1.10^6$ [a] l $mol^{-1}s^{-1}$	$k_1.10^6$ [b] kg $mol^{-1}s^{-1}$	Ref.
35	7.37	2.0		7
	7.50		2.7 ± 0.3	
80	7.00	182.0		9
	7.50		4.2 ± 0.5	
	8.00	33.4	1.6 ± 0.2	9
			2.8 ± 0.4 *	
	9.00	8.3	0.2 ± 0.0	9

[a] Literature data, [b] Calculated from this work, * Duplication experiment Nastke.

Concentrations of the various functional groups were estimated using the rate constants obtained by Nastke et al. The input data are tabulated in Table VI.3. The resulting concentration-time plot was compared with the experimental plot constructed from the data given in his Ph.D.Thesis [14], as shown in Figure VI.4. It can be concluded that (i) the calculated concentrations of -NH, CH_2O and -NCH_2N- agree well with the experimental values and (ii) the calculated concentrations of -NCH_2OH deviate strongly from the experimental values. The lower calculated values of -NCH_2OH groups are due to the high rate of methylene-ether bridge formation ($1.02\ 10^{-2}$). Nastke et al. did not actually measure the concentrations of methylene-ether bridges as a function of time. Therefore they were not able to check the rate constants of methylene bridge formation and decomposition obtained by their model. The concentrations of methylene-ether bridges calculated via the rate constants obtained by Nastke are significant higher than our experimentally observed concentrations (see Fig.VI.2) and do not fit our experimental data.

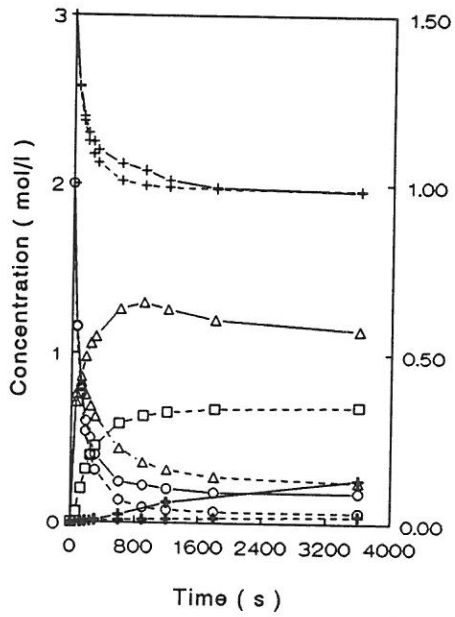

Figure VI.4 Experimental (–) and calculated (--) concentration-time relationships for a MF resin with [F] 1 mol l^{-1}, F/M 2 at 80°C. Data taken from Ref.14. Left + -NH, Right ○ CH_2O, ▵ CH_2OH, + -$NH(R')CH_2NH$- □ -$NHCH_2OCH_2NH$-.

Table VI.5 Comparison of the rate constants of methylene-ether bridge formation and decomposition at 80°C obtained in our investigations with those obtained by Nastke et al. [9].

pH	$k_2.10^6$ [a] $lmol^{-1}s^{-1}$	$k_2.10^6$ [b] $kgmol^{-1}s^{-1}$	$k_{-2}.10^4$ [a] s^{-1}	$k_{-2}.10^4$ [b] s^{-1}
7.0	6500		1.5	
7.5		2.5 ± 0.5		0.9 ± 0.2
8.0	10200	0.9 ± 0.2	3.8	0.20 ± 0.03
		1.1 ± 0.2 *		0.5 ± 0.1 *
9.0	14800	1.2 ± 0.1	9.1	0.30 ± 0.05

[a] Obtained by Nastke et al., [b] Calculated from this work,

* Duplication experiment Nastke.

5 *Discussion*

5.1 *Methylolation*

At the reaction temperatures from 85°C to 95°C methylolation and demethylolation reactions are so fast that equilibrium is reached very quickly (within ± 7 min. at 85°C). The equilibrium constants can be calculated from the molar concentrations at equilibrium. ^{13}C NMR provides differentiation between mono- and dimethylolated amino groups and the following equilibrium constants can be defined:

$$K = [\text{-NHCH}_2\text{OH}] \,/\, (2[\text{-NH}_2][\text{F}]) \qquad (26)$$

$$K' = 2[\text{-N(CH}_2\text{OH)}_2] \,/\, ([\text{-NHCH}_2\text{OH}][\text{F}]) \qquad (27)$$

Equilibrium was also established for the methylolation of methylene bridges, as discussed earlier and the equilibrium constant can be expressed as

$$K'' = [\text{-NR'CH}_2\text{NH-}] \,/\, (2[\text{-NHCH}_2\text{NH-}][\text{F}]) \qquad (28)$$

In order to calculate the equilibrium constants the concentrations of the various functional groups listed in Tables 12-25 (see appendix) were calculated in mol l^{-1} by using a density of 1.2 kg l^{-1} for a 50% resin prepared from F/M 1.7. Table VI.8 lists the K values for various pH values and temperatures.

It can be seen from the data in Table VI.6 that the equilibrium constants are independent of pH within experimental error. The lower values of K' and K" with respect to K indicate that the formation of disubstituted nitrogens is energetically less favourable. This means that the reactions will finally lead to formation of monosubstituted nitrogens. Nearly identical values of the equilibrium constants for the methylolation of a monomethylolated amino group and of a methylene bridge were obtained. Tomita et al. [2] have estimated the equilibrium constants for the nine individual reversible methylolation reactions. From these data an averaged value for K of 3.0 ± 0.9 kJ mol^{-1} and for K' of 2.1 ± 0.7 kJ mol^{-1} at pH 9 and 48°C can be calculated. It can be concluded that the values for K agree well with those obtained by Tomita et al. although they were obtained in a different way.

Table VI.6 Equilibrium constants for methylolation of a primary amino group (K), a monomethylolated amino group (K') and a methylene bridge (K").

T °C	pH	K l mol^{-1}	K' l mol^{-1}	K" l mol^{-1}
85	7.5	3.60	1.54	1.66
	8.0	3.63	1.46	1.80
	9.0	3.45	1.54	
	9.25	3.45	1.36	
	9.5	3.40	1.36	
90	7.5	3.56	1.49	1.64
	8.0	3.46	1.54	1.73
	9.0	3.31	1.46	
	9.5	3.40	1.27	
95	7.5	3.55	1.54	1.71
	8.0	3.46	1.64	1.58
	9.0	3.40	1.43	
	9.25	3.30	1.47	
	9.5	3.39	1.31	

Error 4%.

5.2 *Dependence of the rate constant of methylene bridge formation on pH*

The pH dependence of the rate constant of methylene bridge formation at 85°C, 90°C and 95°C is depicted in Figure VI.5. The log k-pH prophile can be interpreted in terms of an acid catalyzed reaction [15].

$$k_{obs} = k_0 + k_H[H_3O^+] \qquad (29)$$

where k_0 is the rate constant of the uncatalyzed (or solvent catalyzed) reaction and k_H is the rate constant of the H_3O^+ catalyzed reaction.

In the pH 7.5-8 range log k against pH gives a straight line with a slope of -1. In this region $k_H[H_3O^+]$ contributes mainly to k_{obs} and the methylene bridge formation follows an acid catalyzed mechanism. Extrapolation of this line to higher pH values (dashed line) shows the ever decreasing contribution from H_3O^+ catalyze in the increasingly alkaline medium. From pH 9 methylene bridge formation becomes very slow and is only slightly dependent on pH. In the pH 9-9.5 range the contribution of k_0 increases and the contribution of k_H decreases to k_{obs}.

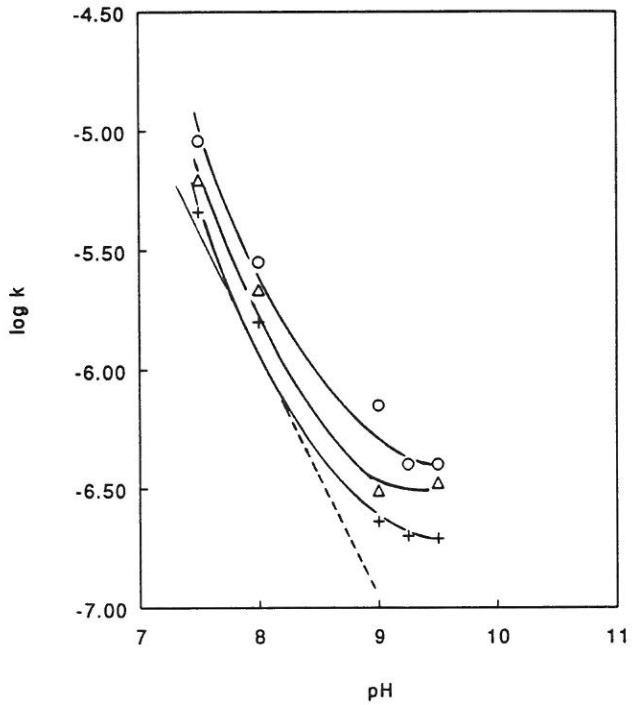

Figure VI.5 Dependence of the rate constant of methylene bridge formation on pH for an MF(1.7) resin at 85°C (+), 90°C (△) and 95°C (o).

Nastke et al. [9] concluded from their polarographic measurements that methylene bridges are also formed in alkaline media. However, they found a considerable dependence of the rate constants on F/M molar ratio in the base pH region. For F/M ratios of 2 and 3 the rate of methylene bridge formation increased again from pH 9.5-10, as shown in Figure I.3. Our results do not preclude that the rate constants of methylene bridge formation will increase again from pH 9.5. However, at high pH values the Cannizzaro reaction is favoured so that experimental confirmation would be difficult.

5.3 *Dependence of the rate constants of methylene-ether bridge formation and decomposition on pH.*

The dependence of the rate constants of methylene-ether bridge formation and decomposition at 85°C, 90°C and 95°C on pH is shown in Figure VI.6.

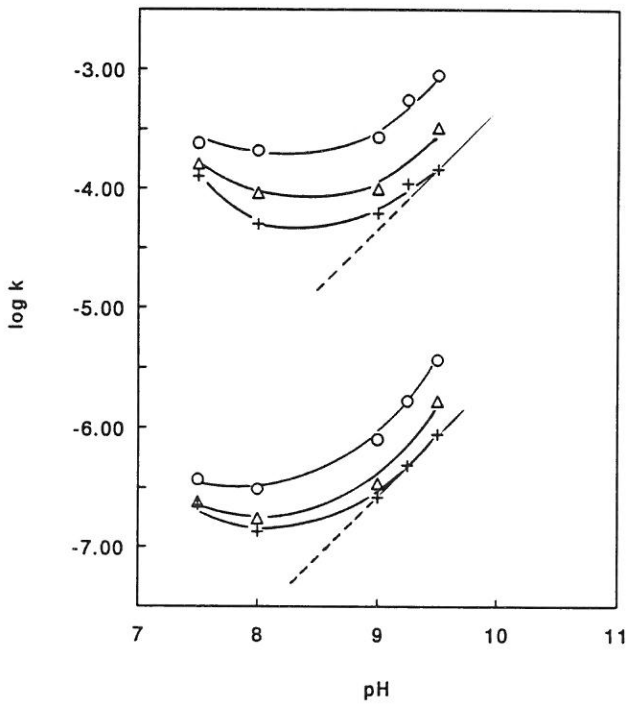

Figure VI.6 Dependence of the rate constants of methylene-ether bridge formation (lower) and decomposition (upper) on pH for a MF(1.7) resin at 85°C (+), 90°C (Δ) and 95°C (o).

The rate constants of both methylene-ether formation and decomposition passe a minimum at pH 8. The constitution of the log k-pH prophiles of the methylene-ether bridge formation and decomposition is determined by the relative magnitudes of k_0, k_H and k_{OH}, like that of a acid-base catalyzed reaction [15].

$$k_{obs} = k_0 + k_H[H_3O^+] + k_{OH}[OH^-] \qquad (30)$$

At pH values > 9 a linear relationship (slope 1) was found between log k_2 (k_{-2}) and pH. At pH 9.25 and 9.5 the third term on the right hand side of eq.(30) contributes mainly to k_{obs}. Thus, the methylene-ether bridge formation is catalyzed by OH^- ions in this pH region. With increasingly acid medium the contribution of the base-catalyzed mechanism decreases and the contributions of k_0 and k_H become more and more significant. At pH 7.5, the rate constants of both the forward and reverse reactions start to increase again. This may indicate that methylene-ether bridge formation is catalyzed by H_3O^+ ions in more acid media. This will be demonstrated by the results of hydrolysis experiments of methylene-ether dimelamine.

The results of the variation of the rate constant of the hydrolysis of methylene-ether dimelamine at 85°C with pH are shown in Figure VI.7. Methylene-ether dimelamine was collected by HPLC on analytical scale and the decomposition of methylene-ether dimelamine in diluted aqueous solutions as a function of pH was followed by HPLC.

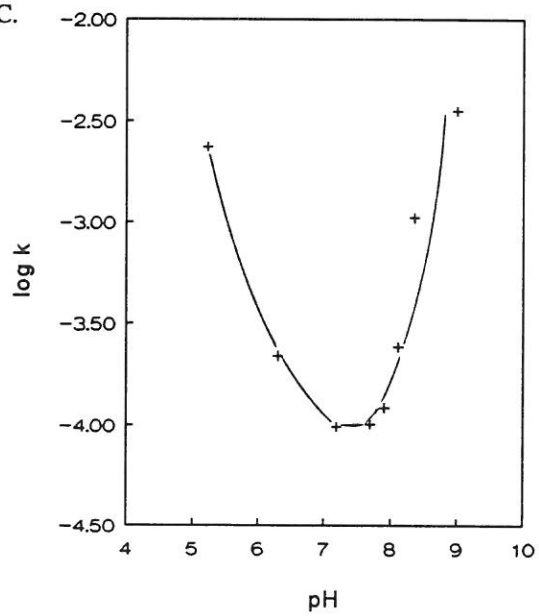

Figure VI.7 Rate constants of the hydrolysis of methylene-ether di-melamine as a function of pH at 85°C.

It is clear that besides OH^--catalyze the hydrolysis reaction is also catalyzed by H_3O^+ ions. This would only become apparent at low pH values. It is impossible to measure the forward reaction in this low pH range because of the fast increase of the condensation rate. Theoretically the equilibrium constant should be independent of pH, so the rate constant of the methylene-ether bridge formation may be expected to be also catalyzed by H_3O^+ ions. The methylene bridge formation is also catalyzed by H_3O^+ ions. This results in a competition between methylene and methylene-ether bridge formation reactions during the final cure process under acid conditions.

5.4 Rate constants as a function of temperature

The rate constants k_1, k_2 and k_{-2} were estimated at three different temperatures 85°C, 90°C and 95°C, respectively. Hence, the activation energies could be calculated from the slope of the Arrhenius plot. As an example, the Arrhenius plots obtained for the methylene bridge formation at various pH values are shown in Figure VI.8.

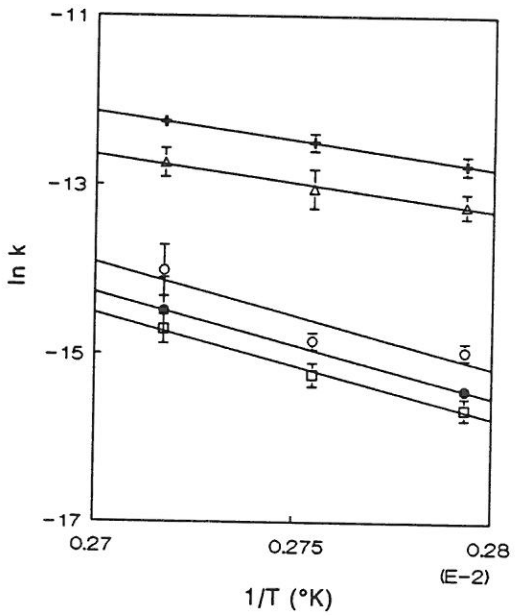

Figure VI.8 The temperature dependence of the rate constants of methylene bridge formation. pH 7.5 + , pH 8 ▵ , pH 9 ○ , pH 9.25 ● , pH 9.5 □

The activation energies for the methylene bridge formation, methylene-ether bridge formation and decomposition are tabulated in Table VI.7. As argued above, the relative contributions of k_0, k_H and k_{OH} to k_{obs} change with pH. In the pH 7.5-8 range the activation energy for the methylene bridge formation corresponds to the acid catalyzed mechanism and in the pH 9-9.5 range the activation energies for the methylene-ether bridge formation and decomposition correspond to a base catalyzed mechanism. In the other pH regions k_H , k_{OH} as well as k_0 contribute to the experimentally observed rate constant and the mechanisms for the methylene, methylene-ether bridge formation and decomposition are no longer unambigious.

The mean activation parameters ($\Delta^{\neq}H$, $\Delta^{\neq}G$, $\Delta^{\neq}S$) are tabulated in Table VI.8. $\Delta^{\neq}H$ was obtained from the slope of the Eyring plot in which ln(k/T) is plotted against 1/T. $\Delta^{\neq}G$ was obtained by using the following equation:

$$k = RT/Nh \exp(-\Delta^{\neq}G/RT) \qquad (31)$$

in which R is the molar gas constant, N is Avogadro's number and h is the Planck constant. Finally $\Delta^{\neq}S$ was calculated from equation (32)

$$\Delta^{\neq}S = (\Delta^{\neq}H - \Delta^{\neq}G)/T \qquad (32)$$

Table VI.7 Apparent activation energies of the condensation reactions.

	pH	E_a (kJ mol^{-1})
Methylene bridge formation	7.5	73 ± 15
	8.0	56 ± 20
	9.0	108 ± 48
	9.25	100 ± 25
	9.5	120 ± 44
Methylene-ether bridge formation	7.5	67 ± 20
	8.0	99 ± 23
	9.0	136 ± 14
	9.25	134 ± 7
	9.5	156 ± 5
Methylene-ether decomposition	7.5	65 ± 35
	8.0	115 ± 30
	9.0	150 ± 17
	9.25	170 ± 30
	9.5	171 ± 36

Table VI.8 Mean activation parameters over the temperature range 358-368°K

	pH range	$\Delta^{\neq}H$ kJ mol^{-1}	$\Delta^{\neq}G$ kJ mol^{-1}	$\Delta^{\neq}S$ J mol^{-1}K^{-1}
Methylene bridge formation	7.5-8.0	64 ± 13	104 ± 3	-144 ± 13
Methylene-ether bridge formation	9.0-9.5	141 ± 10	102 ± 3	107 ± 10
Methylene-ether bridge decompostion	9.0-9.5	167 ± 26	95 ± 2	200 ± 27

5.5 *Equilibrium constant for methylene-ether bridge formation as a function of temperature*

ΔH^0 for the methylene-ether bridge formation can be calculated from the temperature dependence of the equilibrium constant according to the van't Hoff equation (33).

$$\Delta H^0 = -R[\delta \ln K / \delta(1/T)] \qquad (33)$$

An averaged value of -14.3 ± 6.0 kJ mole^{-1} was calculated for the standard heat of the methylene-ether bridge formation. The value of ΔH^0 is similar within experimental error to that obtained from the DSC measurements. The standard free energy change ($\Delta G^0 = -RT \ln K$) and the standard entropy change ($\Delta S^0 = [\Delta H^0 - \Delta G^0] / T$) for the methylene-ether bridge formation were calculated at 363 K, giving values of 9.4 ± 0.2 kJ mol^{-1} and -64.5 ± 6 J mol^{-1} K^{-1}, respectively.

6 *Conclusions*

Rate constants for methylene bridge formation (either non-substituted or methylol substituted), methylene-ether bridge formation and decomposition have been determined for an MF(1.7) resin as a function of pH and temperature. Two different approaches were used to determine the rate constants of the condensation reactions. In the first approach the rate constants for two MF dimers were esimated from the quantitative analysis of melamine species by HPLC. In the second approach, the rate constants for methylene bridge formation, methylene-ether bridge formation and hydrolysis were estimated from concentrations of the functional groups ($-NH_2$, $-NHCH_2OH$, $-N(CH_2OH)_2$ etc.) detected by ^{13}C NMR as a function of time.

The rate constants of methylol-substituted methylene bridge formation are practically identical to those of the non-substituted bridge formation. Similar values were calculated for the equilibrium constants of the methylolation of a methylene bridge and the methylolation of a monomethylolated amino group. The rate constants for methylene bridge formation, methylene-ether bridge formation and hydrolysis are clearly dependent of pH. Methylene bridge formation is catalyzed by H_3O^+ ions. Methylene-ether bridge formation and hydrolysis are catalyzed by H_3O^+ and OH^- ions. For the equilibrium constant of reversible methylene-ether bridge formation a value of 0.05 ± 0.01 kg mol^{-1} was obtained at 90°C in the pH 9-9.5 range. Activation energies for the methylene bridge formation, methylene-ether bridge formation and hydrolysis were calculated from the temperature dependence of the rate constants. The enthalpy for the methylene-ether bridge formation was calculated from the temperature dependence of the equilibrium constant. This value is in accordance with that obtained by DSC.

7 *Experimental*

7.1 *Resin preparation*

The aqueous melamine formaldehyde resins were all synthesized in 230 g batches from melamine, 32 % (m/m) formalin and an appropriate amount of water resulting in a resin with a given solids content (s.c.). The solids content of an MF resin is defined as:

$$s.c.(\%) = \frac{m\,M + m\,F}{m\,M + m\,F + m\,H_2O} \times 100 \qquad (34)$$

in which m is the mass

After addition of water to formalin the required pH was adjusted at room temperature by the addition of 1M aqueous sodium hydroxide solution. The resins were synthesized in a three necked vessel (250 ml) to allow insertion of pH and temperature probes and a stirrer. The raw materials were placed into the vessel and the moment of mixing was taken as t=0. The reaction mixture was heated very quickly so that the reaction temperature (85, 90, 95°C) was reached in about 2 minutes and the pH was adjusted continuously by the addition of 1M NaOH or 1M HCOOH. The pH was controlled continuously with an electrode calibrated at the reaction temperature. The variation of the reaction conditions is summarized in Table VI.9. Samples taken after reaction for several lengths of time, were analyzed by ^{13}C NMR and HPLC. The NMR analysis of the resins was conducted within one or two days. In the mean time the resin solutions were placed in a refrigerator at 4°C to ensure that the resin structure remained unchanged (checked by ^{13} NMR). The HPLC experiments were carried out within one day. The samples dissolved in eluent were also placed in a refrigerator at 4°C in the mean time.

Table VI.9 Synthesis parameter variation.

T (°C)	F/M	s.c.	Constant pH
85	1.7	50%	7.5 8.0 9.0 9.25 9.5
90	1.7	50%	7.5 8.0 9.0 9.5
95	1.7	50%	7.5 8.0 9.0 9.25 9.5

7.2 *Methods*

13C NMR

^{13}C NMR spectra from the aqueous MF resins were obtained on a Varian unity-400 spectrometer. DMSO-d_6 was added as a locking reagent to the aqueous MF resin solutions. The carbon chemical shifts were calibrated by defining the ^{13}C chemical shift of DMSO-d6 as 39.5 ppm. For quantitative measurements a preparation time of 12.5 seconds between repetitive acquisitions was shown to be adequate from spin-lattice relaxation time (T_1) measurements (Chapter 2).

HPLC

A model 1050 liquid chromatograph (Hewlett Packard), equipped with a calibrated Linear UVIS 206 detector was operated at room temperature for the analysis of the aqueous MF resins. Liquid chromatography was applied for the quantitative analysis of methylolmelamines, some distinct dimers and free formaldehyde in the MF reaction mixtures. Melamine, mono- and di-methylolmelamine were determined at 235 nm and the other methylolmelamines and dimers were determined at 210 nm. A stainless steel Chrompack column (250 mm x 4.6 mm i.d.) was used with Inertsil ODS-2 as a stationary phase. The eluent used was an acetronitrile-water (1 g phosphoric acid/l water adjusted at pH 6.8 with 1 M NaOH) mixture at a combined flow rate of 1 ml min^{-1}. The solvent programme is given in Table VI.10.

Table VI.10 Solvent programme for HPLC analysis.

Time (min.)	% CH_3CN
0	1
40	10
50	20
55	1

Determination of the response factors of methylolmelamines and dimers

Relative response factors (with respect to melamine) were defined for the various methylolmelamines, methylene-ether dimelamine and monomethylolated methylene-ether dimelamine because (i) melamine is the only pure component and (ii) the methylolmelamines and methylene-ether dimelamines decompose on dissolution in water. The relative response factors (R) were determined in the following way. The various methylolmelamines and methylene-ether dimelamines were collected by HPLC. Each isolated peak was further diluted with eluent and the vial was sealed. They were immediately placed in a refrigerator to ensure that no further decomposition took place. One part of the isolated methylolmelamines was reinjected and the peak area with regard to the methylolmelamine ($A_{methylol}$) was measured. The other part was decomposed at 60°C into melamine and free formaldehyde and the peak area of melamine ($A_{melamine}$) was measured. R was calculated from the ratio of the area of the methylolmelamine to the area of melamine.

$$R = A_{methylol} / A_{melamine} \qquad (35)$$

Values of 2.00 and 2.20 area / mmole were estimated for the molar relative response factors of methylene dimelamine and monomethylolated methylene dimelamine, respectively.

For quantitative measurements it is necessary to use a fixed wavelength detector, e.g., a Zn lamp λ 214 nm. This is necessary because small deviations in the wavelength adjustment of the detector can cause large analysis errors. A second possibility is the use of a 'high precision' variable wavelength detector. However, in this case the relative response factors have to be determined with that specific detector because the accuracy of the relative response factors is strongly dependent on the accuracy with which the wavelength of the detector can be adjusted or reproduced (high precision). The molar relative response factors of the various methylolmelamines and dimers to a Linear UV 206 detector at 210 nm and 235 nm are given in Table VI.11.

*Table VI.11 Molar relative response factors of methylolmelamines and dimers to a Linear UVIS 206 detector at 210 nm and 235 nm *.*

Compound	Factor (area/mmole)
melamine	1.00 *
mono-methylolmelamine	1.43 *
N,N di-methylolmelamine	2.22 *
N,N' di-methylolmelamine	1.95 *
N,N,N' tri-methylolmelamine	1.40
N,N',N" tri-methylolmelamine	1.58
N,N,N',N' tetra-methylolmelamine	1.30
N,N,N',N" tetra-methylolmelamine	1.47
penta-methylolmelamine	1.36
hexa-methylolmelamine	1.29
methylene dimelamine	2.00
monomethylolated methylene dimelamine	2.20
methylene-ether dimelamine	2.20
monomethylolated methylene-ether dimelamine	2.40

Determination of the free formaldehyde content

The free formaldehyde contents of the MF reaction mixtures were determined by means of a post-column derivatization reaction in which formaldehyde reacts at 95°C with 2,4-pentadione and ammonium acetate to give diacetyldihydrolutidine [16]. The formed diacetyldihydrolutidine was determined by fluorescence detection at 510 nm and excitation at 410 nm.

Hydrolysis of methylene-ether dimelamine

Methylene-ether dimelamine was collected by HPLC on an analytical scale. The collected peaks were further diluted with water and adjusted to pH at the temperature at which the decomposition is studied with an electrode also calibrated at that temperature. This solution was distributed over several glass-tubes. Each tube was sealed-melted to prevent loss of material and then placed in a water bath regulated at the desired temperature for a certain length of time.

7.3 *pH measurement*

The pH of MF reaction mixtures can be measured at room temperature after cooling the resin solution to room temperature or at the reaction temperature. In alkaline media, it was observed that the pH value measured at room temperature is about 1.5 pH units higher than that measured at 95°C. These large differences ask for further explanation. First, the ion product of water is a function of temperature. The temperature dependence of pH for solutions of strong acids and strong bases is given in equations (36) and (37), respectively.

$$\frac{\delta p_H}{\delta T} = -\left(\frac{\delta \log \gamma}{\delta T}\right) \tag{36}$$

$$\frac{\delta p_H}{\delta T} = -\left(\frac{\delta \log K_w}{\delta T}\right) + \left(\frac{\delta \log \gamma}{\delta T}\right) \tag{37}$$

where γ is the activity coefficient of an average univalent ion. The temperature coefficients of log K and log γ, in terms of which the temperature coefficient of pH is expressed, can readily be obtained for many buffer systems from data in literature [17]. It can be noticed that the change of the activity coefficient with temperature is so small that it is often completely overshadowed by $\delta \log K / \delta T$. The large negative temperature coefficient of pK_w (-0.0330) accounts for the large decrease of the pH value in alkaline media with increase of temperature. In addition the buffer capacity of formaldehyde may change as a function of temperature.

For kinetic purposes, it is interesting to know the activity of H_3O^+ ions at the various reaction temperatures by which the rate constants were estimated. Since the potentiometrically measured pH value is a direct measure for the activity of H_3O^+ ions the pH was always measured at the reaction temperature with an electrode also calibrated at the reaction temperature.

8 *References*

[1] M.Gordon, A.Halliwell and T.Wilson, *J.Appl.Polym.Sci.*, 10, 1153 (1966).

[2] B.Tomita, *J.Polym.Sci.,Polym.Chem.Ed.* , 15, 2347, (1977).

[3] K.Sato, *Bull.Chem.Soc.Jpn.*, 40, 2963 (1967).

[4] K.Sato and S.Ouchi, *Polymm.J.*, 10, 1 (1978).

[5] M.Okano and Y.Ogata, *J.Am.Chem.Soc.* 74, 5728 (1952)

[6] K.Sato, *Bull.Chem.Soc.Jpn.* 41, 7 (1968)

[7] K.Sato and T.Naito, *Polym.J.* 5(2), 144 (1973)

[8] A.Berge, *Adv.Org.Coat.Sci.Technol.Ser*, 1, 23 (1979).

[9] R.Nastke, K.Dietrich, G.Reinisch, G.Rafler, *J.Macromol.Sci.Chem.*, A23(5), 579 (1986).

[10] A.Kumar and V.Katiyar, Macromolecules, 23, 3729 (1990).

[11] S.K.Gupta, A.K.Gupta, A.K.Ghosh, A.Kumar, *Frontiers in Chemical Reaction Engineering*, L.K.Doraiswamy, R.A.Mashelkar, Eds., Wiley Eastern, New Delhi, India, 1984.

[12] S.K.Gupta, *J.Appl.Polym.Sci.*, 31, 2805 (1986).

[13] J.Aldersley, M.Gordon, A.Halliwell, T.Wilson, *Polymer*, 9(7), 345 (1968).

[14] R.Nastke, Ph.D.Thesis, DDR, 1982.

[15] H.Maskill, *The physical basis of organic chemistry*, Oxford University Press, New York, 1985.

[16] S.Belman, *Anal.Chem.Acta*, 29, 120 (1963).

[17] R.G.Bates, Determination of pH; Theory and Practice, 2nd.Ed., Wiley, New York.

CHAPTER 7

STUDY OF MF RESIN FORMATION IN THE EARLY STAGES OF THE CONDENSATION

1 Introduction

Melamine-formaldehyde resin formation consists of two stages. In the first stage a low molecular weight resin is produced that is suitable for the manufacture of adhesives, moulding powders, laminates etc. Manufacturing of these resins can be done by impregnation or by blending the resin with fillers or pigments. During the curing (second) stage these intermediates are transformed to the desired MF materials. Precise control of the evolution and the extent of the reaction is essential for a successful manufacture of the intermediate MF resins [1,2]. In industrial practice the MF reaction is still checked by measurement of bulk properties such as pH, cloud point and water tolerance. The water tolerance is defined as the maximum degree of dilution of an MF resin solution with water until turbidity persists.

Herma et al. [3] have studied the influence of pH, temperature and F/M molar ratio on the chemical composition of melamine-formaldehyde moulding powders. The evolution of the condensation was followed by determining the water tolerance and the number of methylene bridges. A decrease in the water tolerance with an increasing number of methylene bridges was observed. However, a quantitative relation between both parameters could not be derived. Polarography was used for the determination of the methylol groups and methylene bridges. The formaldehyde bound in ether structures was determined by oxidation. They found that the concentration of methylene bridges increases with a decreasing pH value whereas the concentration of ether-formaldehyde increases with an increasing pH value and F/M ratio. Subsequently the relation between the composition of the resin and the manufacturing of the resins and the resin properties has been studied by the same authors [4-6].

In this chapter the chemical structure of industrial MF resins has been studied. These resins differ from those studied in the former chapter since the pH is not kept

constant during reaction. The chemical structure of these industrial MF resins is studied as a function of pH, F/M molar ratio, solids content and reaction time by means of ^{13}C NMR. Secondly attention is paid to the relation between the evolution of pH and water tolerance and the evolution of the bridges during the resin synthesis.

2 *The influence of the reaction parameters on the chemical structure of MF resins*

The functional group analysis obtained by ^{13}C NMR is given in Tables 1-11 (see appendix) for the various resin formulations. The concentrations of the various methylene carbons are expressed in mole per kg resin. The calculation of the concentrations of the various functional groups from the intensities of the carbon resonances is described in Chapter 2. In subsequent sections the effect of the initial formalin pH, the effect of F/M ratio and the effect of solids content will be dealt with.

2.1 *Effect of initial formalin pH*

The ^{13}C NMR results of the MF resins prepared from various formalin pH values varied between 7 and 10 listed in Tables 1-6 show (i) a clear dependence of the concentrations of methylene bridge and methylene-ether bridges on the pH value, (ii) a similar chemical composition for the MF resins with and without acidification during the synthesis, (iii) the presence of a relatively large amount of substituted methylene bridges for resins prepared at lower pH values and (iv) variations in the concentration of dimethylolated amino groups as a function of pH after reaction for 30 min.

Figure VII.1 shows the concentrations of methylene and methylene-ether bridges at various reaction times for the MF resins prepared from various formalin pH values. The resins prepared from lower formalin pH's contain relatively more methylene bridges and those prepared from higher formalin pH's contain relatively more methylene-ether bridges. In more alkaline media, methylene-ether bridges are formed faster but are also more quickly subjected to hydrolysis. The evolution of the methylene and methylene-ether bridges as a function of time will be discussed in more detail in the next section.

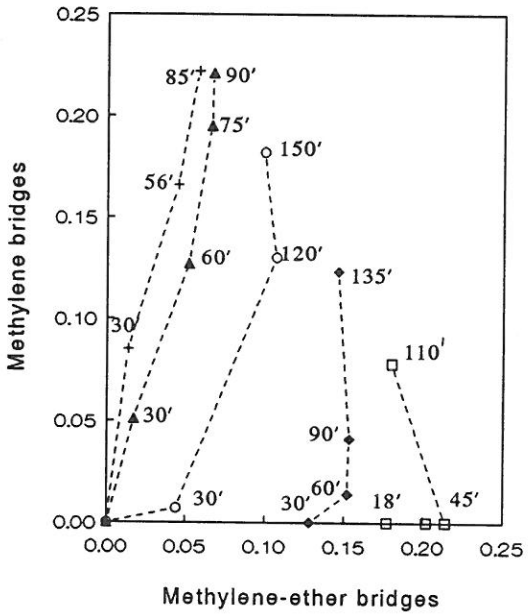

Figure VII.1 Concentrations of methylene and methylene-ether bridges (mole / mole M) at various reaction times at 95°C for MF(1.7) resins prepared from various formalin pH values: 10 (□), 9.5 (◆), 9 (○), 8 (▲) and 7 (+).

Secondly, the effect of a sudden acidification during the resin synthesis on the chemical structure of the MF resin is studied. The MF resin prepared from an initial pH value of 9.5 was suddenly acidified to pH 7.0 after reaction for 30 minutes. Figure VII.2 shows the concentrations of methylene and methylene-ether bridges as a function of time for the MF resins with and without acidification during the resin synthesis. Interestingly both resins finally have the same chemical composition. The only difference is the duration of reaction to reach this degree of condensation.

A third observation which emerges from the data in Tables 1-6 is the larger amount of substituted bridges for MF resins prepared from pH 7-8 than the resins prepared in more alkaline medium. The ratio of substitued to non-substituted bridges is about 0.4 for the pH (7-8) resins and about 0.2 for the pH (9-10) resins. The methylene bridges were mainly substituted by a methylol group as was observed from the appearance of a distinct shoulder on the carbon signal at 71.6 ppm of methylol groups substituted on a tertiairy nitrogen simultaneously with the substituted methylene bridges in the ^{13}C NMR spectrum (Chapter 2).

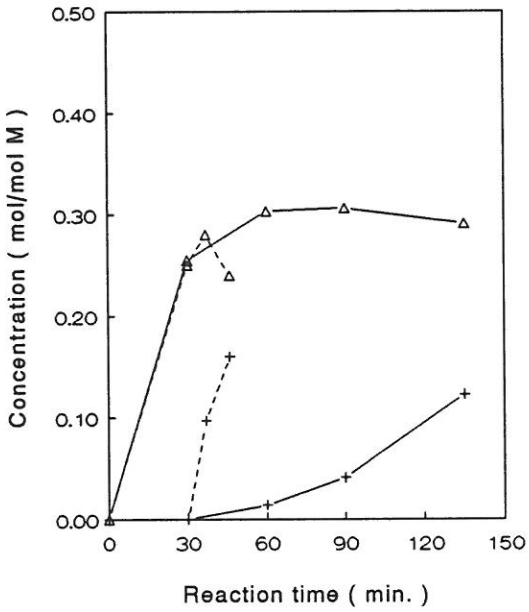

Figure VII.2 Concentration-time relationships of methylene (+) and methylene-ether (△) bridges at 95°C for MF(1.7) resins prepared from pH 9.5 with (--) and without (–) acidification after 30 minutes.

The fourth remarkable fact derived from the ^{13}C NMR results is the variation in the concentration of dimethylolated amino groups with pH after reaction for 30 min. The MF resins prepared from pH 9.5 and 10 contain a smaller number of dimethylolated amino groups relative to monomethylolated amino groups than the pH (7-9) resins. Since the molecular methylol distribution can be studied in more detail by HPLC the observed variations will be explained by means of the following experiment. The variations of the methylol distribution were followed by HPLC for an MF resin (F/M 1.5, pH 9 and s.c. 50%) that was heated with a heating rate of 1°C/min to 95°C. The variations of the methylol distribution during reaction at 95°C are shown in Fig.VII.3. In the beginning the formation of higher methylol homologues is observed. However, fast rearrangement of methylol groups among different methylolmelamine species takes place and the reactions lead finally to formation of monosubstituted nitrogens. This is caused by the fact that substitution on a secondary nitrogen is unfavoured compared to substitution on a NH_2 group. The rate constants of methylolation and demethylolation increase significantly from pH 9 to higher pH values, as shown in Figure I.1.

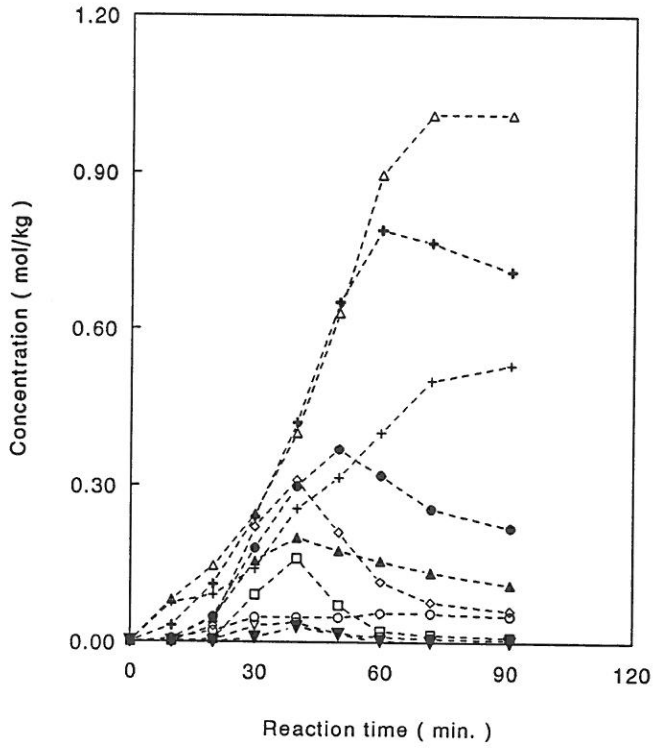

Figure VII.3 Concentration of each methylolmelamine as a function of time at 95°C for MF(1.7), pH 9.5. Left I (+), II' (△), II (○), III' (+), III (▲) Right IV' (●), IV (▽), V (◇), VI (□). Symbols see Figure I.1.

So, the dimethylolated amino groups are converted more rapidly to monomethylolated ones for MF reaction mixtures prepared at higher pH values. This explains the lower concentration of dimethylolated amino groups after reaction for 30 minutes for the resins prepared at higher pH values compared to those prepared at lower pH values.

2.2 *Effect of F/M molar ratio*

In this study the changes in chemical composition of MF resins prepared from F/M molar ratios of 1.5, 1.7, 2.2 and 3.0 were examined. The functional group analysis obtained by ^{13}C NMR for these MF resins is presented in Tables 4, 7, 8 and 9, respectively.

Figure VII.4 shows an increasing number of methylene-ether bridges with increasing F/M ratio. Methylene-ether bridges are formed by reaction of two $-NCH_2OH$ groups whereas methylene bridges are formed by reaction of a -NH group and a $-NCH_2OH$ group. The relative increase in the concentration of $-NCH_2OH$ groups to that of -NH groups with increasing F/M ratio favours the methylene-ether bridge formation rather than methylene bridge formation. The evolution of the methylene and methylene-ether bridges as a function of time will be discussed in more detail in the next section.

The incorporation of a greater amount of formaldehyde into the resin increases the likelihood of formation of $-N(CH_2OH)_2$ groups and substituted bridges as shown in Tables 8 and 9. The substituent on the bridges can either be a methylol group, a methylene bridge or a methylene-ether bridge. In the ^{13}C NMR spectrum of the MF resin (F/M 3 pH 9.5 reacted for 108 min. at 95°C) a relatively larger intensity of substituted methylene and methylene-ether bridges is accompanied by the appearance of a much smaller shoulder at 71.6 ppm (Fig. VII.5) compared to the MF 1.7 resin shown in Figure II.6. This implies that more cross-links (bridges substituted by another bridge) were formed in the MF 3.0 resin than in the 1.7 resin.

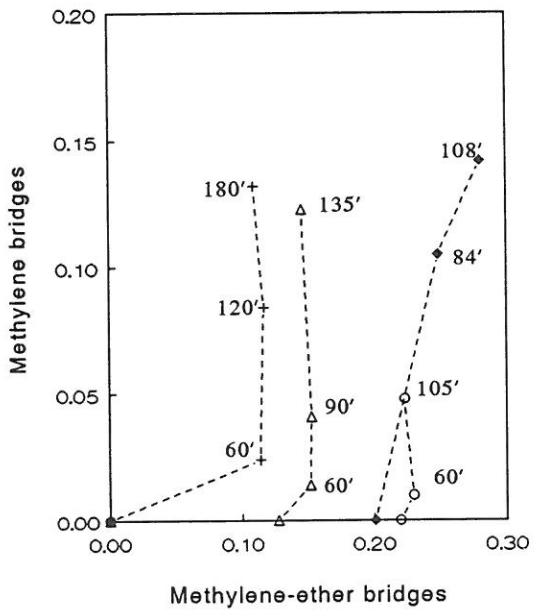

Figure VII.4 Concentrations of methylene and methylene-ether bridges (mole / mole M) at various reaction times at 95°C for MF resins with various F/M ratios. + F/M 1.5, ▵ F/M 1.7, O F/M 2.2, ◆ F/M 3.

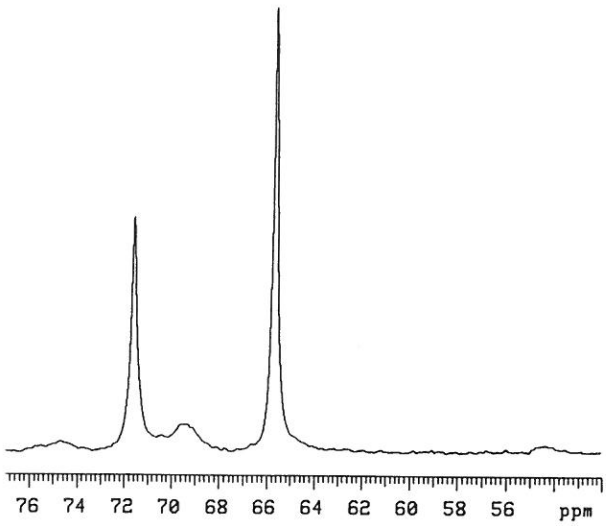

Figure VII.5 ^{13}C NMR spectrum from 52-77 ppm of a MF resin (F/M 3.0 pH 9.5 cured for 108 min. at 95°C).

Methylene bridges of which the two amino groups are disubstituted are not present at levels detectable by ^{13}C NMR, in agreement with findings of Tomita et al. [7] and Pash et al. [8]. There is no consensus in the published literature concerning the formation of these methylene bridges in MF resins. Studies by Tomita and Ono and by Pasch et al. indicate that these bridges are absent (< detection limit) in MF resins. Studies on a model compound for alcoholated MF resins, e.g., N,N dimethoxymethyl-N',N',N",N"-tetramethylmelamine by Wicks and Hsia [9] showed the formation of a cyclic trimer by reaction of this model compound with water in the presence of a catalyst. The structure of the cyclic trimer was confirmed by NMR, elemental analysis and mass spectrometry.

2.3 *Effect of solids content*

All MF resins studied so far were synthesized from a 50% solids content. The chemical structure of the resin resulting from synthesis at a lower concentration, i.e., 10% and 25 %, will be studied in this section. The functional group analysis of the three MF resins obtained by ^{13}C NMR is shown in Tables 4, 10 and 11, respectively. First, an increase in the fraction of unreacted formaldehyde can be observed with a lowering of the solids content. The percentage free formaldehyde

detected after reaction for 30 min. increases from 2.1 to 6.3 when going from a 25% to a 10% resin. Secondly, large differences in the relative ratio of methylene and methylene-ether bridges are observed for the various resins, as shown in Figure VII.6. From Fig.VII.9 it can be seen that the pH falls more rapidly for lower concentration resins. For the 10% resin the pH already reached a value of 7.92 after reaction for 30 min. Figure VI.5 and 6 show that in this pH region methylene bridges are formed rather than methylene-ether bridges. So, the large differences in methylene versus methylene-ether bridge formation as a function of the solids content originate from a different evolution of pH during reaction. This will be discussed in more detail in the next section.

It can be concluded that the resin concentration has a significant effect on the chemical composition of the low molecular weigt MF resin.

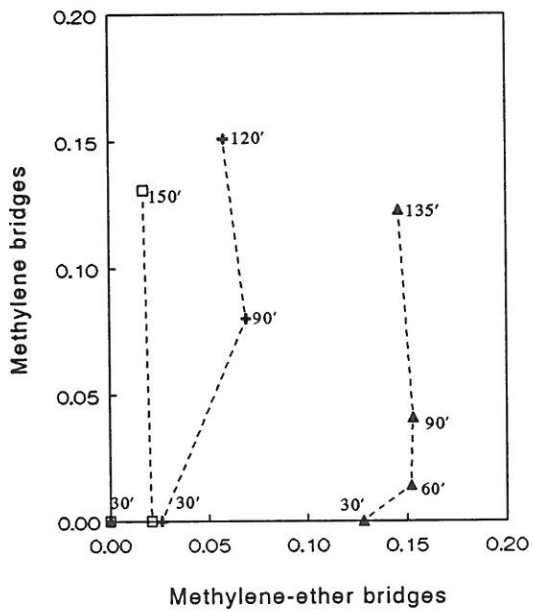

Figure VII.6 Concentrations of methylene and methylene-ether bridges (mole / mole M) at various reaction times at 95°C for 50% (▲), 25% (+) and 10% (□) MF(1.7) resins.

3 *MF resin formation*

Industrial MF resins are usually made by a batch process. The formalin adjusted to pH and melamine are charged into a kettle and the reaction is started. The extent of the condensation reaction is checked regulary by measuring the water tolerance of the MF resin solution. In this section the chemical aspects of (i) the evolution of pH and (ii) the evolution of the water tolerance are studied.

3.1 *Chemical aspects of the evolution of pH*

Figure VII.7 shows the evolution of pH at 95°C during reaction of melamine with formaldehyde for MF resins prepared from F/M 1.7 and various formalin pH values. The observed evolution of pH in the beginning results from a combination of the heating of the electrode and the reaction mixture, a decrease of the buffer capacity of formaldehyde due to consumption of formaldehyde in the methylolation reactions and a change in the composition of the reaction medium. The formation of formic acid by the Cannizzaro reaction [10-12] shown in equation (1) and changes in the buffer capacity of formaldehyde and melamine are the main reasons for the fall of pH during reaction.

$$2\ CH_2O + H_2O \rightarrow HCOOH + CH_3OH \qquad (1)$$

The Cannizzaro reaction is catalysed by alkalies and occurs at pH values > 8.6. This reaction also depends on the concentration of free formaldehyde which in turn is determined by the F/M ratio and the concentration. The evolution of pH during reaction at 95°C for the resins prepared from various F/M molar ratios and various solids contents is shown in Figures VII.8 and VII.9, respectively.

The evolution of the methylene and methylene-ether bridges has been determined as a function of time by means of ^{13}C NMR (see appendix Tables 1-11). The evolution of the bridges as a function of time is determined by the kinetics of the condensation reactions and the concentrations of -NH and -NCH_2OH groups. As shown in Chapter 6 the rate constants of the bridge formation are strongly dependent of pH.

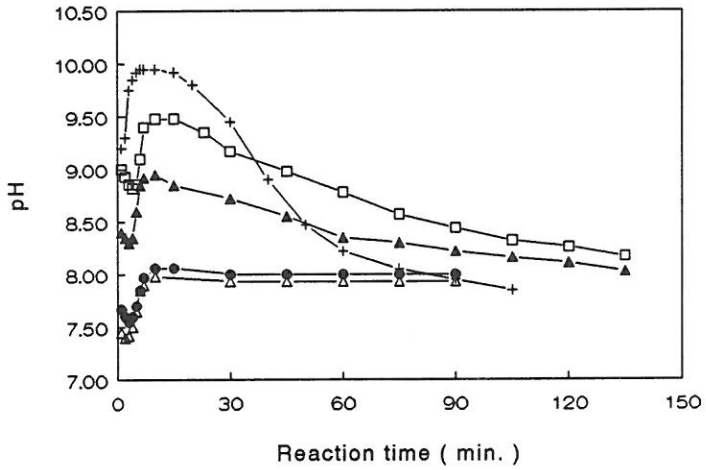

Figure VII.7 Evolution of pH during reaction at 95°C of 50% MF resins prepared from F/M 1.7 and various initial pH values: 10 (+), 9.5 (□), 9 (▲), 8 (●), 7 (△).

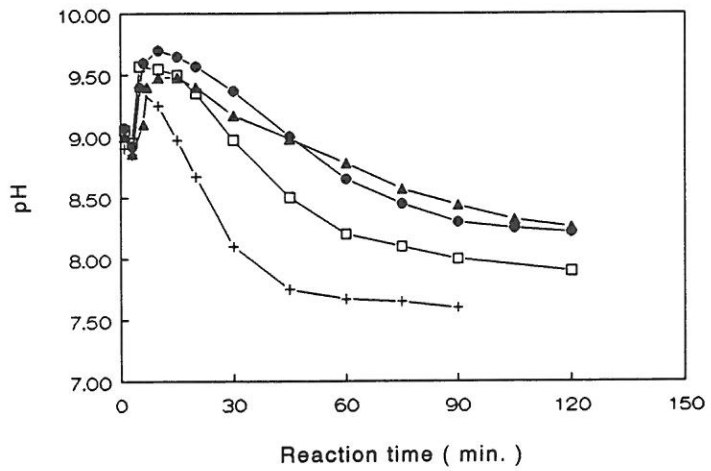

Figure VII.8 Evolution of pH during reaction at 95°C of 50% MF resins prepared from pH 9.5 and various F/M ratios: 3 (+), 2.2 (□), 1.7 (▲) and 1.5 (●).

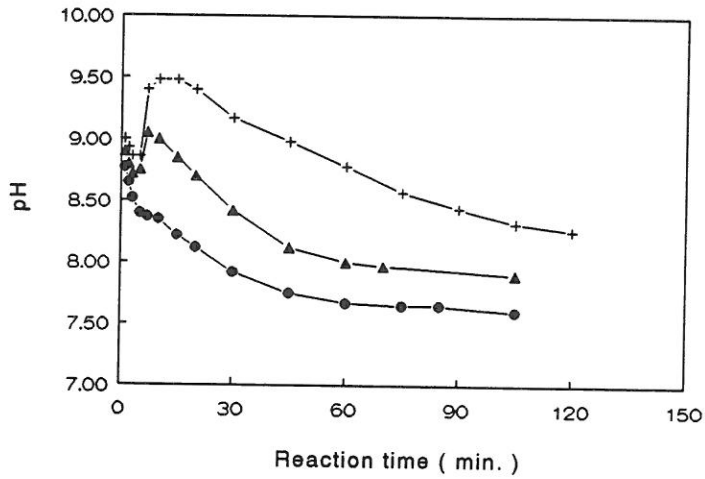

Figure VII.9 Evolution of pH during reaction at 95°C of MF resins prepared from F/M 1.7 pH 9.5 at three different concentrations: 50% (+), 25% (▲) and 10% (●).

By assuming that the time intervals are short enough to allow a mean pH value to be indicative over the selected time intervals rate constants corresponding to the mean pH can be used in order to calculate the changes in the concentrations of the bridges over the selected time intervals. In Chapter 6 the rate constants of the non-substituted methylene bridge formation, methylene-ether bridge formation and decomposition were calculated as a function of pH and temperature. So, the changes in the concentrations of the non-substituted methylene and methylene-ether bridges over the selected time intervals at 95°C can be calculated from eqn. (2) and (3).

$$\Delta [MB] = k_1 [-NH_2] [-NHCH_2OH] \Delta t \qquad (2)$$

$$\Delta [EB] = \{k_2 [-NHCH_2OH]^2 - k_{-2} [NHCH_2OCH_2NH]\} \Delta t \qquad (3)$$

in which k_1, k_2, k_{-2} are the rate constants of methylene bridge formation, methylene-ether bridge formation and decomposition, respectively at the mean pH value of the selected time intervals. Methylolation and demethylolation of bridges are not taken into account. The concentrations of the various functional groups are tabulated in Tables 1-11 (see appendix) for the various resin formulations.

The resulting concentrations of the non-substituted methylene and methylene-ether bridges were compared with the experimentally observed ones. The calculated and experimental plots are shown for two MF resin formulations prepared from a formalin pH of 9.5, and 9 in Figures VII.10 and 11, respectively.

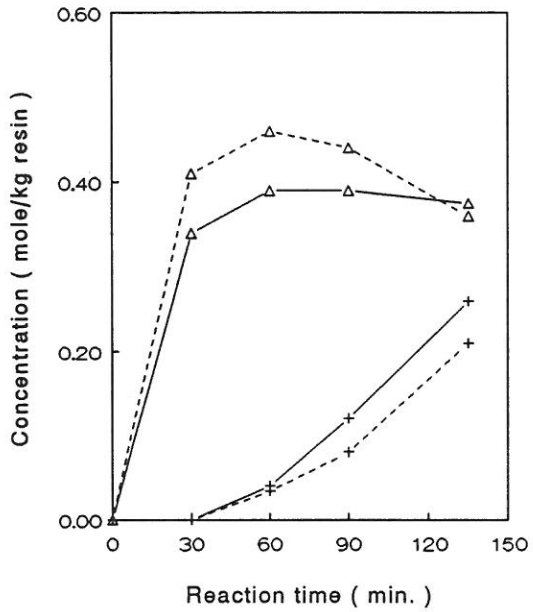

Figure VII.10 Experimental (—) and calculated (--) concentration-time relationships of methylene and methylene-ether bridges for the MF resin with F/M 1.7 pH 9.5 at 95°C. + -$NHCH_2NH$- ▵ -$NHCH_2OCH_2NH$-

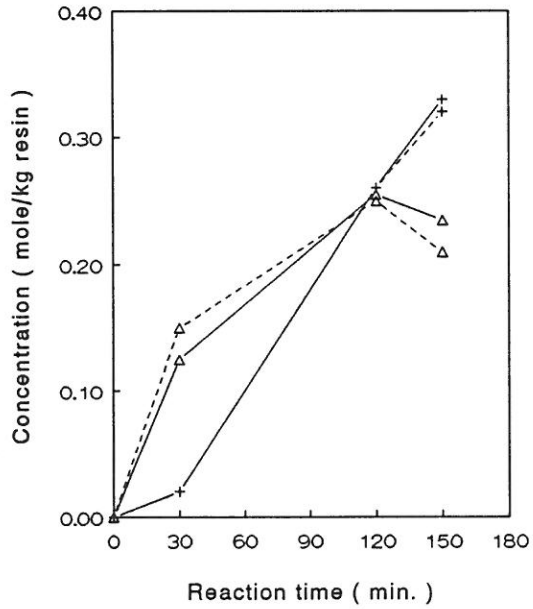

Figure VII.11 Experimental (—) and calculated (--) concentration-time relationships of methylene and methylene-ether bridges for the MF resin with F/M 1.7 pH 9 at 95°C. +-$NHCH_2NH$- ▵ -$NHCH_2OCH_2NH$-

It can be concluded that the concentration-time plots of the methylene and methylene-ether bridges calculated with the experimentally determined rate constants are almost identical with the experimental plots. Similar agreements were found for the MF resins prepared from a formalin pH of 7, 8 and 10.

The concentrations of non-substituted methylene and methylene-ether bridges for the resins prepared from various F/M ratios and various solids contents can be calculated in the same way from the rate constants obtained for the MF(1.7) by assuming that the rate constants of the condensation reactions are independent of F/M molar ratio and solids content. The calculated concentrations of the non-substituted methylene and methylene-ether bridges bridges are compared with the experimental data for the resins with various F/M ratios and various solids contents in Table VII.1 and 2, respectively. Good agreement is found between the calculated and experimental concentrations.

It can be concluded that the rate constants of methylene and methylene-ether bridge formation are independent of F/M ratio in accord with the observations of Kumar and Katiyar [13] and of solids content. These satisfying conformities between calculated and experimental concentration-time plots indicate that the evolution of the methylene and methylene-ether bridges during the resin synthesis can be described very well given (i) the evolution of pH and (ii) the rate constants at the various pH values.

Table VII.1 Experimental values of methylene and methylene-ether bridges and calculated values from the rate constants obtained for the MF(1.7) resin.

F/M	Reaction time, min.	MB, mole/kg		EB, mole/kg	
		calc.	exp.	calc.	exp.
3.0	30	0.02	0.00	0.42	0.46
	84	0.32	0.24	0.58	0.58
	108	0.43	0.33	0.64	0.65
2.2	30	0.00	0.00	0.52	0.58
	60	0.06	0.02	0.57	0.60
	105	0.18	0.13	0.64	0.59
1.5	60	0.09	0.07	0.35	0.33
	120	0.26	0.25	0.43	0.34
	180	0.42	0.39	0.49	0.32

Table VII.2 Experimental values of methylene and methylene-ether bridges and calculated values from the rate constants obtained for the 50% MF(1.7) resin.

s.c.	Reaction time, min.	MB, mole/kg calc.	exp.	EB, mole/kg calc.	exp.
25%	30	0.004	0.000	0.040	0.040
	90	0.090	0.090	0.087	0.090
	120	0.130	0.150	0.080	0.085
10%	30	0.002	0.000	0.005	0.020
	150	0.040	0.050	0.000	0.010

3.2 Chemical aspects of the evolution of water tolerance

The water tolerance of the various resin formulations was measured as a function of time. The data are presented in Tables 1-11 (see appendix). Initially formaldehyde is added to melamine, which results in a mixture of methylol-melamines. These methylolmelamines can tolerate an infinite amount of water. With increasing time of condensation the water tolerance of the resin solutions decreases gradually. In this section attention is paid to the chemical aspects of the evolution of the water tolerance during the resin synthesis. Figure VII.12 shows the relation between methylene and methylene-ether bridge formation and the evolution of the water tolerance for various MF resin formulations. From Fig.VII.12 it can be observed that the ratio of methylene to methylene-ether bridges can be totally different for MF resins with a similar water tolerance. Nevertheless, a linear relationship was found between the water tolerance and the total number of bridges (either methylene bridges or methylene-ether bridges) for all 50% resins, as shown in Figure VII.13. For the lower concentration resins the water tolerance correlates with a lower degree of condensation and deviates from the relation for the 50% resins. Therefore, a more general parameter which is no longer dependent on the water content of the resin is introduced, the so called "critical solids content". The critical solids content (csc) is defined in the same way as the solids content (s.c.).

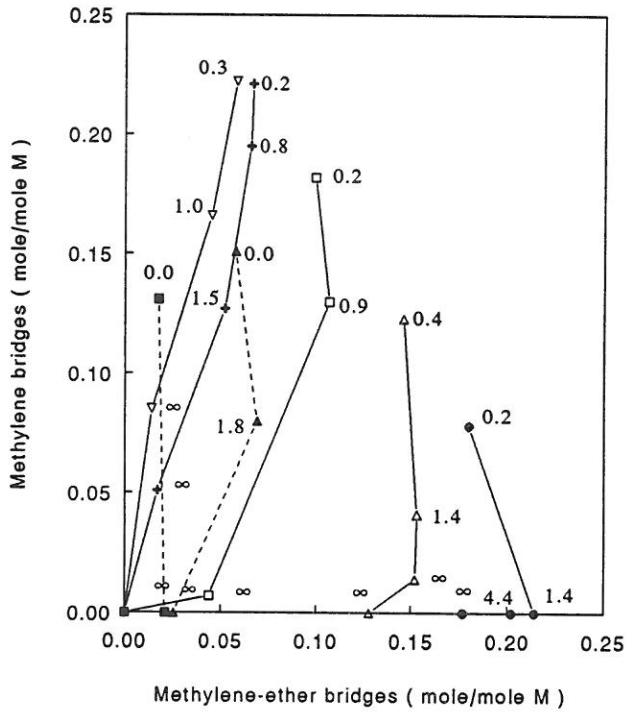

Figure VII.12 Evolution of water tolerance in conjunction with the methylene and methylene-ether bridge formation during during the synthesis of the MF resins: 50% ● pH 10, ▲ pH 9.5, □ pH 9, + pH 8, ▽ pH 7, 25% pH 9.5 --▲--, 10% pH 9.5 --□--.

However it is expressed in grams of solid contents of a MF resin per gram of total water:

$$csc = \frac{s.c.}{1 - s.c. + w.t.} \qquad (4)$$

The relation between the critical solids contents values and the total number of bridges is shown in Figure VII.14. It is shown that the solids content values of the 10% and 25% resins fit in with those of the 50% resins.

In this section, the evolution of the water tolerance has been mapped out in conjunction with the methylene and methylene-ether bridge formation during the synthesis of the MF(1.7) resins. It is possible to determine the chemical constitution of a MF resin from Fig.VII.12 given the initial formalin pH value, the water tolerance, the solids content and the reaction time.

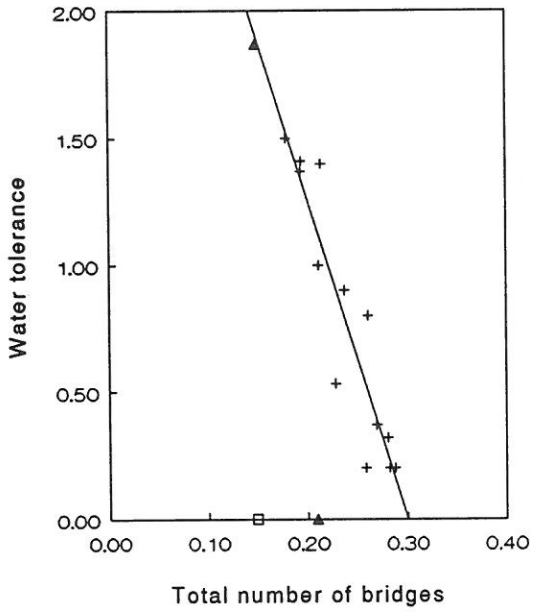

Figure VII.13 Relation between water tolerance and the total number of bridges in mole / mole M, for MF(1.7) resins. 50% (+), 25% (▲) and 10% (□).

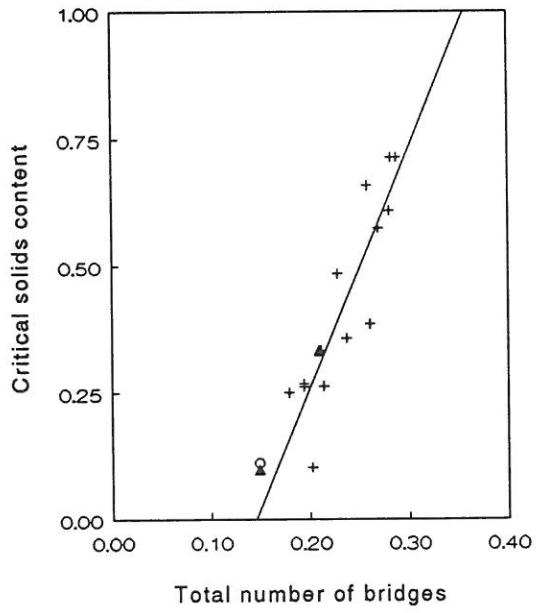

Figure VII.14 Relation between the critical solids content and the total number of bridges in mole / mole M, for MF(1.7) resins. 50% (+), 25% (▲) and 10% (o) .

4 *Conclusions*

The chemical structure of the low molecular weight MF resins has been examined as a function of pH, F/M molar ratio, solids content and reaction time by means of ^{13}C NMR. The pH is one of the most important factors in governing the methylene versus methylene-ether bridge formation. MF resins prepared from a lower formalin pH contain beside non-substituted methylene bridges, a relatively large amount of methylol-substituted methylene bridges. Methylene bridges of which the two amino groups are disubstituted were not detected (<detection limit) in this study. The incorporation of a larger amount of formaldehyde into the resin favours the formation of methylene-ether bridges due to a relative larger amount of methylol groups. The number of substituted methylene and methylene-ether bridges increases with an increasing F/M ratio. The chemical composition of the low molecular weight resins is strongly dependent on the solids content.

The relation between the evolution of pH and the evolution of the bridges during the resin synthesis has been studied. The evolution of the bridges as a function of time can be described very well from the evolution of pH and the rate constants corresponding to the various pH values.

Insight into the chemical aspects of the evolution of water tolerance has been obtained by ^{13}C NMR. A linear relationship has been found between water tolerance and the total number of bridges for a given solids content. A new parameter, the critical solids content, has been introduced which is no longer dependent on the water content of the resin and thus eliminates the influence of the solids content of the resin .

5 *Experimental*

Resin preparation

The aqueous melamine formaldehyde resins were all synthesized in 230 g batches from melamine, 32 % (m/m) formalin and an appropriate amount of water resulting in a resin with a given solids content (s.c.). After addition of water to formalin the required pH was adjusted at room temperature by the addition of 1M aqueous sodium hydroxide solution. The resins were synthesized in a three necked vessel (250 ml) to allow insertion of pH and temperature probes and a stirrer. The raw materials were placed into the vessel and the moment of mixing was taken as t=0. The reaction mixture was heated to 95°C in approximately 20 minutes. Without further adjustment of pH, the pH falls throughout the reaction. The pH was monitored continuously at 95°C with an electrode calibrated at 95°C. The variation of the reaction conditions is summarized in Table VII.3 The extent of the condensation reaction of the MF resin was checked regularly by measuring its water tolerance. To determine the water tolerance, 10 g of MF resin at 20°C was diluted with water at 20°C until the turbidity persists. The amount of water is a measure of the water tolerance, which is expressed in grams of water per gram of resin. The condensation reaction was continued until a water tolerance of 0.2-0.3 was reached. Samples taken after reaction for several lengths of time, were analyzed by ^{13}C NMR. The NMR analysis of the resins was conducted within one or two days. In the mean time the resin solutions were placed in a refrigerator at 4°C to ensure that the resin structure remained unchanged.

Table VII.3 Synthesis parameter variation.

T (°C)	F/M	pH	s.c.	Variation
95	1.7		50%	formalin pH: 7.0 8.0 9.0 9.5 10.0
95		9.5	50%	F/M: 1.5 1.7 2.2 3.0
95	1.7	9.5		s.c.: 10% 25% 50%

Methods

13C NMR

Typical conditions for recording the ^{13}C NMR spectra have been given in Chapter 6.

HPLC

The experimental details of the HPLC measurements have been described in Chapter 6.

pH measurement

The pH was measured continuously at 95°C with an electrode calibrated at 95°C. For further details see Chapter 6.

6 *References*

[1] P.O.Powers, Amino Resins and Plastics, in Kirk-Othmer Encyclopedia of Chemical Technology, A.Standen and J.Scott,eds., 1st ed., 1, 741, Interscience Publishers, Inc., New York (1947).

[2] J.R.Ebdon, B.J.Hunt and M.Al-Kinany, *Spec.Publ.R.Soc.Chem.*, 87, 109 (1991).

[3] H.Herma, K.Dietrich, B.Schilling, C.Schulze, B.Aleithe, W.Teige, *Plaste und Kautschuk*, 30(3), 132 (1983).

[4] H.Herma, K.Dietrich, B.Schilling, C.Schulze, B.Aleithe, W.Teige, *Plaste und Kautschuk*, 30(4), 200 (1983).

[5] H.Herma, K.Dietrich, B.Schilling, C.Schulze, W.Teige, *Plaste und Kautschuk*, 31(1), 9 (1984).

[6] H.Herma, K.Dietrich, C.Schulze, W.Teige, *Plaste und Kautschuk*, 33(9), 9 (1986).

[7] B.Tomita, H.Ono, *J.Polym.Sci.Polym.Chem.Ed.*, 17, 3205 (1979).

[8] H.Pash, G.Hovakeeman, S.Lahalih, *J.Polym.Sci.Polym.Chem.*, 29, 525 (1991).

[9] Z.W.Wicks Jr., D.Y.Y.Hsia, *J.Coat.Techn.*, 55(702), 29 (1983).

[10] J.F.Walker, *Formaldehyde, American Chemical Society Monograph No.159, 3rd ed.*,Reinhold, New York (Chapman & Hall, London), 1964.

[11] R.A.Lapina and F.G.Zhurina, *J.Appl.Chem. USSR*, 42, 2028 (1969).

[12] H.Michaud, *Kunststoffe*, 47, 686 (1957).

[13] A.Kumar and V.Katiyar, *Macromolecules*, 23, 3729 (1990).

CHAPTER 8

STUDY OF THE FINALLY CURED MF RESINS BY A COMBINATION OF ^{13}C CP/MAS NMR AND FT-RAMAN SPECTROSCOPY

1 Introduction

While the structure of MF resins in the early stages of condensation has been studied by a number of authors [1-4], the molecular structure of fully cured resins has been studied only fragmentary despite the importance for material properties. O'Rourke [5] used ^{13}C CP/MAS NMR to investigate the structure of two MF resins prepared from F/M 1.3 and 2.3 cured at 150°C. He concluded that the resin prepared from F/M 2.3 contains relatively more methylene-ether bridges compared to the F/M 1.3 resin. Ebdon et al. [6] examined the structure of some fully-cured MF resins (prepared from F/M 1.5 and 3.0) by CP/MAS ^{13}C and ^{15}N NMR. The ^{13}C CP/MAS NMR spectra show the conversion of methylol groups to methylene bridges, the methylene-ether bridges on the contrary overlap with the residual methylol groups. The presence of residual methylol groups was checked by studying the ^{15}N CP/MAS NMR spectra of the resins and it was concluded that the resins contain few free methylol groups. It was concluded that the resin prepared from F/M 1.5 contains predominantly methylene bridges and that prepared from F/M 3 contains an equal number of methylene and methylene-ether bridges. Difficulties in obtaining detailed structural information of cured resins is the main reason for this few number of studies reported on the full cure of MF resins.

The combination of ^{13}C CP/MAS NMR and FT-Raman spectroscopy, as evidenced in Chapters 3 and 4, is powerful in the determination of the structure of cured MF resins. The number of methylene bridges can be determined by ^{13}C CP/MAS NMR, whereas the percentage residual methylol groups can be calculated from the Raman bands around 1000 cm^{-1}. The Raman band at 900 cm^{-1} is thought to be indicative for the presence of methylene-ether bridges, but this band is very difficult to quantify. However, the percentage methylene-ether bridges can be estimated from the difference between the percentage reacted methylol groups and

the percentage methylene bridges.

In this Chapter the relation between the resin recepy and the molecular structure of the finally cured resin will be studied by systematic variation of the reaction parameters. The following parameters have been varied: (i) the initial formalin pH, (ii) the F/M molar ratio, (iii) the solids content, (iv) the cure temperature and (v) the addition of p-toluene sulfonic acid as catalyst.

2 *Variation of the reaction conditions*

The results of ^{13}C CP/MAS NMR and Raman studies of the various MF resin formulations are discussed in five parts. In subsequent sections the effect of initial formalin pH, the effect of F/M molar ratio, the effect of solids content , the effect of cure temperature and the effect of p-toluene sulfonic acid as catalyst will be dealt with. The chemical structure of the various MF resins prior to cure is given in Chapter 7.

2.1 *Effect of initial formalin pH*

In the early stages of resin formation it was shown that the methylene versus methylene-ether bridge formation at each time is governed by, among others, the pH value of the reaction mixture. So, the chemical constitution just prior to cure at 120°C was totally different for the MF resins prepared from various initial pH values as shown in Table VIII.1.

Table VIII.1 Chemical constitution (in mol% ,total F = 100%) obtained by ^{13}C liquid NMR of the MF resins prepared from F/M 1.7 and various initial pH values just prior to cure.

Initial pH	7.0	8.0	9.0	9.5	10.0
-NR'CH_2NR'-	12.9	12.9	11.2	7.1	4.6
-NR'CH_2OCH_2NR'-	3.5	3.8	5.9	8.6	10.6
-NR'CH_2OH	80.1	79.5	77.0	75.7	74.1

R' = H or CH_2-

The evolution of pH (Fig. VII.7) was followed at 95°C during the early condensation stage for the various MF resins and the pH varied only between 7.9 and 8.1 at the moment that samples were taken for further cure experiments at 120°C. So the MF resins prepared from various initial formalin pH's were all cured at approximately the same pH value for 4 hours at 120°C in a non-sealed reaction vessel.

The concentrations of methylene bridges and of the sum of methylol groups and methylene-ether bridges, obtained by ^{13}C CP/MAS NMR are listed in Table VIII.2. Beyond all expectations, the cured MF resins prepared from an initially higher pH value contain at least as many methylene bridges in comparison with those prepared from a lower pH value. The relative distribution of N-CH_2-N (1435 cm^{-1}) and N-CH_2-O (1450 cm^{-1}) structures in the methylene bending region of the Raman spectra shown in Figure VIII.1, is consistent with the ^{13}C CP/MAS NMR results. From the ratio of the 1000 cm^{-1} bands to the triazine band at 975 cm^{-1} the mole percentage of residual methylol groups can be calculated. This amount of residual methylol groups coincided with the mole percentage of methylol groups determined by ^{13}C liquid NMR (see appendix Tables 1-6). The mole percentage of residual methylol groups for the cured MF resins can then be calculated from the ratio of the 1000 cm^{-1} bands to the triazine band in the Raman spectra after cure. Values of 6 and 12 mol% of residual methylol groups were calculated for the pH (7-9.5) resins and the pH(10) resin, respectively. The presence of methylene-ether bridges can be observed from the Raman band around 900 cm^{-1}. The intensity of the 900 cm^{-1} band is quite similar for all MF resins shown in Fig. VIII.1. The mol% methylene-ether bridges present can be calculated as one half of the difference between the mol% reacted methylol groups, obtained from the FT-Raman spectra and the mol % methylene bridges, determined by ^{13}C CP/MAS NMR. This results in 16 and 11 mol% methylene-ether bridges for the pH(7-9.5) resins and the pH(10) resin, respectively (see Table VIII.2).

It can be concluded that the structural differences between the cured MF resins prepared from pH values varying between 7 and 9.5 are smaller than can be detected by ^{13}C CP/MAS NMR or FT-Raman spectroscopy. The resin prepared from pH 10 deviates from the other four resins and this is not yet understood.
During cure in aqueous resins it would be expected that methylene-ether bridges are in equilibrium with methylol groups and that the methylol groups react with the amino groups to the thermodynamically more stable methylene bridges. Thus the cured resins are cross-linked predominantly by methylene bridges. However, still 9-15 mole% methylene-ether bridges were observed in the cured MF resins whereas no would been expected. This discrepancy may be caused by (i) vitrification

Table VIII.2 Chemical composition (in mol% ,total F = 100%) obtained from ^{13}C CP/MAS NMR and FT-Raman measurements of cured MF resins prepared from F/M 1.7 and various initial pH values.

Initial pH	N-CH_2-N	N-CH_2O-	N-CH_2OH	N-CH_2OCH_2-N
	^{13}C CP/MAS		Raman	Calc.
7.0	58	42	6	18
8.0	62	38	6	16
9.0	62	38	6	16
9.5	63	37	6	16
10.0	67	33	12	11

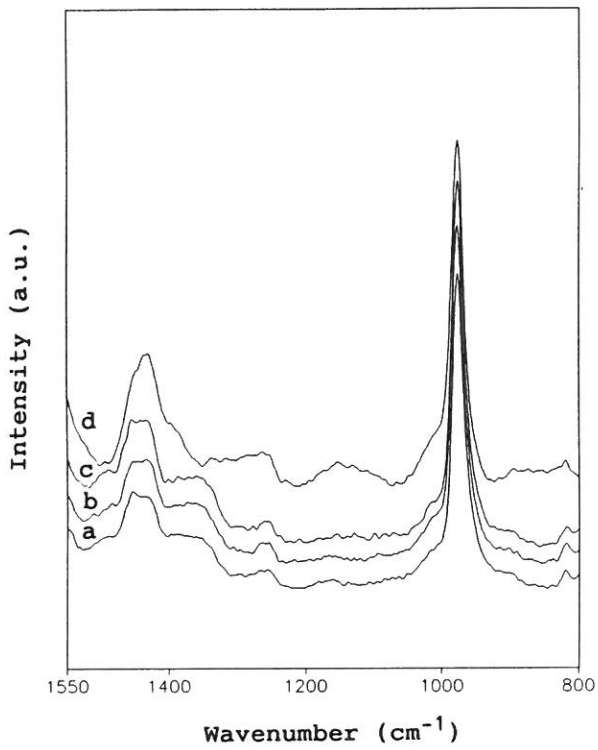

Figure VIII.1 FT-Raman spectra from 800-1550 cm^{-1} of cured MF(1.7) resins prepared from pH 7 (a), 9 (b), 9.5 (c), and 10 (d) at 120°C.

and (ii) inhibition of the hydrolysis of methylene-ether bridges due to phase separation and or evaporation of water. A combination of both effects is likely since a decrease of the amount of water available for hydrolysis slows down the decomposition of methylene-ether bridges and thus the formation of methylene bridges.

2.2 *Effect of F/M molar ratio*

The ^{13}C CP/MAS NMR results of the MF resins prepared from F/M 1.5, 1.7, 2.2 and 3.0, cured in non-sealed vessels at 120°C for 4 hours are listed in Table VIII.3. The corresponding FT-Raman spectra are shown in Figure VIII.2. The ^{13}C CP/MAS NMR results as well as the methylene bending spectral region in the Raman spectra show a decrease in the relative number of methylene bridges for resins prepared from higher F/M ratios. Furthermore, the ^{13}C CP/MAS NMR spectra show a relative increase in the number of substituted methylene and methylene-ether bridges with an increasing F/M ratio as indicated by the increased intensities at 55 ppm and 75 ppm, respectively (Fig. VIII.3). In the 1100-850 cm^{-1} spectral region of the Raman spectra (Fig. VIII.2) two differences with varying F/M ratio can be marked. First, the relative ratio of methylol groups to the melamine content increases with increasing F/M ratio. Values of 5, 6, 16 and 17 mole percent of residual methylol groups were calculated for the resins with increasing F/M ratio, respectively.

Table VIII.3 Chemical composition (in mol% ,total F = 100%) obtained from ^{13}C CP/MAS NMR and FT-Raman measurements of cured MF resins prepared from various F/M ratios.

F/M ratio	$N\text{-}CH_2\text{-}N$	$N\text{-}CH_2O\text{-}$	$N\text{-}CH_2OH$	$N\text{-}CH_2OCH_2\text{-}N$
	^{13}C CP/MAS		Raman	Calc.
1.5	70	30	5	12
1.7	63	37	6	16
2.2	49	51	16	18
3.0	22	78	17	30

Secondly, it can be seen that the broad band around 900 cm^{-1}, representing methylene ether bridges becomes more intense with an increasing F/M ratio. Values of 12, 16, 18 and 30 mol% methylene-ether bridges were calculated from the difference between the mol% reacted methylol groups and the mol % methylene bridges for the resins with F/M ratio of 1.5, 1.7, 2.2 and 3.0, respectively.

The structure of cured MF resins depends on the kinetics of the condensation reactions and the chemical composition of the resin prior to cure. It is assumed that the hydrolysis of methylene-ether bridges can be neglected because water escapes during cure and consequently the equilibrium is shifted in the forward direction. The ratio of methylene (MB) and methylene-ether (EB) bridges for the various MF resins with varying F/M ratio can be calculated from eqn. (1) and (2).

$$\frac{d\,[MB]}{dt} = k_{MB}\,[\text{-NHR'}][\text{-NR'CH}_2\text{OH}] = k_{MB}\,[6\text{-(F/M)}][F/M] \qquad (1)$$

$$\frac{d\,[EB]}{dt} = k_{EB}\,[\text{-NR'CH}_2\text{OH}]^2 = k_{EB}\,[F/M]^2 \qquad (2)$$

with R'= H or CH_2-

The reaction time is similar, so the ratio of methylene and methylene-ether bridges can be calculated in the following simple way. The rate constants k_{MB} and k_{EB} were taken from Chapter 6.

$$\frac{d\,[MB]}{d\,[EB]} = \frac{k_{MB}\,[6\text{-(F/M)}]}{k_{EB}\,[F/M]} \qquad (3)$$

The results presented in Table VIII. 4 show that the calculated and experimental values are in reasonable agreement although the change in the experimentally found MB/EB ratio with F/M ratio is more pronounced.

It is concluded that the changes in the ratio of methylene and methylene-ether bridges originate from the variations in the concentrations of -NH and -NCH_2OH groups with varying F/M ratio.

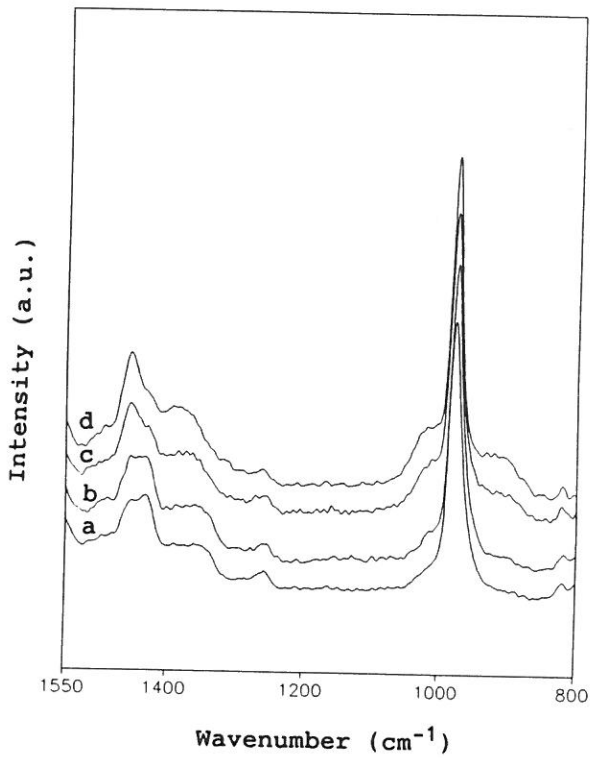

Figure VIII.2 Comparison of the 800-1550 cm^{-1} region of cured MF resins prepared from pH 9.5 and F/M 1.5 (a), 1.7 (b), 2.2 (c) and 3.0 (d) at 120°C.

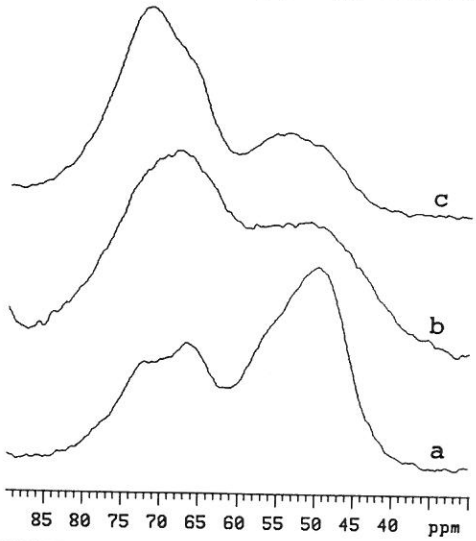

Figure VIII.3 ^{13}C CP/MAS NMR spectra from 30-90 ppm of cured MF resins with different F/M ratio's: 1.7 (a), 2.2 (b) and 3.0 (c) at 120°C.

Table VIII.4 Calculated and experimental ratio of methylene (MB) and methylene-ether (EB) bridges.

F/M ratio	MB / EB	
	exp.	calc.
1.5	5.9	3.6
1.7	3.9	3.1
2.2	2.7	2.1
3.0	0.8	1.2

The resins described in the following sections were cured in sealed tubes and water evaporation is inhibited. Therefore the effect of cure in non-sealed vessels or in sealed tubes (water evaporation) on the final structure of the resin will be discussed firstly. Surprisingly, only slight differences in chemical structure (see Table VIII.5) were observed for the MF resin cured in non-sealed and sealed reaction vessles. The MF resin cured in a sealed tube contains 10 mol% more methylene bridges and a smaller number of methylene-ether bridges (4 mol%) compared to that cured in a non-sealed vessel. This might be caused by the fact that in both cases (sealed and non-sealed) the resin separates from the upper water-layer during cure. So, the resin cured in a sealed tube contains only a small amount of water and the hydrolytic reactions are again slowed down.

Table VIII.5 Chemical composition (in mol% ,total F = 100%) obtained from ^{13}C CP/MAS NMR and FT-Raman measurements of an MF resin (F/M 1.7, pH 9.5) cured at 120°C in a non-sealed vessel and in a sealed tube.

Cure conditions	N-CH_2-N	N-CH_2O-	N-CH_2OH	N-CH_2OCH_2-N
	^{13}C CP/MAS		Raman	Calc.
non-sealed	62	38	6	16
sealed	72	28	4	12

2.3 *Effect of solids content*

MF (F/M = 1.7) resins prepared at different solids contents, namely 10%, 25% and 50% were cured at 120°C for 4 hours in sealed tubes. These resins differ greatly in chemical structural at the beginning of the cure (Table VIII.6). The resins prepared at a lower concentration contain a significant lower content of methylene-ether bridges. The ^{13}C CP/MAS NMR results of the 10 %, 25 % and 50 % MF resins are shown in Table VIII.7. Comparison of these data reveals that the effect of concentration on the final N-CH_2O- / N-CH_2-N distribution is minor. In Figure VIII.4 the 800-1550 cm^{-1} spectral region of the Raman spectra of the various MF resins is shown. The relative distribution of the number of N-CH_2-N and N-CH_2O- structures in the methylene bending region is in agreement with the ^{13}C CP/MAS NMR results. The mole percentage of residual methylol groups is quite similar (± 4%) for all three MF resins. Consequently, it can be concluded that the mole percentage of methylene-ether bridges is also similar (± 13%) for the 10%, 25% and 50% MF resin (Table VIII.7).

No significant effect of the solids content on the structure of the cured MF resins is observed. This can probably be explained by the fact that the resin separates from the upper water-layer and the concentration terms are eliminated.

It can be concluded that the chemical constitution of the cured 10%, 25% and 50% MF resins is rather similar in contrast to the early stages of condensation where the various concentration resins differ greatly in chemical structure.

Table VIII.6 Chemical constitution (in mol% ,total F = 100%) obtained by ^{13}C liquid NMR of the MF resins prepared from various solids content just prior to cure.

Solids content	10%	25%	50%
-NR'CH_2NR'-	8.0	9.1	7.1
-NR'CH_2OCH_2NR'-	1.5	3.5	8.6
-NR'CH_2OH	84.4	81.3	75.7
CH_2O	4.6	2.4	-

R' = H or CH_2-

Table VIII.7 Chemical composition (in mol% ,total F = 100%) obtained from ^{13}C CP/MAS NMR and FT-Raman measurements of cured MF resins prepared from F/M 1.7 , pH 9.5 and various solids contents.

Solids Content	N-CH_2-N	N-CH_2O-	N-CH_2OH	N-CH_2OCH_2-N
	^{13}C CP/MAS		Raman	Calc.
10%	72	28	4	12
25%	71	29	4	12
50%	72	28	4	12

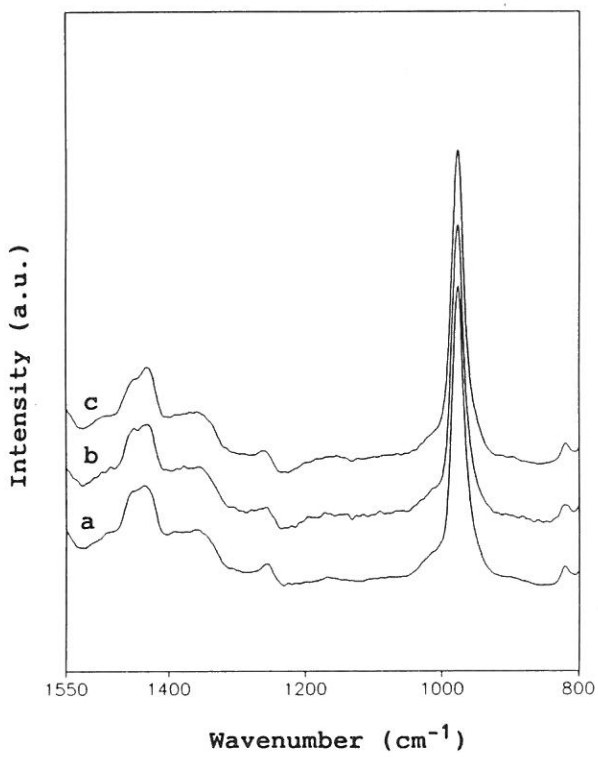

Figure VIII.4 FT-Raman spectra from 800-1550 cm^{-1} of cured MF resins prepared from F/M 1.7, pH 9.5 at three different concentrations 50% (a), 25% (b), 10% (c) at 120°C.

2.4 *Effect of cure temperature*

An MF resin prepared from F/M 1.7 ; pH 9.5 at 95°C was cured for 4 hours in sealed tubes at 120°C, 140°C and 160°C, respectively. From the ^{13}C CP/MAS NMR results in Table VIII.8 and the Raman methylene bending region (Fig.VIII.5), it can be seen that the fraction of methylene bridges increases from 72% to 85% with increasing cure temperature. In Chapter 5 it has been shown that the glass transition equals the cure temperature, vitrification occurs. The onset of the glassy state provides a large barrier to continued MF cure. By increasing the cure temperature, however, further reaction of residual methylol groups can take place. The increase in mole percentage of methylene bridges with increasing cure temperature can not exclusively be due to reaction of residual methylol groups (Table VIII.8). The ^{13}C CP/MAS NMR results and the methylene bending spectral region show that the total number of N-CH_2-0 structures (methylol groups + methylene-ether bridges) further decreases with increasing cure temperature. Furthermore, the intensity of the Raman band at 900 cm^{-1}, representing methylene-ether bridges decreases with increasing cure temperature. This supports the explanation presented before that with increasing cure temperature the cure reactions lead finally to formation of the thermodynamically more stable methylene bridges.

Table VIII.8 Chemical composition (in mol% ,total F = 100%) obtained from ^{13}C CP/MAS NMR and FT-Raman measurements of MF resins (F/M 1.7, pH 9.5) cured at various temperatures.

Cure Temperature	N-CH_2-N	N-CH_2O-	N-CH_2OH	N-CH_2OCH_2-N
	^{13}C CP/MAS		Raman	Calc.
120°C	72	28	4	12
140°C	80	20	3	9
160°C	85	15	3	6

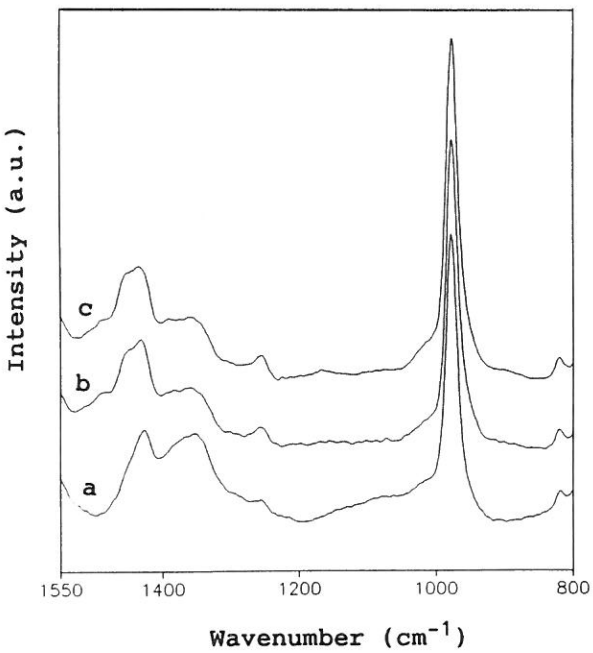

Figure VIII.5 Comparison of the 800-1550 cm^{-1} region of MF resins prepared from F/M 1.7, pH 9.5 cured at 160°C (a), 140°C (b) and 120°C (c).

2.5 *Effect of p-toluene sulfonic acid*

An acid catalyst is usually added just prior to the cure of MF resins to increase the condensation rate. Organic acids such as formic acid, acetic acid or p-toluene sulfonic acid are usually used as catalysts. A standard resin (F/M 1.7 initial pH 9.5) was prepared at 95°C. The MF resin was cooled to room temperature and the pH was measured at room temperature giving a pH value of 8.9. p-Toluene-sulfonic acid (0.05-0.15 w/w%) was added to adjust the pH at room temperature to 8, 7.5, and 7, respectively in order to study the effect of a catalyst (p-toluene-sulfonic acid) on the structure of the cured MF resins. The MF resin without addition of PTSA was taken as reference. The resins were cured in sealed tubes at 120°C for 4 hours. The ^{13}C CP/MAS NMR results are given in Table VIII.9. It is shown that the mole percentage of methylene bridges formed is practically constant and not influenced by the presence of PTSA. No significant differences were observed in the number of residual methylol groups (± 4%) (see Fig. VIII.6) and methylene-ether bridges (± 12%) among those MF resins. The incomplete cure at 120°C after addition

of PTSA is due to vitrification of the resin and the separation of the resin from the water-layer. Thus, in all cases vitrification occurs and the conversion of methylene-ether bridges to the thermodynamically more stable methylene bridges is inhibited.

It can be concluded that addition of p-toluene sulfonic acid has no significant effect on the resin structure and it will only accelerate the condensation reactions.

Table VIII.9 Chemical composition (in mol% ,total F = 100%) obtained from ^{13}C CP/MAS NMR and FT-Raman measurements of cured MF resins with and without p-toluene sulfonic acid.

Catalyst	N-CH_2-N	N-CH_2O-	N-CH_2OH	N-CH_2OCH_2-N
	^{13}C CP/MAS		Raman	Calc.
without PTSA	72	28	4	3
PTSA pH 7	76	24	3	11
PTSA pH 7.5	70	30	3	13
PTSA pH 8	75	25	4	11

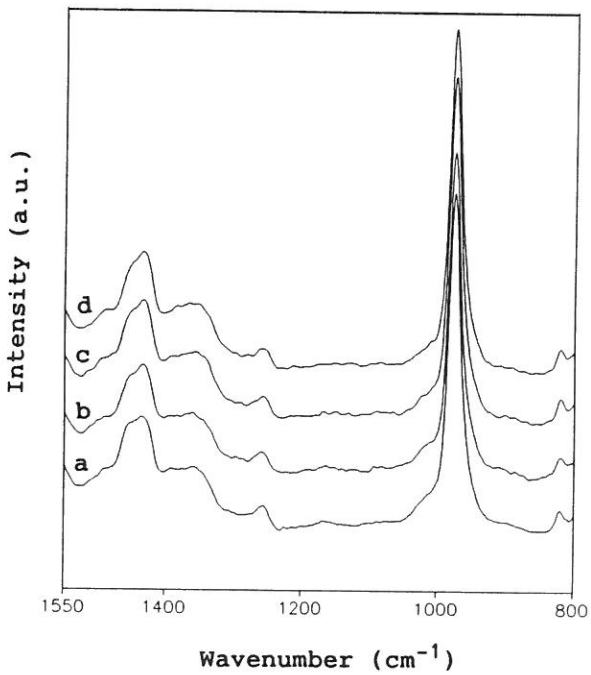

Figure VIII.5 FT-Raman spectra from 800-1550 cm^{-1} of MF (1.7) resins cured at 120°C without PTSA (a), with PTSA pH 8 (b), pH 7.5 (c) and pH 7 (d).

3 *Conclusions*

It is shown that a detailed picture of the network structure of fully cured MF resins can be obtained from a combination of ^{13}C CP/MAS NMR and FT-Raman spectroscopy.

From a systematic study, the following relationships between resin composition and molecular structure of the cured resins can be derived. No significant effect of the initial pH varying between 7 and 9.5, has been observed on the structure of the cured MF resins. The ratio of methylene to methylene-ether bridges appears to be controlled mainly by the F/M molar ratio in the starting mixture. The incorporation of a larger amount of formaldehyde into the resin favours methylene-ether bridge formation and substituted bridge formation. The solids content has no significant effect on the final resin structure. The structure of the MF resins was not influenced by addition of p-toluene sulfonic acid, the cure reactions are only accelerated. With increasing cure temperature, more methylene bridges are formed. The additional thermal energy promotes the conversion of methylene-ether bridges to the thermodynamically more stable methylene bridges.

In this chapter the relation between resin composition and molecular structure of the cured MF resins has been studied in detail. In a next step, the full relation between synthesis of MF resins, the resulting network structure and the final properties will be subject of study. Using these relations guidelines can be derived for optimum resin composition in relation to properties.

4 *Experimental*

MF resins

The synthesis conditions of each MF resin have been given in chapter 7, describing the resin formation in the early stages of the condensation. The resulting low molecular weight resins prepared at 95°C, were cured in two different ways. Some of the resins were cured in non-sealed vessels (vessels covered by a petri dish) whereas the other ones were cured in sealed tubes. In the non-sealed vessels the cure is performed with simultaneous loss of water. However, in both cases the resin separates from the upper water-layer during cure. The separable liquid during cure in the sealed tubes was removed and was not investigated in this study. The cured MF resins were ground to powder. These powders are suitable for ^{13}C CP/MAS NMR and Raman spectroscopic studies.

Methods

NMR

The ^{13}C CP/MAS NMR spectra were recorded on a Varian XL-200 spectrometer. Typical conditions for recording the ^{13}C spectra have been described in Chapter 3.

Raman spectroscopy

Raman spectra were recorded on a Bruker, Model FRA 106 FT-Raman accessoire, attached to a Bruker IFS 66 spectrometer and equipped with a Nd:YAG laser (1064 nm). All spectra were recorded at 4 cm^{-1} resolution with laser powers in the 100 mW range. The Raman spectra result from the accumulation of 150 scans. Spectral deconvolution has been performed on clusters of highly overlapping Raman bands by a commercially-available fitting Routine (Lab Calc.). In order to follow the changes occurring during cure by FT-Raman spectroscopy, not only spectra of the cured resins but also of the initial MF reaction mixtures were recorded. These latter solutions were freeze-dried to get solids suitable for the Raman measurements.

5 *References*

[1] B.Tomita, H.Ono, *J.Polym.Sci.Polym.Chem.Ed.*, 17, 3205 (1979).

[2] T.Gebregiorgis, Ph.D.Thesis, University of Essex, 1982.

[3] H.Herma, K.Dietrich, B.Schilling, C.Schulze, B.Aleithe, W.Teige, *Plaste und Kautschuk*, 30(3), 132 (1983).

[4] R.Nastke, K.Dietrich, G.Reinisch, G.Rafler, *J.Macromol.Sci.Chem.* A23(5), 579 (1986).

[5] S.O'Rourke, Ph.D.Thesis, University of Lancaster, 1984.

[6] J.R.Ebdon, B.J.Hunt, W.T.S.O'Rourke, J.Parkin, *Br.Polym.J.*, 20, 327 (1988).

SUMMARY

A multi-spectroscopic study of the molecular structure of melamine-formaldehyde resins in relation to resin composition is presented in this thesis. The rapid industrial development of MF resin technology has far outdistanced the capability to analyze the MF reaction products. In order to advance the art of state, a more detailed characterization of the MF reaction products should be undertaken. Several spectroscopic tools were evaluated and developed for the characterization of MF resins in the early stages of condensation as well as in the cured stage. The kinetics of methylene bridge formation, methylene-ether bridge formation and decomposition have been studied. The relation between resin composition and resin structure as well in the early stages of condensation as in the cured stage has been studied by systematically varying the reaction conditions around those used industrially.

In Chapter 1 the state of knowledge in the field of MF resins at the beginning of this study, is presented. The chemical complexity and the insolubility of cured MF resins have slowed down elucidation of the chemical structure of MF resins. Periodically new techniques became available and more detailed structural information was generated. The kinetics and mechanisms of methylolation and condensation reactions are described.

In Chapter 2 the powerfulness of ^{13}C NMR in the analysis of MF resins in the early stages of the condensation is demonstrated. Special attention has been paid to the methylene-ether bridge formation. The combination of ^{1}H and ^{13}C NMR opens a way for demonstrating the methylene-ether bridge formation during MF resin cure. The amount of methylene-ether bridges calculated from the amount of water liberated during condensation was in good accordance with that calculated from the number of monomethylolated amino groups consumed during condensation. This combined study has offered some insight into the reaction pathways for the formation of methylol-substituted methylene bridges.

The ^{13}C CP/MAS NMR study described in Chapter 3 shows that the ^{13}C NMR cross polarization technique can be applied for the quantitative analysis of cured MF resins. Furthermore the relative distribution of methylene carbons can be determined quantitatively from a single CT experiment with considerable saving in spectrometer

time. ^{13}C CP/MAS NMR can be used to determine quantitatively the fraction of methylene bridges formed during resin cure. Changes in the averaged mobility of the MF resin with cure were observed from $T_{1\rho}(^1H)$ measurements providing a criterion for the deterimination of the degree of cure.

A Raman spectroscopic study on MF resins is presented in Chapter 4. From the combination of HPLC, ^{13}C liquid and CP/MAS NMR data a significant clarification of the interpretation of MF Raman spectra has been achieved. It has been shown that FT-Raman spectroscopy is a useful complement to 13C CP/MAS NMR for the characterization of cured MF resins. It seems possible to extract quantitative data from FT-Raman spectra by normalizing the measured areas to that of the triazine ring at 975 cm^{-1}. Relative changes in the distribution of N-CH_2-N / N-CH_2-O structures during cure can be observed from the methylene bending region. The amount of residual methylol groups can be determined from the Raman bands around 1000 cm^{-1}. The presence of methylene-ether bridges can be indicated by the band around 900 cm^{-1}. A Raman spectroscopic method, which was further supported by theoretical analysis of the Raman frequencies, has been developed for the determination of the free melamine content in MF resins.

In Chapter 5 the cure behaviour of MF resins is studied by Differential Scanning Calorimetry. MF resin cure was measured under isothermal conditions because the endothermic effect of vaporization of water of condensation otherwise would contribute to the measured heat flow. Reasonable estimates of the enthalpies for the methylene and methylene-ether bridge formation were obtained by a combination of DSC, ^{13}C CP/MAS NMR and FT-Raman spectroscopy. For the methylene bridge formation ΔH is more exothermic (-30 ± 6 kJ/mole) compared to the methylene-ether bridge formation (-19 ± 8 kJ/mole).

In Chapter 6 rate constants for the methylene bridge formation (either unsubstituted or methylol substituted), methylene-ether bridge formation and decomposition have been determined for a standard MF(1.7) resin as a function of pH and temperature. Two different approaches were used to determine the rate constants of the condensation reactions. In the first approach the rate constants for two MF dimers were esimated from the quantitative analysis of melamine species by HPLC. In the second approach, the rate constants for methylene bridge formation, methylene-ether bridge formation and hydrolysis were estimated from concentrations of the functional groups (-NH_2,-$NHCH_2OH$, -$N(CH_2OH)_2$ etc.) detected by ^{13}C NMR as a function of time. Rate constants for the methylol-substituted and non-substituted methylene bridge formation are quite similar. The equilibrium constant of methylolation of a methylene bridge is similar to the equilibrium constant of

secondary methylolation of an amino group. A clear dependence of the rate constants of methylene bridge formation, methylene-ether bridge formation on pH has been shown. The kinetic hydrolysis experiments of methylene-ether dimelamine have shown that the methylene-ether bridge decomposition is catalysed by H_3O^+ ions in acid medium. Activation energies for the methylene bridge formation, methylene-ether bridge formation and hydrolysis were calculated from the temperature dependence of the rate constants. The enthalpy for the methylene-ether bridge formation was calculated from the temperature dependence of the equilibrium constant. This value (-14.3 ± 6.0 kJ/mole) is in accord with that obtained by DSC.

A detailed ^{13}C NMR study of the structure of industrial MF resins as a function of the resin formulation (pH, F/M ratio and solids content) in the early stages of the condensation is dealt within Chapter 7. Methylene versus methylene-ether bridge formation is strongly governed by the pH value of the MF resins. MF resins prepared at low pH values contain a relatively large number of methylol substituted methylene bridges beside non-substituted ones. Large variations in the concentration of secondary methylol groups were observed as a function of pH. With increasing F/M ratio, the number of methylol groups increases relative to that of -NH groups and this favours the methylene-ether bridge formation. The resin structure of MF resins in the early stages of condensation is strongly affected by the solids content. The evolution of pH and the evolution of the water tolerance during the industrial MF resin synthesis were related to the evolution of the methylene and methylene-ether bridges during the resin synthesis. It has been shown that the evolution of the methylene and methylene-ether bridges can be well described from the evolution of pH and the rate constants of the condensation reactions determined in Chapter 6. A linear relationship has been found between water tolerance and the total number of bridges for a given solids content.

A systematically ^{13}C CP/MAS NMR and FT-Raman spectroscopic study of the molecular structure of cured MF resins as a function of resin composition is presented in Chapter 8. The structure of cured MF resins prepared from F/M 1.7 is invariant within experimental error upon variation of the initial formalin pH between 7 and 9.5. The ratio of methylene to methylene-ether bridges appears to be controlled mainly by the F/M molar ratio in the starting mixture. The solids content of the resin has no significant effect on the structure of the cured resin. The resin structure is not influenced by the addition of p-toluene sulfonic acid as catalyst. In all cases vitrification occurs and the conversion of methylene-ether bridges to methylene bridges is inhibited. An increasing cure temperature promotes the formation of the thermodynamically more stable methylene bridges.

SAMENVATTING

Een multispectroscopische studie naar de relatie tussen de moleculaire structuur van melamine-formaldehyde harsen en de hars receptuur wordt beschreven in dit proefschrift. De snelle industriële ontwikkeling van MF harsen had tot gevolg dat de analyse van de MF reaktieprodukten achterop bleef. Een meer gedetailleerd beeld van de mogelijke MF reactieprodukten is vereist om progressie te maken in dit domein. Verschillende spectroscopische technieken werden geëvalueerd en verder ontwikkeld voor de karakterisatie van MF harsen zowel in het initiële als het uitgeharde stadium. De kinetiek van de methyleen brugvorming, methyleen-ether brugvorming en hydrolyse werd bestudeerd. De relatie tussen hars receptuur en hars structuur werd bestudeerd zowel in het initiële stadium van de uitharding als in het uiteindelijk uitgeharde stadium door de industriële reaktieparameters systematisch te variëren.

In hoofdstuk 1 wordt een overzicht gegeven van de kennis op het gebied van MF harsen bij de aanvang van deze studie. De chemische complexiteit van MF harsen en de onoplosbaarheid van uitgeharde MF harsen heeft de opheldering van de chemische structuur van deze harsen aanzienlijk bemoeilijkt. Mettertijd werden nieuwe technieken ontwikkeld welke meer gedetailleerde informatie verschaften. De kinetiek en mechanismen van de methylolering en condensatiereakties worden in detail beschreven.

In het tweede hoofdstuk wordt de kracht van ^{13}C NMR voor het analyseren van MF harsen in het initiële condensatie stadium gedemonstreerd. Er is in het bijzonder aandacht besteed aan de methyleen-ether brugvorming. De vorming van methyleen-ether bruggen tijdens de condensatie van een MF hars is aangetoond door middel van een combinatie van ^{1}H en ^{13}C NMR. Het aantal gevormde methyleen-ether bruggen berekend op basis van de hoeveelheid water vrij gezet tijdens de condensatie stemt goed overeen met dat berekend op basis van het aantal gereageerde mono gemethyloleerde amino groepen tijdens de condensatiereakties. Deze studie heeft verder inzicht verschaft in de reaktiepaden voor de vorming van gemethyloleerde methyleen bruggen.

Hoofdstuk 3 beschrijft de ^{13}C CP/MAS NMR studie op MF harsen en laat zien dat de ^{13}C NMR cross polarisatie techniek kan gebruikt worden voor de

kwantitatieve analyse van uitgeharde MF harsen. Verder is aangetoond dat de relatieve verdeling van de methyleen koolstoffen kwantitatief bepaald kan worden uit één enkel contact-tijd experiment met een enorme besparing in spectrometer tijd als gevolg. De fractie methyleen bruggen gevormd tijdens de uitharding kan kwantitatief bepaald worden met ^{13}C CP/MAS NMR. De veranderingen in de gemiddelde netwerk mobiliteit met toenemende uithardingsgraad komen duidelijk tot uiting in de $T_{1\rho}(^1H)$ metingen en deze laatste kunnen in principe aangewend worden als een criterium voor de bepaling van de uithardingsgraad.

In hoofstuk 4 wordt de Raman spectroscopische studie op MF harsen gepresenteerd. De combinatie van HPLC, ^{13}C vloeistof en vaste stof NMR data hebben bijgedragen tot de interpretatie van de Raman spectra van MF harsen. Er wordt getoond dat FT-Raman spectroscopie een complementaire techniek is aan ^{13}C CP/MAS NMR voor de karakterisatie van uitgeharde MF harsen. Kwantitatieve data kunnen worden afgeleid uit de FT-Raman spectra. De ring breathing vibratie mode van melamine kan gehanteerd worden als interne standaard in de Raman spectra van MF harsen. Relatieve veranderingen in de verdeling van $N\text{-}CH_2\text{-}N$ en $N\text{-}CH_2\text{-}O$ structuren tijdens de uitharding worden geobserveerd in het methyleen bending Raman spectraal gebied. Het percentage residuele methylol groepen kan bepaald worden vanaf de Raman banden bij 1000 cm^{-1}. De Raman band bij 900 cm^{-1} kan gebruikt worden als een indicatie voor methyleen-ether bruggen. Een Raman spectrosocpische methode is ontwikkeld voor de bepaling van de hoeveelheid vrij melamine in uitgeharde MF harsen. Deze methode werd verder ondersteund door een theoretische analyse van de Raman frequenties.

In hoofdstuk 5 is DSC aangewend voor het bestuderen van de uitharding van MF harsen. Om de bijdrage van het endotherme effect van het verdampen van het condensatiewater tot de gemeten reaktiewarmte te omzeilen wordt de uitharding gemeten onder isotherme condities. Redelijke schattingen van de enthalpieën voor de methyleen- en de methyleen-ether brugvorming worden bekomen door gebruik te maken van een combinatie van DSC, ^{13}C CP/MAS NMR and Raman spectrosocpie. ΔH is meer exotherm voor de methyleen brug vorming (-30 ± 6 kJ/mol) dan voor de methyleen-ether brugvorming (-19 ± 8 kJ/mol).

In hoofdstuk 6 worden snelheidsconstanten voor methyleen brugvorming, methyleen-ether brugvorming en hydrolyse bepaald voor een standaard MF (1.7) hars in functie van pH en temperatuur. Er wordt gebruik gemaakt van twee verschillende aanpakken voor de bepaling van deze snelheidsconstanten. In de eerste aanpak worden de snelheidsconstanten voor twee MF dimeren bepaald via een quantitatieve analyse van de melamine moleculaire deeltjes met HPLC. In de tweede aanpak

worden de snelheidsconstanten berekend uit het concentratie verloop van functionele groepen (-NH_2,-$NHCH_2OH$, -$N(CH_2OH)_2$ enz.) in functie van de tijd. Vergelijkbare waarden worden gevonden voor de snelheidsconstanten van de ongesubstitueerde en methylol-gesubstitueerde methyleen brugvorming. De methylolerings evenwichts-constanten van een methyleen brug en van een mono gemethyloleerde amino groep zijn vergelijkbaar. De snelheidsconstanten van de methyleen brugvorming, methyleen-ether brugvorming en hydrolyse zijn sterk afhankelijk van de pH. De kinetische hydrolyse experimenten van methyleen-ether dimelamine hebben aangetoond dat de hydrolyse van methyleen-ether bruggen wordt gekatalyseerd door H_3O^+ ionen in zuur midden. De activeringsenergieën voor de methyleen brugvorming, methyleen-ether brugvorming en hydrolyse zijn berekend uit de temperatuurs-afhankelijkheid van de snelheidsconstanten. De enthalpie voor de methyleen-ether brugvorming is berekend uit de temperatuursafhankelijkheid van de evenwichts-constante. Deze waarde (-14.3 ± 6.0 kJ/mol) is in overeenstemming met de waarde bepaald met DSC.

Een gedetailleerde ^{13}C NMR studie naar de structuur van industriële MF harsen in het initiële condensatie stadium als functie van de hars receptuur (pH, F/M verhouding en vaste stof gehalte) wordt beschreven in hoofdstuk 7. De vorming van methyleen- versus methyleen-ether bruggen wordt in belangrijke mate bepaald door de pH van het MF hars. Naast ongesubstitueerde methyleen bruggen bevatten de MF harsen bereid met een lage formaline pH eveneens relatief veel methylol-gesubstitueerde methyleen bruggen. Het totaal aantal secundaire methylol groepen varieert sterk als functie van de formaline pH. De toename van het aantal methylol groepen ten opzichte van -NH groepen met toenemende F/M verhouding begunstigt de vorming van methyleen-ether bruggen. De hars structuur in het initiële condensatie stadium wordt in belangrijke mate bepaald door het vaste stof gehalte van de hars. Het verloop van de pH en het verloop van de water verdraagzaamheid tijdens de industriële hars synthese werden gerelateerd aan het verloop van de methyleen en methyleen-ether bruggen. Het verloop van de bruggen kan goed beschreven worden aan de hand van het pH verloop en de snelheidsconstanten bij de respectievelijke pH waarden. De waterverdraagzaamheid correleert lineair met de totale hoeveelheid gevormde bruggen voor een bepaald vaste stof gehalte.

De structuur van de uitgeharde MF harsen in functie van de hars receptuur wordt op systematische wijze bestudeerd in hoofdstuk 8. De structuur van de uitgeharde MF harsen wordt praktisch niet beïnvloed bij variatie van de initiële formaline pH tussen 7 en 9.5. De verhouding van methyleen en methyleen-ether bruggen wordt in grote mate bepaald door de F/M verhouding van het initiële

reaktiemengsel. De structuur van de uitgeharde MF harsen wordt praktisch niet beïnvloed door het vaste gehalte van het hars. Het toevoegen van p-tolueen sulfonzuur als katalysator heeft praktisch geen invloed op de structuur van de uitgeharde MF harsen. In alle gevallen treedt verglazing op en dit belemmert de omzetting van methyleen-ether bruggen naar methyleen bruggen. Een hogere uithardingstemperatuur begunstigt de vorming van de thermodynamisch meer stabiele methyleen bruggen.

Appendix

Survey of the various MF resin formulations studied by ^{13}C NMR

Resin No.	T(°C)	s.c.	F/M	pH	
1	95	50%	1.7	initial	7
2					8
3					9
4					9.5
5					9.5 → 7
6					10
7	95	50%	1.5	initial	9.5
8			2.2		
9			3.0		
10	95	25%	1.7	initial	9.5
11		10%			
12	85	50%	1.7	constant	7.5
13					8
14					9
15					9.25
16					9.5
17	90	50%	1.7	constant	7.5
18					8
19					9
20					9.5
21	95	50%	1.7	constant	7.5
22					8
23					9
24					9.25
25					9.5

Resin No.1

Reaction time, s	1800	3360	5100
Water tolerance	∞	1.0	0.3
Concentration, mol C/ kg resin			
-NH_2	3.78	3.54	3.30
-$NHCH_2OH$	3.73	3.32	3.10
-$NR'CH_2OH$	0.77	0.76	0.75
-$NHCH_2NH$-	0.15	0.30	0.41
-$NR'CH_2NH$-	0.09	0.17	0.22
-$NHCH_2OCH_2NH$-	0.08	0.26	0.33
-$NR'CH_2OCH_2NH$-	-	-	-
$HOCH_2OH$ + oligomers	0.08	0.08	0.08

Resin No.2

Reaction time, s	1800	3600	4500	5400
Water tolerance	∞	1.5	0.8	0.2
Concentration, mol C/ kg resin				
-NH_2	3.71	3.54	3.34	3.24
-$NHCH_2OH$	3.78	3.40	3.08	3.04
-$NR'CH_2OH$	0.74	0.75	0.77	0.77
-$NHCH_2NH$-	0.09	0.25	0.38	0.41
-$NR'CH_2NH$-	0.06	0.11	0.17	0.22
-$NHCH_2OCH_2NH$-	0.09	0.29	0.33	0.38
-$NR'CH_2OCH_2NH$-	-	-	-	
$HOCH_2OH$ + oligomers	0.08	0.08	0.10	0.10

Resin No.3

Reaction time, s	1800	7200	9000
Water tolerance	∞	0.9	0.4
Concentration, mol C/ kg resin			
$-NH_2$	4.11	3.51	3.48
$-NHCH_2OH$	3.72	3.17	3.04
$-NR'CH_2OH$	0.82	0.67	0.69
$-NHCH_2NH-$	0.02	0.26	0.33
$-NR'CH_2NH-$	-	0.10	0.18
$-NHCH_2OCH_2NH-$	0.25	0.51	0.47
$-NR'CH_2OCH_2NH-$	-	0.05	0.05
$HOCH_2OH$	-	0.10	0.10
+ oligomers			

Resin No.4

Reaction time, s	1800	3600	4500	8100
Water tolerance	∞	4.4	1.4	0.4
Concentration, mol C/ kg resin				
$-NH_2$	3.95	3.83	3.74	3.56
$-NHCH_2OH$	3.46	3.31	3.20	3.01
$-NR'CH_2OH$	0.63	0.61	0.63	0.63
$-NHCH_2NH-$	-	0.04	0.12	0.26
$-NR'CH_2NH-$	-	-	-	0.09
$-NHCH_2OCH_2NH-$	0.68	0.78	0.78	0.75
$-NR'CH_2OCH_2NH-$	0.05	0.07	0.09	0.06
$HOCH_2OH$	0.10	0.08	0.10	0.10
+ oligomers				

Resin No.5

Reaction time, s	1800	2220	2760
Water tolerance	∞	1.6	0.2
Concentration, mol C/ kg resin			
-NH_2	3.95	3.68	3.37
-$NHCH_2OH$	3.61	3.02	2.95
-$NR'CH_2OH$	0.62	0.67	0.64
-$NHCH_2NH$-	-	0.18	0.34
-$NR'CH_2NH$-	-	0.09	0.13
-$NHCH_2OCH_2NH$-	0.52	0.69	0.64
-$NR'CH_2OCH_2NH$-	0.06	0.11	0.05
$HOCH_2OH$	0.10	0.08	0.08
+ oligomers			

Resin No.6

Reaction time, s	1080	1800	2700	6600
Water tolerance	∞	∞	1.4	0.2
Concentration, mol C/ kg resin				
-NH_2	3.95	3.87	3.84	3.66
-$NHCH_2OH$	3.26	3.10	3.05	2.94
-$NR'CH_2OH$	0.55	0.57	0.56	0.63
-$NHCH_2NH$-	-	-	-	0.22
-$NR'CH_2NH$-	-	-	-	-
-$NHCH_2OCH_2NH$-	0.92	1.05	1.10	0.93
-$NR'CH_2OCH_2NH$-	0.08	0.09	0.11	0.09
$HOCH_2OH$	0.08	0.10	0.08	0.08
+ oligomers				

Resin No.7

Reaction time, s	3600	7200	10800
Water tolerance	∞	1.6	0.4
Concentration, mol C/ kg resin			
$-NH_2$	4.49	4.31	4.15
$-NHCH_2OH$	3.17	2.95	2.67
$-NR'CH_2OH$	0.48	0.49	0.54
$-NHCH_2NH-$	0.07	0.16	0.29
$-NR'CH_2NH-$	-	0.08	0.09
$-NHCH_2OCH_2NH-$	0.63	0.61	0.54
$-NR'CH_2OCH_2NH-$	0.03	0.07	0.10
$HOCH_2OH$	0.06	0.06	0.06
+ oligomers			

Resin No.8

Reaction time, s	1800	3600	6300
Water tolerance	2.2	1.0	0.5
Concentration, mol C/ kg resin			
$-NH_2$	2.80	2.70	2.62
$-NHCH_2OH$	3.39	3.42	3.32
$-NR'CH_2OH$	1.08	1.07	1.07
$-NHCH_2NH-$	-	0.02	0.08
$-NR'CH_2NH-$	-	-	0.05
$-NHCH_2OCH_2NH-$	1.02	1.05	1.01
$-NR'CH_2OCH_2NH-$	0.13	0.16	0.16
$HOCH_2OH$	0.16	0.16	0.20
+ oligomers			

Resin No.9

Reaction time, s	1800	5040	6480
Water tolerance	∞	1.2	0.3
Concentration, mol C/ kg resin			
$-NH_2$	1.33	1.09	1.06
$-NHCH_2OH$	3.45	3.17	2.91
$-NR'CH_2OH$	2.24	2.21	2.25
$-NHCH_2NH-$	-	0.09	0.10
$-NR'CH_2NH-$	-	0.15	0.23
$-NHCH_2OCH_2NH-$	0.67	0.82	0.82
$-NR'CH_2OCH_2NH-$	0.26	0.33	0.47
$HOCH_2OH$	0.32	0.17	0.17
+ oligomers			

Resin No.10

Reaction time, s	1800	5400	7200
Water tolerance	∞	1.9	0.0
Concentration, mol C/ kg resin			
$-NH_2$	1.97	1.88	1.82
$-NHCH_2OH$	1.93	1.71	1.62
$-NR'CH_2OH$	0.33	0.32	0.34
$-NHCH_2NH-$	-	0.09	0.15
$-NR'CH_2NH-$	-	0.02	0.07
$-NHCH_2OCH_2NH-$	0.08	0.18	0.17
$-NR'CH_2OCH_2NH-$	-	0.03	-
$HOCH_2OH$	0.06	0.06	0.06
+ oligomers			

Resin No.11

Reaction time, s	1800	9000
Water tolerance	∞	0.0
Concentration, mol C/ kg resin		
$-NH_2$	0.80	0.75
$-NHCH_2OH$	0.75	0.68
$-NR'CH_2OH$	0.11	0.13
$-NHCH_2NH-$	-	0.05
$-NR'CH_2NH-$	-	0.03
$-NHCH_2OCH_2NH-$	0.04	0.03
$-NR'CH_2OCH_2NH-$	-	-
$HOCH_2OH$	0.06	0.05
+ oligomers		

Resin No.12

Reaction time,s	900	1800	2700	3300	3900
Water tolerance	∞	∞	1.3	0.6	0.4
Concentration, mol/kg					
$-NH_2$	3.98	3.80	3.49	3.56	3.40
$-NHCH_2OH$	3.80	3.60	3.41	3.30	3.25
$-N(CH_2OH)_2$	0.43	0.33	0.30	0.29	0.27
$-NHCH_2NH-$	0.07	0.21	0.29	0.36	0.40
$-NR'CH_2NH-$	-	0.08	0.13	0.17	0.19
$-NHCH_2OCH_2NH-$	0.02	0.05	0.09	0.08	0.09
$-NR'CH_2OCH_2NH-$	-	-	-	-	-
$HOCH_2OH$	0.06	0.09	0.08	0.09	0.07
+ oligomers					

Resin No.13

Reaction time,s	1200	2400	3600	5400	6600	8400
Water tolerance	∞	∞	∞	4.1	1.8	0.8
Concentration, mol/kg						
$-NH_2$	4.08	4.06	3.96	3.68	3.64	3.58
$-NHCH_2OH$	3.98	3.91	3.77	3.58	3.41	3.28
$-N(CH_2OH)_2$	0.40	0.39	0.35	0.32	0.31	0.26
$-NHCH_2NH-$	0.01	0.07	0.13	0.16	0.26	0.33
$-NR'CH_2NH-$	-	-	0.07	0.09	0.12	0.19
$-NHCH_2OCH_2NH-$	0.01	0.02	0.06	0.10	0.11	0.12
$-NR'CH_2OCH_2NH-$	-	-	-	-	-	-
$HOCH_2OH$ + oligomers	0.04	0.04	0.10	0.06	0.09	0.07

Resin No.14

Reaction time,s	1200	2400	3600	7200	10800	14400
Water tolerance	∞	∞	∞	∞	∞	4.0
Concentration, mol/kg						
$-NH_2$	4.05	4.13	4.25	4.21	4.04	3.93
$-NHCH_2OH$	3.86	3.77	3.76	3.61	3.51	3.33
$-N(CH_2OH)_2$	0.40	0.38	0.38	0.34	0.33	0.29
$-NHCH_2NH-$	-	-	-	-	0.03	0.06
$-NR'CH_2NH-$	-	-	-	-	-	-
$-NHCH_2OCH_2NH-$	0.07	0.10	0.12	0.19	0.26	0.31
$-NR'CH_2OCH_2NH-$	-	-	-	0.03	0.03	0.07
$HOCH_2OH$ +oligomers	0.05	0.08	0.06	0.05	0.05	0.05

Resin No.15

Reaction time,s	1800	3600	5400	8100	10800	13500
Water tolerance	∞	∞	∞	-	3.7	1.8
Concentration, mol/kg						
$-NH_2$	4.20	4.02	4.03	3.99	3.99	3.87
$-NHCH_2OH$	3.77	3.77	3.49	3.33	3.22	3.24
$-N(CH_2OH)_2$	0.37	0.33	0.31	0.29	0.27	0.23
$-NHCH_2NH-$	-	-	0.02	0.02	0.03	0.06
$-NR'CH_2NH-$	-	-	-	-	-	-
$-NHCH_2OCH_2NH-$	0.11	0.19	0.25	0.32	0.36	0.38
$-NR'CH_2OCH_2NH-$	-	-	-	0.06	0.08	0.06
$HOCH_2OH$ + oligomers	0.10	0.06	0.07	0.06	0.07	0.06

Resin No.16

Reaction time,s	1200	2100	3000	4800	6600	8400
Water tolerance	∞	∞	∞	6.0	2.6	2.2
Concentration, mol/kg						
$-NH_2$	4.18	4.22	4.13	4.01	3.95	3.93
$-NHCH_2OH$	3.81	3.80	3.50	3.34	3.27	3.18
$-N(CH_2OH)_2$	0.35	0.34	0.31	0.28	0.26	0.25
$-NHCH_2NH-$	-	-	-	0.01	0.02	0.04
$-NR'CH_2NH-$	-	-	-	-	-	-
$-NHCH_2OCH_2NH-$	0.12	0.17	0.22	0.31	0.33	0.37
$-NR'CH_2OCH_2NH-$	-	-	0.06	0.08	0.09	0.09
$HOCH_2OH$ + oligomers	0.07	0.05	0.07	0.06	0.07	0.05

Resin No.17

Reaction time,s	600	1020	1440	1860	2280	2700
Water tolerance	∞	∞	-	1.2	0.7	0.4
Concentration, mol/kg						
$-NH_2$	3.95	3.81	3.71	3.47	3.55	3.42
$-NHCH_2OH$	3.78	3.60	3.51	3.37	3.24	3.24
$-N(CH_2OH)_2$	0.39	0.35	0.33	0.33	0.31	0.29
$-NHCH_2NH-$	0.08	0.16	0.24	0.30	0.35	0.40
$-NR'CH_2NH-$	-	0.07	0.10	0.12	0.17	0.20
$-NHCH_2OCH_2NH-$	0.04	0.06	0.07	0.09	0.12	0.08
$-NR'CH_2OCH_2NH-$	-	-	-	-	-	-
$HOCH_2OH$ + oligomers	0.10	0.08	0.08	0.06	0.05	0.06

Resin No.18

Reaction time,s	900	1800	2700	4200	5700	7200
Water tolerance	-	-	-	-	-	-
Concentration, mol/kg						
$-NH_2$	4.29	4.00	3.92	3.71	3.60	3.49
$-NHCH_2OH$	3.78	3.75	3.63	3.46	3.24	3.18
$-N(CH_2OH)_2$	0.42	0.36	0.36	0.30	0.29	0.29
$-NHCH_2NH-$	0.03	0.05	0.15	0.25	0.31	0.37
$-NR'CH_2NH-$	-	0.04	0.08	0.11	0.14	0.17
$-NHCH_2OCH_2NH-$	0.04	0.05	0.06	0.08	0.09	0.13
$-NR'CH_2OCH_2NH-$	-	-	-	-	-	-
$HOCH_2OH$ + oligomers	0.07	0.09	0.06	0.07	0.06	0.05

Resin No.19

Reaction time,s	1800	3600	5400	7800	10320	12600
Water tolerance	∞	∞	∞	∞	2.5	1.3
Concentration, mol/kg						
$-NH_2$	4.16	4.09	4.07	3.89	3.90	3.84
$-NHCH_2OH$	3.72	3.68	3.45	3.34	3.18	3.18
$-N(CH_2OH)_2$	0.39	0.34	0.32	0.29	0.27	0.26
$-NHCH_2NH-$	-	-	0.03	0.06	0.08	0.12
$-NR'CH_2NH-$	-	-	-	0.02	0.04	0.06
$-NHCH_2OCH_2NH-$	0.11	0.13	0.20	0.28	0.29	0.31
$-NR'CH_2OCH_2NH-$	-	0.04	0.09	0.06	0.09	0.09
$HOCH_2OH$ + oligomers	0.09	0.08	0.06	0.07	0.07	0.05

Resin No.20

Reaction time,s	900	1800	2700	3600	4800	5700
Water tolerance	∞	∞	∞	5.0	1.7	1.2
Concentration, mol/kg						
$-NH_2$	4.11	4.00	4.00	3.94	3.95	3.98
$-NHCH_2OH$	3.83	3.50	3.34	3.26	3.20	3.13
$-N(CH_2OH)_2$	0.33	0.28	0.27	0.25	0.25	0.24
$-NHCH_2NH-$	-	0.01	0.02	0.02	0.03	0.03
$-NR'CH_2NH-$	-	-	-	-	-	-
$-NHCH_2OCH_2NH-$	0.16	0.26	0.34	0.38	0.42	0.44
$-NR'CH_2OCH_2NH-$	-	0.05	0.06	0.08	0.07	0.08
$HOCH_2OH$ + oligomers	0.06	0.06	0.07	0.06	0.06	0.06

Resin No.21

Reaction time,s	480	780	1080	1380	1680	1980
Water tolerance	∞	∞	-	3.2	1.9	0.9
Concentration, mol/kg						
$-NH_2$	4.02	3.98	3.82	3.76	3.71	3.61
$-NHCH_2OH$	3.83	3.74	3.61	3.56	3.42	3.35
$-N(CH_2OH)_2$	0.39	0.40	0.36	0.31	0.30	0.28
$-NHCH_2NH-$	0.04	0.14	0.17	0.22	0.28	0.32
$-NR'CH_2NH-$	-	-	0.07	0.13	0.13	0.16
$-NHCH_2OCH_2NH-$	0.03	0.04	0.05	0.06	0.07	0.08
$-NR'CH_2OCH_2NH-$	-	-	-	-	-	0.02
$HOCH_2OH$	0.10	0.08	0.08	0.08	0.08	0.06
+ oligomers						

Resin No.22

Reaction time,s	600	1200	1800	2700	3600	4500
Water tolerance	∞	∞	∞	9.4	1.9	0.8
Concentration, mol/kg						
$-NH_2$	4.28	4.10	3.97	3.79	3.66	3.68
$-NHCH_2OH$	3.75	3.71	3.67	3.51	3.40	3.24
$-N(CH_2OH)_2$	0.43	0.41	0.38	0.33	0.31	0.25
$-NHCH_2NH-$	0.03	0.07	0.12	0.19	0.27	0.33
$-NR'CH_2NH-$	-	-	0.04	0.08	0.11	0.15
$-NHCH_2OCH_2NH-$	0.04	0.05	0.09	0.11	0.12	0.09
$-NR'CH_2OCH_2NH-$	-	-	-	-	-	0.05
$HOCH_2OH$	0.10	0.07	0.05	0.07	0.08	0.09
+ oligomers						

Resin No.23

Reaction time,s	1200	2100	3000	4500	6300	7800
Water tolerance	∞	∞	∞	2.6	1.3	1.2
Concentration, mol/kg						
$-NH_2$	4.14	4.09	4.03	3.94	3.89	3.86
$-NHCH_2OH$	3.79	3.69	3.63	3.39	3.21	3.16
$-N(CH_2OH)_2$	0.38	0.34	0.33	0.29	0.24	0.23
$-NHCH_2NH-$	-	-	0.04	0.05	0.08	0.14
$-NR'CH_2NH-$	-	-	-	-	0.06	0.07
$-NHCH_2OCH_2NH-$	0.11	0.18	0.22	0.27	0.31	0.34
$-NR'CH_2OCH_2NH-$	-	-	-	0.06	0.07	0.04
$HOCH_2OH$ + oligomers	0.06	0.09	0.06	0.08	0.08	0.06

Resin No.24

Reaction time,s	600	1200	1800	3000	4200	5400
Water tolerance	∞	∞	∞	2.8	1.7	1.3
Concentration, mol/kg						
$-NH_2$	4.50	4.10	4.14	4.00	3.96	3.95
$-NHCH_2OH$	3.82	3.67	3.64	3.34	3.19	3.11
$-N(CH_2OH)_2$	0.40	0.36	0.33	0.27	0.27	0.24
$-NHCH_2NH-$	-	-	-	0.02	0.06	0.07
$-NR'CH_2NH-$	-	-	-	-	-	-
$-NHCH_2OCH_2NH-$	0.10	0.20	0.25	0.32	0.33	0.34
$-NR'CH_2OCH_2NH-$	-	-	-	0.06	0.10	0.14
$HOCH_2OH$ + oligomers	0.06	0.06	0.06	0.06	0.05	0.05

Resin No.25

Reaction time,s	600	1020	1440	2160	3060	3960
Water tolerance	∞	∞	-	1.9	-	1.3
Concentration, mol/kg						
$-NH_2$	4.07	3.98	4.02	4.00	4.00	4.00
$-NHCH_2OH$	3.72	3.55	3.41	3.34	3.19	3.19
$-N(CH_2OH)_2$	0.32	0.30	0.25	0.24	0.23	0.22
$-NHCH_2NH-$	-	-	-	0.02	0.03	0.05
$-NR'CH_2NH-$	-	-	-	-	-	-
$-NHCH_2OCH_2NH-$	0.14	0.22	0.34	0.39	0.43	0.44
$-NR'CH_2OCH_2NH-$	0.04	0.05	0.06	0.07	0.07	0.06
$HOCH_2OH$ + oligomers	0.05	0.05	0.06	0.05	0.06	0.05

LIST OF ABBREVIATIONS

M	melamine
F	formaldehyde
R	melamine species minus one amino group
MM	methylolmelamine
MB	methylene bridge
EB	methylene-ether bridge
s.c.	solids content
c.s.c.	critical solids content
PTSA	p-toluene sulfonic acid